FEBRUARY 1989

ENVIRONMENTAL PROGRESS

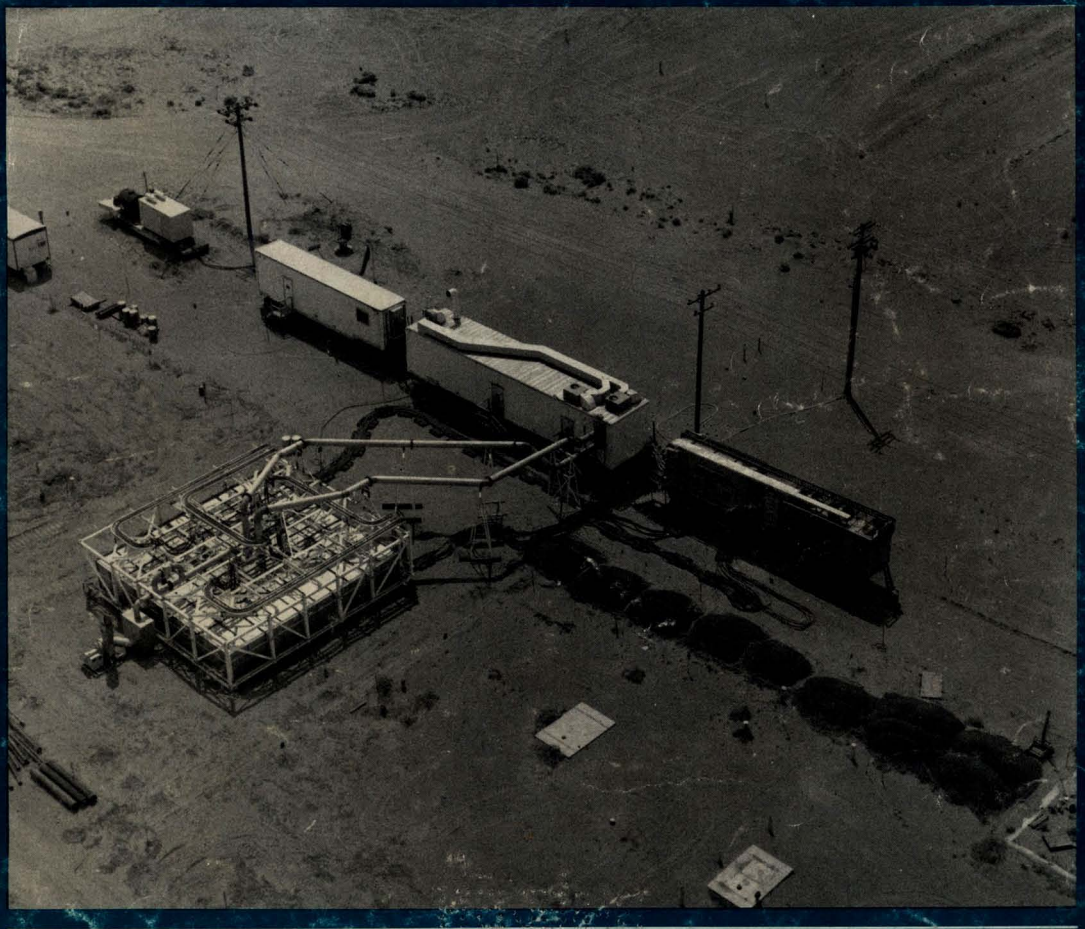

ISV, a chemical and hazardous waste process. Photo courtesy of Geosafe Corporation, Kirkland, WA.

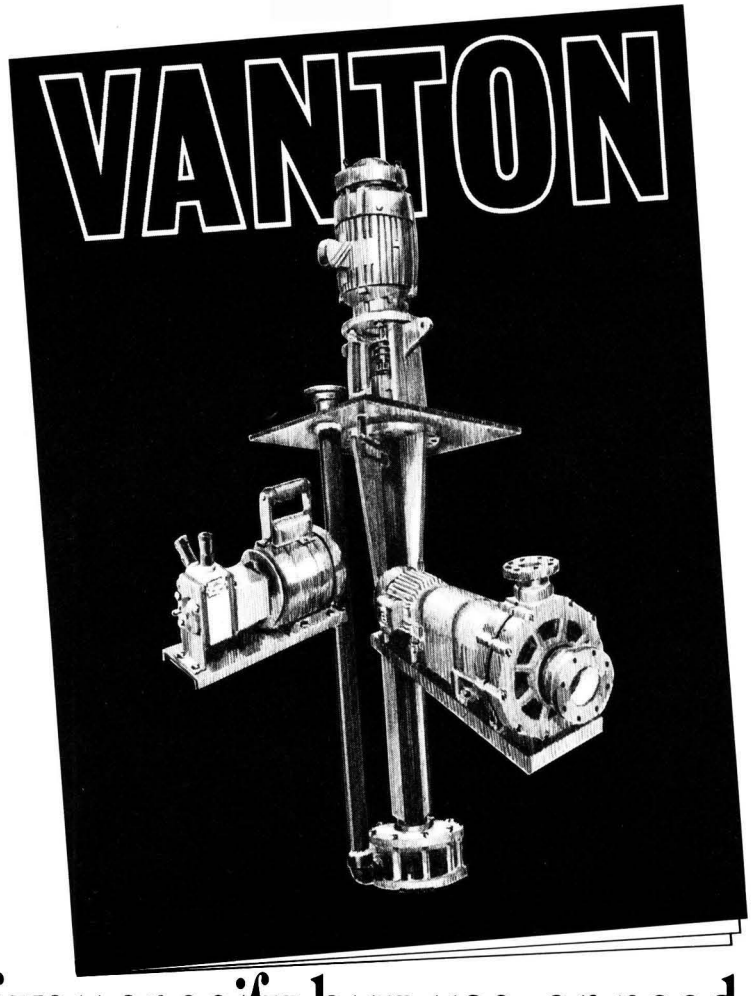

If you specify, buy, use, or need non-metallic pumps, here's a company you should know more about.

CHEM-GARD® horizontal, heavy-duty plastic centrifugal pumps with capacities to 1000 gpm, for temperatures to 275°F and heads to 240'. Self priming and close-coupled models to 250 gpm. Available in Polypropylene, PVC, CPVC, PVDF, and ECTFE.

FLEX-I-LINER® sealless, self-priming plastic pumps in capacities to 40 gpm, discharge pressures to 45 psig, for temperatures to 250°F. Recommended for corrosive, abrasive and ultra-pure liquid or gas service. Only two non-metallic components, pump body and the flexible liner, contact the fluid.

SUMP-GARD® heavy-duty engineered vertical plastic centrifugal sump pumps in capacities to 1000 gpm, temperatures to 275°F, heads to 210' and depth to 20'. Available in Polypropylene, PVC, CPVC and PVDF in standard and "bearingless" cantilevered designs. No metal components in contact with fluid.

VANTON

"The Pump Professionals Prefer"

Vanton Pump & Equipment Corp., 201 Sweetland Avenue, Hillside NJ 07205 • (201) 688-4216 • Fax (201) 686-9314

ENVIRONMENTAL PROGRESS

Environmental Progress is a publication of the American Institute of Chemical Engineers. It will deal with multi-faceted aspects of the pollution problem. It will provide thorough coverage of abatement, control, and containment of effluents and emissions within compliance standards. Papers will cover all aspects including water, air, liquid and solid wastes. Progress and technological advances vital to the environmental engineer will be reported.

Publication Office, 215 Canal Street, Manchester, N.H. Published quarterly by the American Institute of Chemical Engineers, 345 East 47 St., New York, N.Y., 10017. (ISSN 0278-4491). Manuscripts should be submitted to the Manuscript Center, American Institute of Chemical Engineers, 345 East 47 St., New York, N.Y. 10017. Statements and opinions in *Environmental Progress* are those of the contributors, and the American Institute of Chemical Engineers assumes no responsibility for them. Subscription price per year: $50. Outside the U.S. please add $5 per subscription for postage and handling. Single copies $18. Outside the U.S. please add $2 for postage and handling. Payment must be made in U.S. dollars. Second-class postage paid at New York, N.Y. and additional mailing offices.

Volume 8

Contents

Number 1

Environmental Progress fee code: 0278-4491/89 $2.00. Postmaster: Please send change of addresses to *Environmental Progress*, AIChE, 345 East 47 Street, New York, N.Y. 10017.

Making Superfund Work

by

Thomas P. Grumbly

Clean Sites Inc., Alexandria, VA.

The nation's hazardous waste cleanup program is at a crossroads. Aimed at cleaning up uncontrolled hazardous waste sites, the Superfund program is one of the most ambitious and expensive environmental efforts ever attempted. The EPA has already spent over $4 billion on the program, and is committed to spending an additional $6 billion over the next three years. It is estimated that the price tag for cleaning up only the 1,175 sites on the EPA's National Priorities List is over $30 billion.

While EPA has made substantial strides in its efforts to implement the Superfund program, there is still a widespread perception that the health and environmental risks posed by hazardous waste sites are not being effectively managed. The Nation's progress in solving the uncontrolled waste site problem has been slower than expected. Furthermore, the problem is larger than expected.

The magnitude of the task at hand, and the amounts of time and money it will take to clean up the growing number of hazardous waste sites require that significant improvement be made in the implementation of the program. Over the past few years EPA has done a good job, using Fund monies, of getting more and more sites "in the pipeline." In the next year or two, many sites will move into the remedial design stage. As a result, Fund monies will be almost fully committed in the next year. This underscores the need for increased private party cleanups to augment those financed by the Fund.

Many of the problems that are currently being discussed—lack of incentives for responsible parties to volunteer to clean up sites, confusion about appropriate site remedies, criticism about inconsistent cleanup levels—can be corrected by changing the way EPA is implementing the program under current law. Attention is already being focused on the 1991 reauthorization as a way to remedy these problems. However, the advent of a new Administration presents an ideal opportunity to implement significant mid-course corrections to give the Superfund program the best chance of success. The current statute should be implemented to the fullest before Congress begins the reauthorization process.

EPA is just beginning to utilize fully its enforcement and settlement powers to create a strong cleanup program conducted and financed by the parties responsible for the hazardous waste sites. The process for selecting a site remedy is still slow, lacks clear definition and frustrates all involved, including government personnel. The lack of a strong management relationship at EPA between Headquarters and the Regions and among EPA Headquarters' offices impairs the Superfund program's effectiveness. Finally, current measures of program success do not provide meaningful indicators to the public, Congress, and other interested parties about the pace and quality of site cleanups. While the Agency's proposed revisions to the National Contingency Plan augur well for improved implementation of the Superfund program, there is still more to be done.

Improvements in program implementation must be made in four key areas: a more vigorous enforcement and settlement strategy; clearer policies for the selection of a site remedy; improved internal management operations; and more dynamic measures of program success.

An effective Superfund program depends on a stronger relationship between the EPA and the private sector. EPA and the Department of Justice must provide responsible parties with adequate incentives to finance and conduct cleanups. In addition, EPA must be prepared to move more vigorously against those who fail to cooperate with cleanups.

EPA also must implement a more clearly defined policy that articulates how the different cleanup criteria embodied in Section 121 of the statute are to be evaluated and weighed in selecting a remedy. Clearer remedy-selection criteria will help EPA staff making controversial and expensive decisions, guide responsible parties in estimating likely cleanup costs and give citizens a yardstick to evaluate the appropriateness of different remedies. This is an area in which chemical engineers can make particular contributions because of their process engineering experience.

Internally, EPA must clarify the lines of authority and responsibility within and between EPA Headquarters and the Regional Offices. To ensure implementation of EPA policy, Regional Administrators should be made accountable for achieving national program policies and goals.

Finally, EPA needs to develop new measures of program success that focus on achievements—such as the speed with which sites are being remediated, the number of site cleanups financed by responsible parties, the number of orphan sites cleaned up by EPA—rather than simply on inputs, such as the number of remedial investigations initiated. Information on EPA's progress should be communicated to the public regularly in a readily available and easily understandable fashion.

The new Administration has the opportunity to make the Superfund program a success. There are clear lessons that can be learned from EPA's experience in implementing the program over the past eight years. All involved can benefit from understanding where the program has been successful and where it has faltered. To ignore what we have learned would be a loss for the new Administration, for the EPA, and for the country.

Now is the time to make the Superfund program work.

Clean Sites Inc., was established in 1984 to encourage the cleanup of hazardous waste sites by those responsible for them. Clean Sites helps responsible parties divide cleanup costs and acts as an informal mediator to help the parties and governments achieve settlement agreements. It also reviews technical studies, manages cleanups and cleanup funds and conducts public policy and education efforts to facilitate the development of a regulatory system that encourages private party cleanups. Thomas P. Grumbly was named president in 1987.

Environmental Shorts

Water Quality Concerns Spur Increasing Demand by European Market

Water pollution along Europe's coastal and inland waters has in recent years become more apparent, igniting concern among the European public to demand stricter controls, local, national, and international in the need for purer process water. Manufacturers of water/waste treatment equipment are clearly in the right business at the right time.

A report by Frost and Sullivan says this market includes all of Western Europe plus Yugoslavia, with West Germany as the largest market. The Iberian market (Spain and Portugal) is however the fastest growing market in all of Europe.

Looking at types of equipment used, the Frost and Sullivan report finds growth market for all categories, but sees some of the most rapid market growth coming in types of equipment used for polishing fresh water (5.47% annual growth rate and for tertiary processing of liquid effluents (5.59%) annual growth). This reflects the increasing pressure for better water quality and less damaging waste discharges.

In examining the equipment and processes for water and waste water treatment, the report identifies problem areas such as nitrate removal, and decreasing the amounts of heavy metals in sludges where there is a neeed for better methods and advanced processes. A number of trends, general and specific are taking shape. They include increased investment in treatment to overcome the problem of high nitrate levels, either by ion exchange or by biological processes. The proportion of packaged plants for the purpose of activated sludge treatment is also increasing.

In its analysis of manufacturing and marketing processes, the report notes that "remarkably few companies have failed" in this industry even during the recession of the early 1980's. A number of companies are profiled individually. Companies such as the British Biwater Group, which has achieved success especially with its potable water equipment packages, and the large Swedish centrifuge-maker, Alfa-Laval, which has recently developed strong interests in biotechnology, with the full purchase of Chemap and the introduction of the AX range of disc centrifuges (with their very high separating power).

The section in the report on legislation and organizational activities covers both international and national controls—from pressure being brought to bear on the UK in 1988 to stop dumping in the North Sea to the fragmented picture in West Germany and the traditionally liberated attitude in Southern Europe towards control of any kind.

CALL FOR PAPERS

Annual AIChE Environmental Division Student Award

1st Place—$300.00
2nd Place—$200.00
3rd Place—$100.00

Certificates and awards will be presented at the Summer National AIChE Meeting to be held in Philadelphia, Pennsylvania on August 20-23, 1989. The AIChE will also provide the 1st place winner with the lowest cost airfare and two (2) days accommodation for attendance at the awards presentation. In addition, the paper is intended for publication in *Environmental Progress.*

Contest Entry Rules:

a. The work must be a first paper (i.e., report on original unpublished work)
b. The paper must report on research or investigation related to an environmental program
c. The author must be the sole author and must be a full-time undergraduate student in a school with an accredited chemical engineering program
d. The student author must be a member of the student chapter of AIChE

Submit manuscript with cover letter by May 14, 1989, to the Second Vice Chairman of the Environmental Division:

Dr. Joseph J. Cramer
Stone & Webster Engineering Corporation
245 Summer Street—11th floor
Boston, MA 02107

Washington Environmental Newsletter

New EPA Administrator

As you probably know, President Bush has selected Bill Reilly of the Conservation Foundation and the World Wildlife Fund as the next EPA Administrator. His early confirmation by Congress is expected. Although a number of names for this post were being speculated on in Washington, Reilly's nomination has had broad support from environmental leaders, industry executives, state governors and other participants in environmental issues. It is generally felt that his record of accomplishments at the Conservation Foundation, his willingness to take on controversial issues, and his ability to build consensus should make him an outstanding choice for this demanding job. Following his confirmation, AIChE's Washington representatives will be meeting with him to continue the rapport that the Institute has enjoyed over the past years by submission of position papers and cooperative programs such as the CCPS projects, the Emergency Response Program., etc.

EPA Proposed as a Cabinet Level Department

New legislation that would raise EPA to the Cabinet level has been introduced by Sen. David. F. Durenberger (R. Minn.) and Sen. Frank R. Lautenberg (D. NJ). On the House side, the bill will be proposed by Rep. James Florio (D. NJ) and Rep. Sherwood Boehlert (R. NY). Durenberger said it is necessary to improve the relationship between the President and the head of EPA. We have long supported this concept, since EPA needs to be on an equal footing with other Cabinet departments—some of which are among the nation's biggest polluters. The legislation makes no changes in the structure of EPA, it just elevates the functions across the board. This newest bill addressing the issue seems to have more and broader bipartisan support than a similar bill proposed in June of 1988. Sponsors hope that action on the bill will be forthcoming early this year.

Science and Engineering Community Hopes for Bush Choice of Science Advisor

As this column goes to press, there are high expectations that President Bush will deliver on his promise to appoint a science advisor with rank of assistant to the President, and a council of science advisors. This is also an issue that has been supported by the Government Programs Steering Committee in concert with other professional engineering and scientific societies. If such an appointment comes about, the technical community will have a champion who has the President's ear and a better chance of having sound scientific and engineering principles included in high level decisions.

Proposed Institute for Pollution Prevention

AIChE, through its GPSC, in conjunction with the EPA Office of Pollution Prevention, SOCMA, academia, industry reps and environmental groups, is part of an ad-hoc group studying the feasibility of forming a private/public coalition which would establish a Pollution Prevention Institute. Funding for such an effort would come from government, industry and foundations. The proposed Institute would serve as a clearing house for source reduction research, technology transfer; sponsor national and international symposia on the issue of waste minimization, and other activities designed to address the problems of hazardous and solid waste prevention and management.

This material was prepared by AIChE's Washington Representative, Siegel • Houston & Associates, Inc. Suite 333,1707 L Street, N.W., Washington, D.C. 20036. Tel. (202) 223-0650

On the 1988 Environmental Division Student Paper Contest

by

Robert W. Peters

Energy & Environmental Systems Division, Argonne National Laboratory, 9700 South Cass Avenue Argonne, Illinois 60439

2nd Vice-Chairman, Environmental Division, AIChE

The 1988 American Institute of Chemical Engineers' (AIChE's) Environmental Division Student Paper Contest had eight entries submitted for the contest. The contest entry rules are listed below:

(1) The paper is the student's first paper (i.e., unpublished work).
(2) The paper pertains to research or an investigation related to an environmental topic.
(3) The student is a full-time undergraduate student in an accredited program.
(4) The student must be a member of the local student chapter of AIChE.

The award winners receive a monetary award of $300, $200, and $100 for the first, second, and third place winners, respectively, along with an award certificate commemorating their achievement.

Listed below are the eight papers that were submitted for this year's contest:

1. "Methylmethacrylate Vapor Suppression with CGAs," by Christopher Berrey, Virginia Polytechnic Institute and State University, Blacksburg, VA; Faculty Advisor: Donald L. Michelsen.
2. Safety Systems Management for Design of Hazardous Technologies," by Gabrielle V. Brown, California State University at Long Beach, Long Beach, CA; Faculty Advisor: Hamid Kavianian.
3. "Biosolubilization of Coal," by Loni M. Gibbs, Colorado State University, Fort Collins, CO; Faculty Advisor: Vincent G. Murphy.
4. "Use of Ligand-Modified Micellar-Enhanced Ultrafiltration in the Selective Removal of Metal Ions from Water," by Joseph Klepac, University of Oklahoma, Norman, OK; Faculty Advisor: John F. Scamehorn.
5. "Feasibility Study of Using TMP Sludge as Feedstock for the TVA Acid Hydrolysis Process", by Thomas M. McMillan, Mississippi State University, Mississippi State, MS; Faculty Advisor: George R. Lightsey.
6. "Electrophysical Sorption of Halogenated Aliphatic Solvents onto Soils", by Jonathan Mokrauer, Rutgers University, Piscataway, NJ; Faculty Advisor: David S. Kosson.
7. "An Analysis of the Dispersion of Dioxins in British Columbia", by Wendi L. Rottluff, University of British Columbia, Vancouver, British Columbia, Canada; Faculty Advisor: Joel L. Bert.
8. "Used Oil: Waste Processes", by Taunia S. Wilde, University of Utah, Salt Lake City, UT; Faculty Advisor; A. Lamont Tyler.

This collective group of papers was sent out for review to a Peer Review Committee consisting of 14 professional personnel involved in environmental operations. The compositional make-up of the committee involved the following: academia (6), consultants (3), national laboratories (2), and industry (3). The committee was asked to review each paper in regards to its:

(1) organization (clarity and logic)
(2) experimental (procedure and method)
(3) tables/figures (clarity, content, and style)
(4) technical content/merit (results and discussion)
(5) conclusions (justified)

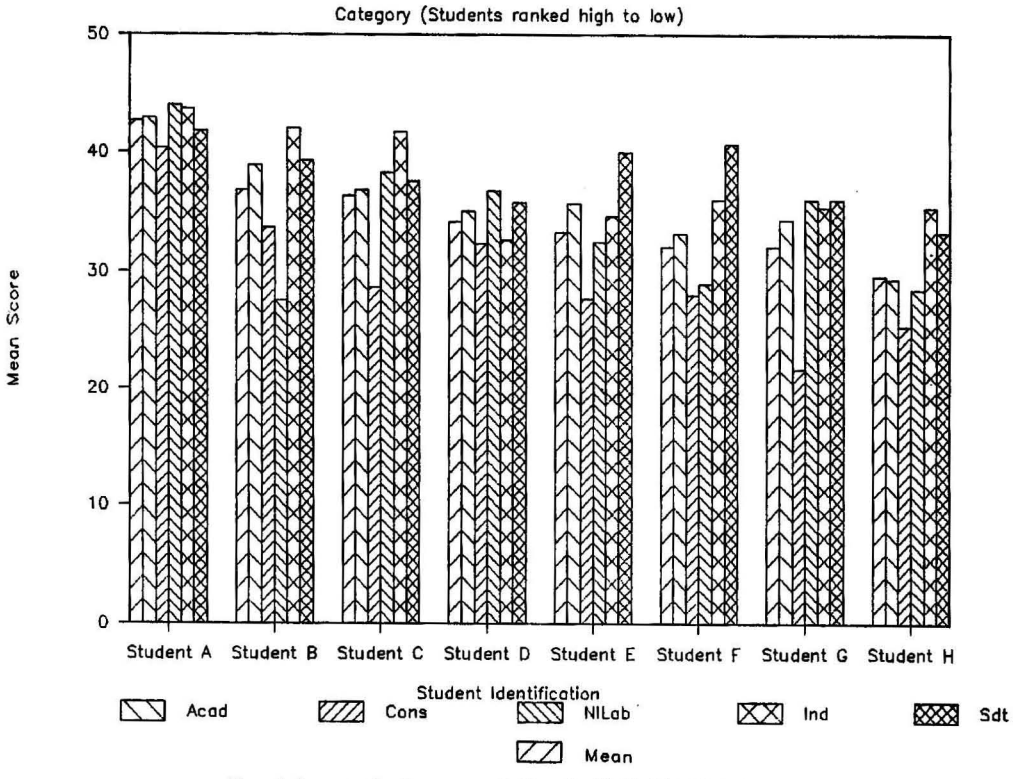

Figure 1. Summary of review paper evaluations classified by job sector category.

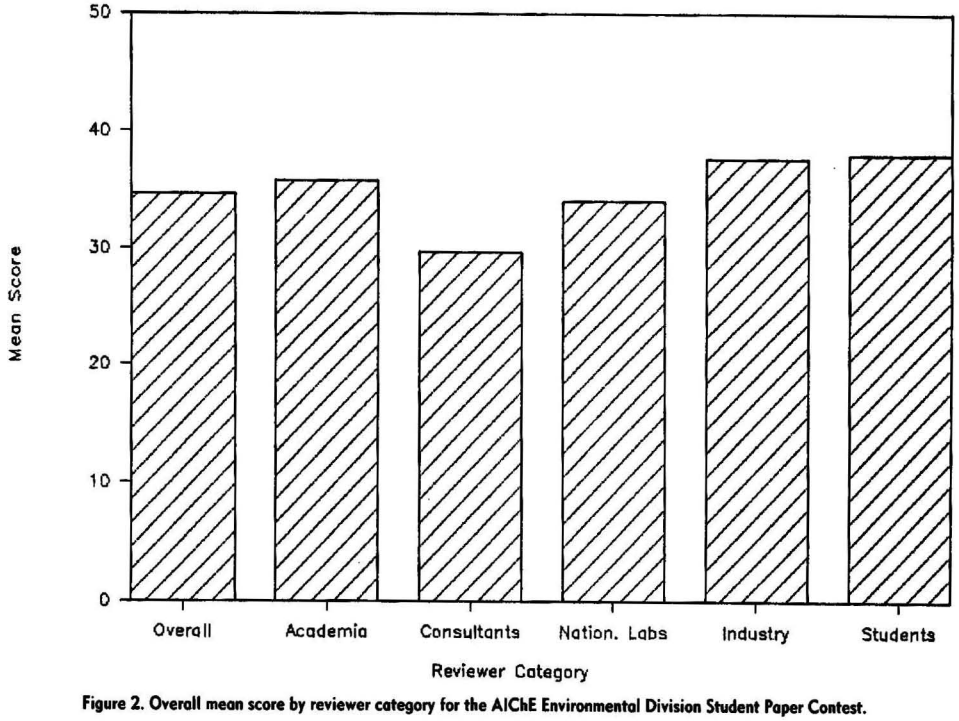

Figure 2. Overall mean score by reviewer category for the AIChE Environmental Division Student Paper Contest.

TABLE 1. SIGNIFICANT COMPARISONS BETWEEN JOB SECTOR EVALUATIONS

Student Identification	Job Sector Comparison	Level of Significance
Student B	Academia-National Laboratories	0.00191
	Students-National Laboratories	0.04895
Student C	Consultants-Industry	0.01776
Student F	National Laboratories-Industries	0.01920
	Students-Overall	0.00910
	Students-Academia	0.02997
	Students-Consultants	0.03731
	Students-National Laboratories	0.03431
Student H	Academia-Industry	0.03341
	Consultants-Industry	0.02803

Each of the papers were judged according to these five categories, providing a numerical score (of 10 points maximum) for each category. The sum of all five categories provided the total score for the paper (maximum score = 50 points). Each reviewer reviewed all eight papers.

For comparison purposes, the papers were also sent to each of the students for their own peer review of the papers (reviewing each paper except for their own paper) in accordance with the procedures developed for the Peer Review Committee.

The results of the individual evaluations, broken down by job sector, are shown graphically in Figure 1. The results of the evaluations are ranked according to score from high to low; the results presented in Figure 1 bare no resemblance to the alphabetical listing of the papers submitted, previously described. Inspection of the mean scores for each job sector group indicate the consultants tended to be more critical in their reviews; the mean scores tended to be lowest for this job sector (they gave the lowest mean score for 7 of the 8 papers). The highest scores tended to be given by the students and industry job sectors. These observations are confirmed in Figure 2, which lists the mean score (averaged over all eight papers) within a particular job sector group. There was quite a discrepancy between the groups concerning the ranking of any individual paper, although everyone agreed concerning which paper was the best. The discrepancy between the rankings is shown by the fact that academia, consultants, and industry rated one paper as the second best paper, while the national laboratories' personnel judged it to be the eighth best paper.

The mean results for each student paper were compared between the various job sector classifications using t-tests. For the majority of cases, the difference between the mean scores between the job sector categories were statistically insignificant (level of significance = 0.05). Those comparisons showing up as being statistically significant are summarized in Table 1. Due to the higher mean scores provided by the industrial personnel, those comparisons involving the industrial job sector tended to be statistically different from the other job sectors.

The eight papers submitted for the Environmental Division Student Paper Contest resulted in a very competitive contest. On the basis of the Peer Review Committee's evaluations, the award winners for this year's contest were: (1) Jonathan Mokrauer of Rutgers University, (2) Wendi Rottluff of the University of British Columbia, and (3) Joseph Klepac of the University of Oklahoma. These particular people, plus the other contestants, are commended for their very fine efforts and papers submitted for the contest. The top award paper appears immediately after this commentary on page 1 of this issue of *Environmental Progress*. The efforts of the Peer Review Committee proved to be especially helpful in choosing the contest winners. The scope and range of the papers submitted represents a diverse array of environmental topics being investigated. The number of excellent papers submitted shows an increased concern for our environment and our nation's resources within the chemical engineering community.

Electrophysical Sorption of Single Carbon Halogenated Solvents onto Soil

J. E. Mokrauer and D. S. Kosson
Department of Chemical and Biochemical Engineering,
Rutgers, The State University of New Jersey,
Piscataway, New Jersey

Sorption of halogenated single carbon organic contaminants onto a sandy loam has been found to be controlled by the electrostatic attraction between a slightly negatively (δ^-) charged clay particle and a positively (δ^+) charged carbon atom within the solvent molecule. Adsorption isotherms for chloroform, bromodichloromethane and methylene chloride indicate that the extent of sorption appears to have a direct functional relationship to the molecular charge distribution within the solvent molecule, and to the atomic radii of the molecular substituents of the contaminant. When a carbon atom is saturated with highly electronegative substituents (e.g. carbon tetrachloride), an electron cloud surrounds the molecule and shields the slightly positive (δ^+) carbon nuclei. This shielding effect limits the sorption that occurs. A study on carbon tetrachloride sorption resulted in no detectable sorption onto the sandy loam soil. This theory of adsorption is defined as Electrophysical Sorption (EPS) because it reflects the combination of electrostatic and physical contributions to sorption.

INTRODUCTION

Groundwater contamination from inappropriate disposal of hazardous and toxic chemicals poses a major environmental problem to the entire United States. Testing performed on public water supplies as a consequence of New Jersey Assembly Bill A-280 has shown chlorinated aliphatic hydrocarbons to be present as contaminants in many New Jersey potable water resources. To fully understand contaminant attenuation in groundwater systems, all related processes (i.e. sorption, reaction and dispersion) must be considered. Sorption most commonly involves the uptake of solutes (contaminants) by solid substrates (soil) [*1*]. The intent of this paper is to develop a mechanistic framework for the interpretation of contaminant partitioning in groundwater/soil systems.

As contaminated groundwater flows continuously through soil, some contaminants sorb to the surface of soil constituents, attenuating contaminant levels in the water. Furthermore, at equilibrium, for most priority pollutants, the concentration of contaminants in the soil phase is at least that of the aqueous phase. In turn, this yields an apparent concentration at the soil water interface that is greater than or equal to the aqueous phase concentration [*1*]. Current theories describe adsorption of contaminants in an aqueous soil system as partitioning between an organic soil phase and an aqueous phase [*2, 3, 4*]. However, recent studies on competitive adsorption of contaminants onto soil have produced results inconsistent with the pre-

A modified version of this paper won first place in the 1988 AIChE Environmental Division National Student Paper Competition.

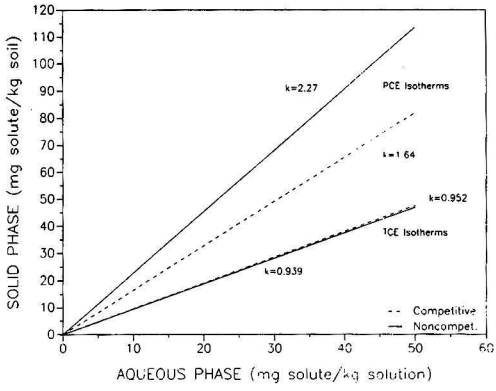

Figure 1. Competitive adsorption effects of a binary system.

vailing theory. Isotherms from the competitive adsorption of trichloroethylene (TCE) and tetrachloroethylene (PCE) onto the sandy loam observed during this study are presented in Figure 1. This data was generated using methods explained in subsequent sections of this paper. These results indicate that sorption of TCE is unaffected by the presence of PCE, in a binary system. For the single solute (noncompetitive) system the linear partitioning coefficient [k] for TCE was 0.939, whereas for the binary system (competitive) k = 0.952. This is not a significant difference. However, PCE sorption was significantly altered in the binary system, especially at higher aqueous phase concentrations. At PCE concentrations between 0.5 and 10 mg/l, the isotherm was relatively unchanged (Figure 2) and yielded a k = 2.48 compared to k = 2.27 for the single solute system. At PCE concentrations greater than 10 ppm, k approached 1.41, i.e., competitive effects were observed.

The accepted theory predicts no competitive effects for the simultaneous uptake of these solutes (pollutants). In fact, it treats the partitioning of contaminants between soil phases and water in a manner similar to that of an organic solvent extraction [2, 3, 4]. The study described in this paper was carried out to develop a new model for the mechanism of adsorption, to assist in the analysis of such cases. The model is based on the physical and electronic differences among adsorbing molecules. Chemical differences were ignored because no reaction occurs during the limiting time period of simple adsorption.

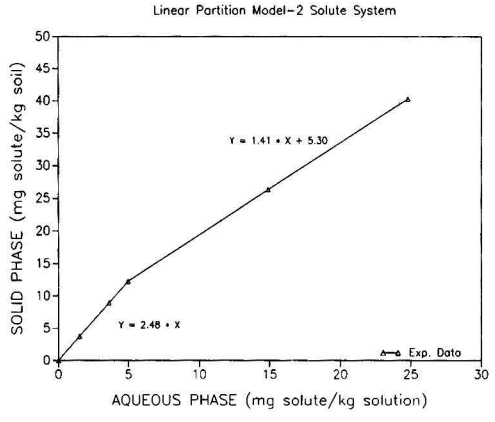

Figure 2. Adsorption of tetrachloroethylene.

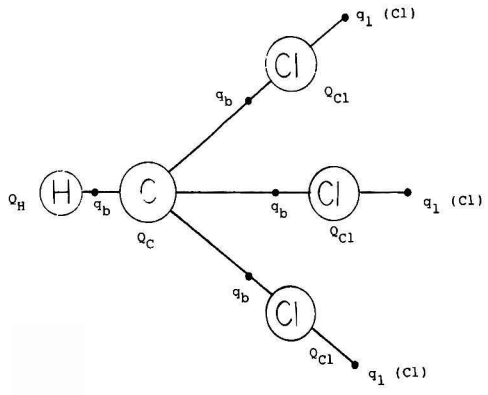

q_b = bond charge

Q_{Cl} = chlorine atomic charge

Q_C = carbon atomic charge

Q_H = hydrogen atomic charge

q_l = lone pair charge

Figure 3. New point charge model [8].

EPS THEORY AND QUANTIFICATION

The clay mineral constituents of soil were chosen as the basis of the sorption theory because of high surface area and sorptive capacity [5]. Soils chosen for experimental verification were selected based on relatively low soil organic matter content. In addition, recent experimentation has shown aqueous adsorption of fluridone (herbicide) to be related not only to organic matter but also to clay content [6]. A plausible explanation for this is that, an electrostatic attraction exists between slightly negatively (δ^-) charged silicate clay molecules and slightly positively (δ^+) charged carbon atoms. The slightly negative charge on the clay surface is a result of (*i*) unsaturated valence states surrounding the exterior of the molecule, and (*ii*) exposed oxygen and hydroxyl groups that behave as negatively charged active sites [5]. The slight positive charge on contaminant carbon atoms results from highly electronegative substituents, e.g., chlorine atoms, attached to the carbon atom. In general, the greater the electronegativity and frequency of substitution of such substituents, the higher the local charge (δ^+) on the carbon atom. When the two charged particles are present in the same system, an electrostatic attraction between a δ^+ carbon atom and a δ^+ clay particle acts to bind the contaminant to the surface of

TABLE 1. CALCULATED Q VALUES FOR ATOMS (charge eV)

	Q_H	Q_C	Q_{Cl}
CH_2Cl_2	0.203	0.038	0.029
$CHCl_3$	0.203	0.263	0.029
CCl_4	—	0.488	0.029

$q_b = 0.0$

$q_l = -0.051$

Covalent Atomic Single Bond Radii (A)

Carbon = 0.77 Hydrogen = 0.30 Chlorine = 0.99

soil particles. Analogous theories have been used to explain cation adsorption to clays [7]. Consequently, in the EPS theory, the greater the δ^+ charge on the carbon the greater the tendency to sorb. However, when the carbon atom is saturated with highly electron withdrawing groups other effects should be seen. The electronegative substituents surrounding the carbon atom create an electron cloud resulting in a negative shielding effect that leads to anion repulsion rather than the expected attraction.

CHARGE QUANTIFICATION

To quantify the δ^+ charge on the carbon atom(s) of the molecules studied, the 'New Point Charge Model' was used [8]. In this model, atoms, bonds, and lone pairs are all compressed to point charges according to their electron density, as illustrated in Figure 3. The calculation of the point charges on the molecules is carried out with measurable dipole moments and core binding energies [8]. Unfortunately, these charges on the atom do not correspond to traditional atomic charges. To calculate the δ^+ charge (Q_a), q_l and the atom's share of q_b (bond charge) must be added to the atom point charge. This share is inversely proportional to the ratio of the covalent atomic radii of the atoms [8]. Accurate values for q_b are not available. As outlined by Coppens [8], q_b can be assumed to be zero, although lesser accuracy is the result. Table 1 illustrates values for the respective charges; covalent atomic radii also are provided for three of the molecules studied [8, 9].

In addition to these electronic effects, the size of the carbon substituents should play a major role in the adsorption of certain organic contaminants. The larger the substituent, the smaller the area available for attachment to the soil and increased hindrance should occur. The ratio of the atomic covalent radii of the substituents has been used to quantify these physical effects on sorption.

Correlating both the electronic and physical factors to sorption yields the EPS equation:

$$K_a/K_b = (Q_{ac}/Q_{bc})/\prod_{i=1}^{n} (r_{ai}/r_{bi}) \quad (1)$$

where a and b represent the respective contaminants, k_a represents the partitioning coefficient of contaminant a, Q_{ac} represent the charge on the carbon atom of contaminant a, n represents the number of substituents, represents the product of the contaminants present and r_{ai} represents the atomic covalent radii of substituent i on contaminant a.

Isotherm Model

To explore the EPS theory experimentally, the relative sorptive capacities of single carbon contaminants were determined. To correlate the results of sorption measurements, data for each solute was regressed to a form of the Freundlich model. The model is an empirical equation that takes the form:

$$q = k \cdot c^{1/n} \quad (2)$$

where q is mg of solute per kg of soil, c is mg of solute per kg solution, k is the partitioning coefficient between water and soil; lastly, n is the linearity constant. This model suggests that the energy of sorption decreases logarithmically as the fraction of surface covered increases [10]. A major problem with this model is that the slope of the isotherm should be finite at infinite dilution but is not unless n is equal to one [11].

The linear partition model is the Freundlich model with n = 1. It has the form:

$$q = k \cdot c \quad (3)$$

In the area of soil chemistry, this is the case for model adsorption onto soils and clays. As a result, all adsorptions studied were fit to this model.

EXPERIMENTAL AND ANALYTICAL METHODS

The following experimental procedures were used to quantify sorptive interactions of solute species (methylene chloride, chloroform, carbon tetrachloride, bromochloromethane and bromodichloromethane) with a sandy loam soil. This soil was assayed and found to have the following composition on a mass basis: 72% sand, 16% silt, 12% clay, and 1.8% organic matter. Initially, bottles were filled with sifted, air-dried soil and water and sealed with teflon/silicon septa. Solute in methanol solution was injected, to attain concentrations of 2, 5, 10, 50, 100, and 200 ppm (within the solubility limit of all solutes used). Competition for sites between methanol and solute has been found to be minimal at low methanol concentrations (0.1% in this case) [10]. Each concentration was run in duplicate, together with controls. Care was taken to minimize head space in all samples and controls, to avoid vapor losses.

Samples were placed on an isothermal (25°C) shaker for at least 24 hours, at 250 rpm, to allow close approach to equilibrium. Following equilibration and centrifuging, the aqueous phase was extracted with pentane and analyzed.

The equilibration time was calculated from a kinetic study in which bottles filled with water, soil, and TCE were placed on a shaker, at 250 rpm, and taken off at regular intervals. Aqueous phase TCE concentration as a function of time was plotted; see Figure 4. The curve leveled off after approximately one hour and adsorption was assumed to be complete at this time; longer times were used to insure equilibrium.

After shaking, soil samples were centrifuged at 3500 rpm for 4.0 hours to prepare them for extraction into pentane. Next, the aqueous phase was sampled and syringe filtered into an equal amount of chilled (4°C) pentane. Syringe filtration was utilized to minimize any losses through volatilization. This extraction step was the highest error generating procedure in the experimentation (9.4%), necessitating six extractions for each sample. An experiment, carried out using known amounts of halogenated hydrocarbons, pentane, and water to test this extrac-

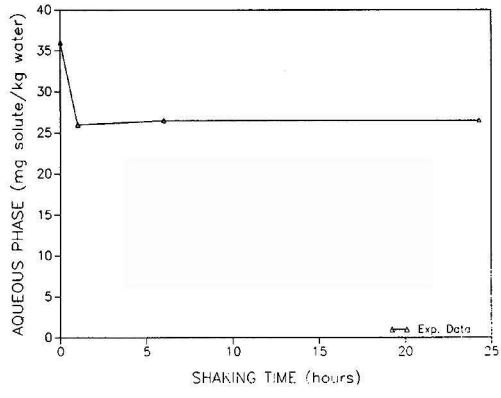

Figure 4. Equilibration time.

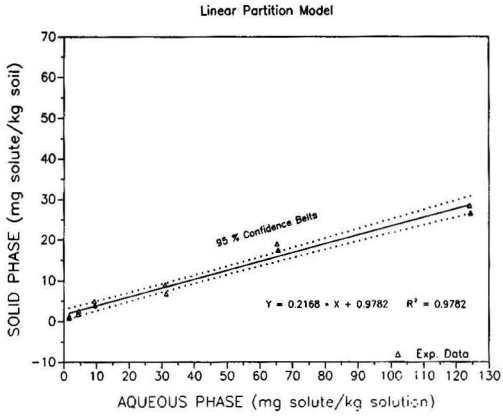

Figure 5. Adsorption of methylene chloride.

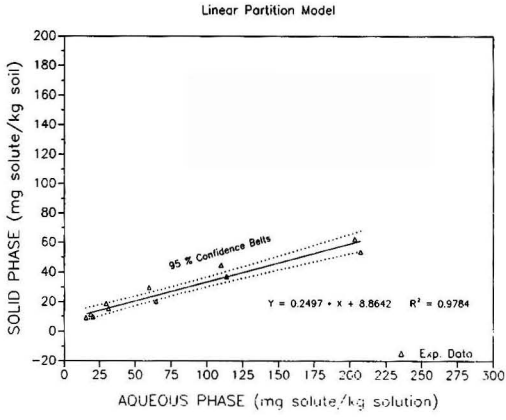

Figure 7. Adsorption of bromochloromethane.

tion procedure attained recovery in the pentane phase of greater than 97%.

Solute concentrations in pentane from the extraction step were determined using a Hewlett Packard 5890A Gas Chromatograph (GC) equipped with an O.I. Model 4420 electrolytic conductivity detector (ELCD) and a 1% SP-1000 60/80 Carbopack stainless steel column. The GC utilized an 4-minute isothermal run at an oven temperature of 200°C, an injection temperature of 210°C and a detector temperature of 210°C. The detection limit for this method was less than or equal to 300 ppb for all halogenated hydrocarbons.

Gas chromatograph output peak areas were compared to a standard curve to calculate aqueous phase solute concentrations. Standards for the development of standard curves were prepared in HPLC grade n-pentane on a volumetric basis. Data for the standard curves was linearly regressed and used to calculate sample solute concentrations. These concentrations were normalized for variance in water weight in each bottle. A total solute mass balance was utilized to calculate the concentration of sorbate on soil. The difference between the blank concentration and the aqueous phase concentration was the amount adsorbed. This concentration was renormalized for variance of soil weight in each bottle. Reduction of solute in the soil sample via degradative mechanisms was ignored due to the short duration of this experiment.

RESULTS OF SINGLE CARBON SPECIES ADSORPTION

Data for the sorption of methylene chloride and chloroform in single solute systems was regressed to the linear partition model; see Figure 5 and 6. The linear regression confirmed that the data was linear over a broad range of aqueous concentrations. The dotted lines on the graphs indicate 95% confidence belts. Partition coefficients (slopes) of 0.22 for methylene chloride and 0.47 for chloroform were observed. Thus, the sorptive loading of chloroform onto a sandy loam is about 2.1 times that of methylene chloride. As noted above, theoretically the extent of sorption should have a direct functional relationship with the intensity of the charge on the carbon atom and an inversely proportional relationship with the atomic radii of the substituents. This charge, as calculated, was 0.038 and 0.263 for the carbon in methylene chloride and in chloroform, respectively. This results in a charge ratio between chloroform and methylene chloride of 6.92. The only substituent difference between the two molecules is the replacement of one hydrogen atom in methylene chloride with a chlorine atom in chloroform. Chlorine, with an atomic radius of 0.99 Angstroms, has a radius of 3.33 times that of hydrogen [9]. Solution of the right side of the EPS equation (Equation (1)) yields a value of 2.07. This calculated value comparing favorably

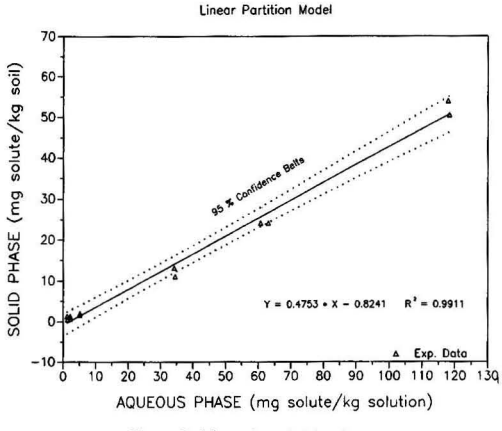

Figure 6. Adsorption of chloroform.

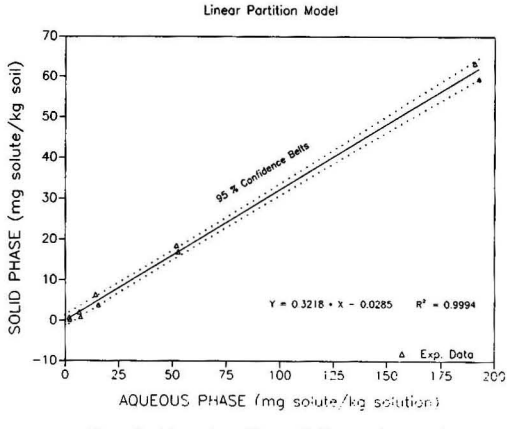

Figure 8. Adsorption of bromodichloromethane.

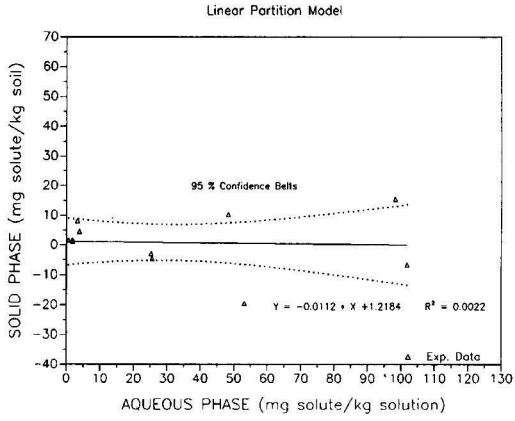

Figure 9. Adsorption of carbon tetrachloride.

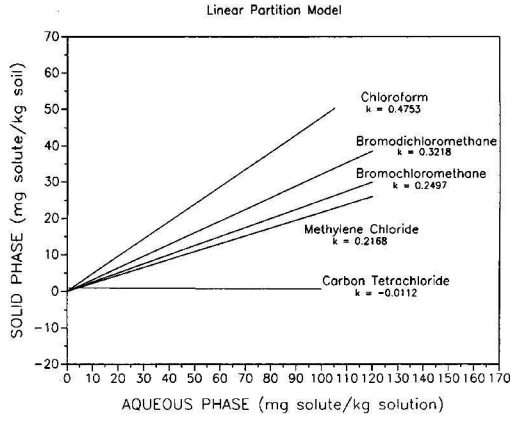

Figure 10. Adsorption of single carbon species.

to the measured adsorption ratio of 2.13, illustrating the direct relationship between the electronic/physical characteristics and the sorptive capacity of the solute molecule.

Although not prevalent in contaminated groundwater systems, both bromochloromethane and bromodichloromethane sorption was investigated to further support the EPS theory. Data for the sorption of these compounds was regressed to the linear partition model; see Figure 7 and 8. The linear isotherms have partitioning coefficients of 0.3218 for bromodichloromethane and 0.2497 for bromochloromethane. As a less electronegative and larger atom than chlorine, a bromine substituent should cause a molecule to sorb less than a chlorine substituent. Comparison of the partitioning coefficients of chloroform (k = 0.4753) and bromodichloromethane (k = 0.3218) illustrates this concept. However, data for bromochloromethane (k = 0.2497) and methylene chloride (k = 0.2168) was inconclusive. The partitioning coefficient for bromochloromethane was 0.03 greater than methylene chloride, but when evaluated statistically no significant difference was observed.

Data for sorption of carbon tetrachloride onto a sandy loam was also regressed on the linear partition model, see Figure 9. Actually, in this experiment no sorption occurred. This is consistent with the hypothesis that electrostatic shielding created by the surrounding chlorine atoms creates anion repulsion between a δ^- soil particle and the CCl_4 molecule. Note, the electronegativity of chlorine and carbon are 3.0 and 2.5, respectively [*12*]. In addition, the carbon is surrounded with chlorine atoms (large substituents) that physically hinder attachment of the solute on the soil. With both the physical size and the electronic shielding factors, the carbon tetrachloride molecule has no ability to sorb. The EPS equation was solved for chloroform and carbon tetrachloride with one modification. For carbon tetrachloride, the sum of the chlorine charges (including lone pair charges) was used for Q_{ac} to account for the envelope of charge shielding the positive charge of the carbon. The value of −0.10 yielded by the equation is very close to the experimental value of −0.01 which was shown to be statistically no different than zero.

A comparison of sorptive data for all the compounds in Figure 10 supports the EPS theory.

CONCLUSION

Electrostatic attraction between a δ^- charged clay particle and charged carbon atom is hypothesized to be the driving force for sorption of halogenated organic contaminants onto a sandy loam. In addition, the extent of sorption was found to be directly proportional to the molecular charge distribution on the contaminant and inversely proportional to the atomic radii of large substituents on the carbon atom. At total saturation of the carbon with highly electronegative substituents, sorption does not occur. The geometric arrangement of substituents around the carbon atom induces a cloud of negative charge which repels negatively charged soil particles.

ACKNOWLEDGMENT

This work was funded in part by the New Jersey Hazardous Substances Management Research Center (Project SITE-12).

LITERATURE CITED

1. Smith, J. M., *Chemical Engineering Kinetics*, McGraw-Hill Book Company, New York, 1981.
2. Chiou, C. T., D. W. Schmedding and M. Manes, *Environmental Science Technology*, 684, 1982.
3. Chiou, C. T., in "Hazard Assessment of Chemicals: Current Developments," J. Saxema and F. Fisher, Eds., Academic Press (New York), Vol. 1, 1981.
4 Chiou, C. T., P. E. Porter and D. W. Schmedding, "Partition Equilibrium of Nonionic Organic Compounds Between Soil Organic Matter and Water," *Environmental Science Technology*, Vol. 17, No. 4, 1983.
5. Brady, N. C., *The Nature and Properties of Soils*, Macmillan Publishing Company Incorporated, New York, 1974.
6. Weber, J. B., "Fluridone Retention and Release in Soils," *Soil Science Society of America Journal*, volume 50, No. 3, 1986.
7. Nir, Shlomo, "Specific and Nonspecific Cation Adsorption to Clays: Solution Concentrations and Surface Potentials," *Soil Science Society of America Journal*, volume 50, No. 1, 1986.
8. Coppens, P. and M. B. Hall, *Electron Distributions and the Chemical Bond*, Plenum Press, New York (NY), 1982.
9. Griswold, E., *Chemical Bonding and Structure*, Raytheon Education Company, New York, 1968.
10. Ollinger, W., "Thermodynamic and Topological Descriptors for the Sorptive Interactions Between Organic Solutes and Apolar Sorbents," *Doctoral Dissertation: Rutgers—The State University*, New Brunswick (NJ), May 1986.
11. Dzombak, D. A., "Estimating Adsorption of Polycyclic Aromatic Hydrocarbons on Soils," *Soil Science*, Vol. 137, No. 5, May 1984.
12. Wingrove, A. S. and R. L. Caret, *Organic Chemistry*, New York (NY), 1980.

Destruction of Aromatic Pollutants by UV Light Catalyzed Oxidation with Hydrogen Peroxide

D. W. Sundstrom, B. A. Weir, and H. E. Klei

Department of Chemical Engineering, The University of Connecticut, Storrs, CT 06268

Toxic and hazardous compounds are often present in water at low concentrations, which can make their removal difficult and costly by conventional treatment processes. A promising method for destroying pollutants in water is ultraviolet (UV) catalyzed oxidation by hydrogen peroxide. The effectiveness of this process was determined for typical aromatic compounds including benzene, toluene, chlorobenzene, phenol, 2-chlorophenol, 2,4-dichlorophenol, 2,4,6-trichlorophenol, dimethyl phthalate, and diethyl phthalate. The reactions were conducted in a quartz annular reactor equipped with a low-pressure mercury lamp. Of the aromatics studied, reaction rates were fastest with 2,4,6-trichlorophenol and slowest with the phthalates. Analyses of reacted samples by HPLC and GC/MS indicated that the aromatics formed many intermediates that could be destroyed by extending the treatment time. An empirical rate expression was developed to correlate the results.

INTRODUCTION

Toxic and hazardous organic compounds are often present in industrial discharges and water supplies. Removal of these compounds may be difficult and costly, especially if very low concentration levels must be achieved. Packed-bed aeration and activated carbon adsorption are common methods for removing residual organic compounds from water. Aeration is only useful for volatile compounds, and adsorption is ineffective with some types of organic molecules. In addition, both techniques are non-destructive, unless followed by thermal or other treatment.

An alternative treatment method for organic pollutants in water is chemical oxidation catalyzed by ultraviolet (UV) light. The UV photons enhance the rate of reaction by producing reactive species from the oxidant. The combination of ozone and UV light has proven effective with many types of aliphatic and aromatic compounds [*1–4*]. The cost of UV/ozone treatment depends upon the type and concentration level of the pollutant, and on the degree of removal required. Fletcher [5] has reported treatment costs from about $0.25/1,000 gal for slightly contaminated groundwater to about $40/1,000 gal for highly contaminated industrial wastewaters. Ozone is an unstable gas that must be generated on site and transferred into

the liquid phase. Ozone generation is also expensive at low production levels.

Hydrogen peroxide is also an effective oxidizing agent for UV catalyzed reactions. It can be stored for use according to process demand, is readily mixed with water, and is less sensitive than ozone to scale of operation. The absorption of UV photons by hydrogen peroxide dissociates it into hydroxyl radicals that attack organic molecules by abstracting hydrogen atoms or by adding to double bonds. Under suitable operating conditions, the final products are water, carbon dioxide, and low molecular weight aliphatic acids, such as acetic and oxalic. Until recently, most studies of the peroxide/UV process have involved acetates, explosives, organic acids, and process water contaminants [6–9].

BACKGROUND

Sundstrom et al. [*10*] studied the destruction of typical halogenated aliphatics by the combination of UV light and hydrogen peroxide. The chlorinated compounds with carbon-to-carbon double bonds, such as trichloroethylene, degraded much faster than the other compounds studied. The reacted chlorine was converted quantitatively to chloride ion, indicating that the chlorinated structures were effectively destroyed.

Weir et al. [*11*] studied the effects of process operating conditions on the destruction of benzene by UV and hydrogen peroxide. The rates of reaction were strongly affected by the concentration of hydrogen peroxide and the intensity of UV radiation. Many reaction intermediates were formed, but they could be eliminated by extending the treatment time.

Hager et al. [*12–14*] have developed pilot-plant and commercial-scale water treatment systems for the UV catalyzed hydrogen peroxide process. Groundwater at several sites contaminated with mixtures of hazardous aliphatic compounds were treated in pilot scale equipment [*14*]. Initial concentrations of 1 to 9,000 mg/l were reduced below regulatory levels in less than 60 min residence time. Hydrogen peroxide was fed at rates from 7 to 300 mg/l-min and UV output from the lamps varied from 160 to 590 watts/l. Based on these results, treatment costs were estimated to range from $1.37/1,000 gal for low levels of contaminant (1 mg/l) to $58.51/1,000 gal for concentrated leachates (9,000 mg/l). In a separate study [*13*], groundwater contaminated with 1 to 10 mg/l trichloroethylene was purified at estimated treatment costs of $0.68 to $1.95 per 1,000 gal. Hager et al. [*14*] report the installation of two UV/peroxide groundwater systems treating 60,000 gal/day and 600,000 gal/day, respectively. As another promising application of this technology, Hager et al. [*12*] suggest destroying concentrated organic contaminants in condensate from steam regeneration of activated carbon.

The encouraging results from UV catalyzed treatment of contaminated water suggest the need for further studies to define the effectiveness of this process on a wide range of priority pollutants in water. The purpose of this research was to examine the destruction of typical aromatic pollutants in water by the UV/peroxide process. The priority pollutants studied were benzene, toluene, chlorobenzene, phenol, 2-chlorophenol, 2,4-dichlorophenol, 2,4,6-trichlorophenol, dimethyl phthalate, and diethyl phthalate. The three monosubstituted benzenes were selected to examine the effect of a single substituent group on the rate of reaction of benzene. The effect of adding chlorine atoms to a ring was explored through the series of chlorophenols. Finally, the phthalate esters were studied because they are commonly found in industrial discharges.

EXPERIMENTAL METHODS

The experiments were conducted in a recirculating flow reactor system, which has been previously described [*11*]. The annular reactor consisted of two 20 cm quartz tubes with inner and outer diameters of 2.5 cm and 5.4 cm. A low-pressure ultraviolet lamp of 1.6 cm diameter was located within the inner tube. The lamp had an output of about 5.3 watts at 254 nm. Since the output of a UV lamp varies with temperature, the lamp surface was maintained at 40°C by a stream of air. The UV radiation passed radially through the annular region containing the reacting liquid.

The reactor was operated in a recirculating mode by pumping the solution from a reservoir through the reactor and back to the reservoir. Liquid temperature was controlled at 25°C, and pH was maintained at 6.8 by a phosphate buffer. The aromatics were dissolved in buffer and added to the reactor system along with the desired amount of hydrogen peroxide. The liquid volume in the system was brought to 3,300 ml and the UV lamp was turned on. For some runs, a small amount of solution was circulated through a flow cell in a spectrophotometer set at 254 nm.

Samples from the reactor were analyzed for pollutant concentration by injection into a Gow-Mac gas chromatograph equipped with a flame ionization detector. The column was packed with 3% SP-1500 on 80/120 mesh Carbopack B. Hydrogen peroxide concentrations were determined by a glucose oxidase-peroxidase method.

Samples from a few runs were analyzed for reaction intermediates by high performance liquid chromatography (HPLC) and by GC/MS. For HPLC analyses, samples were acidified, extracted into ethyl acetate, and dried. The residue was dissolved in methanol and analyzed by a Waters HPLC using a C_{18} Radial-Pak column. The GC/MS samples were prepared by the same extraction procedure used for HPLC and were analyzed by a Hewlett-Packard system with a cross-linked dimethyl silicone capillary column.

RESULTS AND DISCUSSION

Effect of UV and H_2O_2

The aromatic compounds studied were benzene, toluene, chlorobenzene, phenol, 2-chlorophenol, 2,4-dichlorophenol, 2,4,6-trichlorophenol, dimethyl phthalate, and diethyl phthalate. A previous study with benzene [*11*] showed the major process variables influencing reaction rates were the molar ratio of hydrogen peroxide to pollutant and intensity of UV radiation. Here, the intensity of the UV lamp was set at its maximum value (5.3 watts) and the molar ratio of peroxide to pollutant was varied. The initial concentration of pollutant in water was about 0.2 mM for each run.

The effect of hydrogen peroxide to pollutant ratio on rates of reaction is illustrated for benzene, phenol, 2,4,6-trichlorophenol, and diethyl phthalate in Figures 1 to 4. With UV light alone, a moderate rate of reaction was observed for all of the compounds studied, except the phthalates. The combination of hydrogen peroxide and UV light was much more effective than UV alone in destroying the compounds, except for 2,4,6-trichlorophenol. The aromatic compounds are attacked by both UV photons and hydroxyl radicals generated from the hydrogen peroxide. As the molar ratio of peroxide to pollutant is increased, more hydroxyl radicals are available to attack the aromatic structures and the rates of reaction are increased.

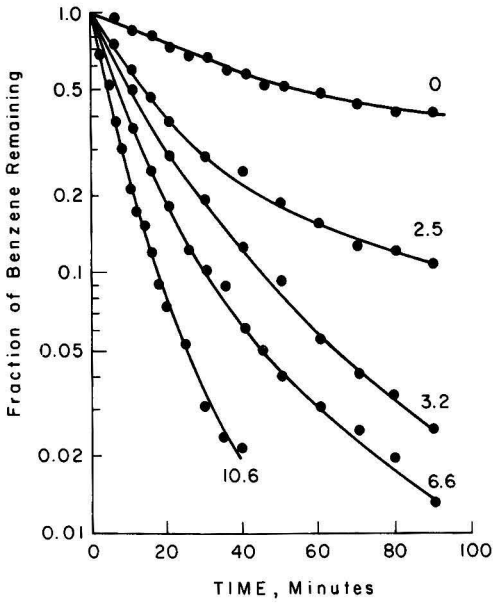

Figure 1. Effect of initial molar ratio of H_2O_2 to benzene on decomposition of benzene at 25°C and pH 6.8. Initial benzene = 0.2 mM.

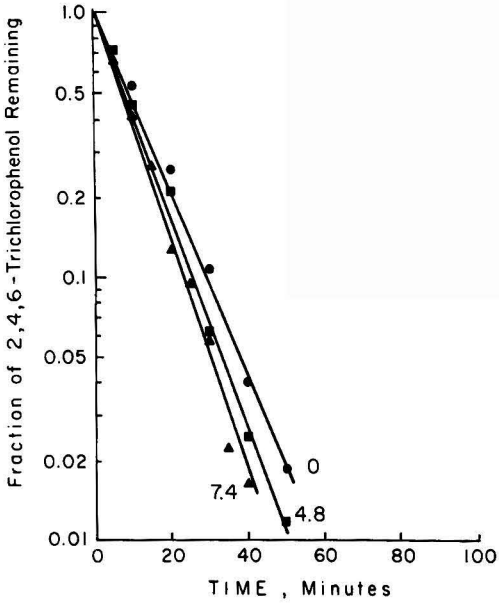

Figure 3. Effect of initial molar ratio of H_2O_2 to 2,4,6-trichlorophenol on decomposition of 2,4,6-trichlorophenol at 25°C and pH 6.8. Initial 2,4,6-trichlorophenol = 0.2 mM.

A comparison of the rates of reaction of benzene and monosubstituted benzenes at a peroxide to pollutant ratio of 7 is shown in Figure 5. The rates of reaction are of similar magnitude for these four aromatics, suggesting that the substituent groups have a small effect on attack of a benzene ring by UV plus hydrogen peroxide. With UV light alone, all of the reaction rates were much lower, especially in the case of phenol.

The hydroxyl radical acts as an electrophilic reagent in its attack of a benzene ring. The presence of electron-donating groups such as OH on an aromatic ring is known to activate the ring for electrophilic substitution reactions. Thus, phenol is more susceptible to electrophilic attack by hydroxyl radicals than benzene so that the presence of hydrogen peroxide accelerates the phenol reaction more than the benzene reaction.

The rates of reaction of phenol and chlorinated phenols are compared in Figure 6. With both UV light and hydrogen peroxide, phenol, 2,4-dichlorophenol and 2,4,6-trichlorophenol had similar reaction rates, but 2-chlorophenol reacted at a slower rate. As shown in Figures 2

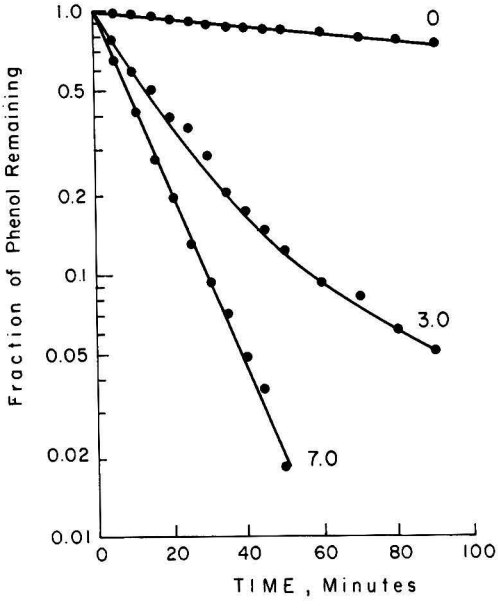

Figure 2. Effect of initial molar ratio of H_2O_2 to phenol on decomposition of phenol at 25°C and pH 6.8. Initial phenol = 0.2 mM.

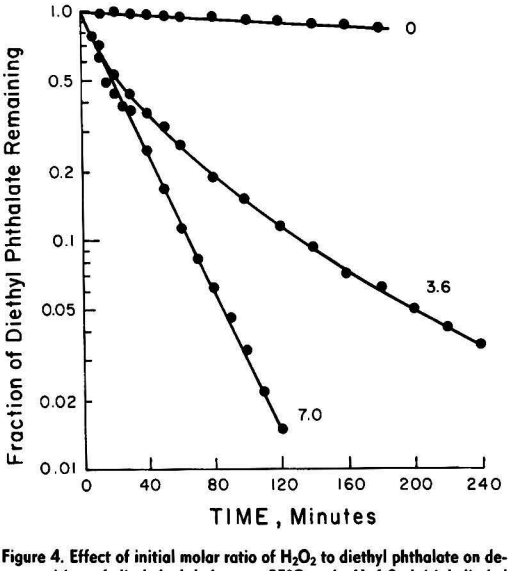

Figure 4. Effect of initial molar ratio of H_2O_2 to diethyl phthalate on decomposition of diethyl phthalate at 25°C and pH 6.8. Initial diethyl phthalate = 0.2 mM.

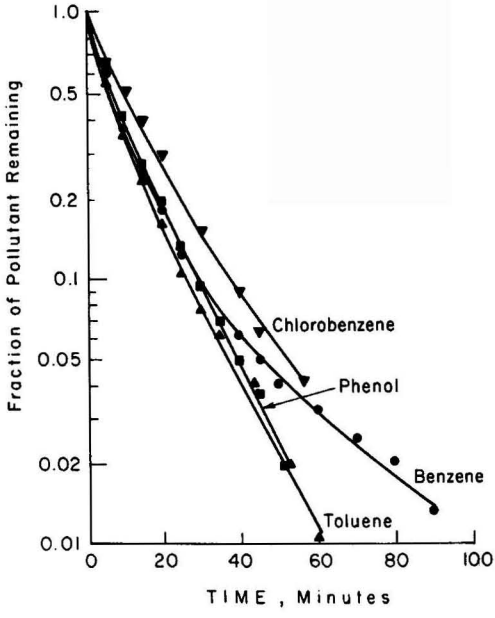

Figure 5. Comparison of rates of reaction of benzene, toluene, chlorobenzene, and phenol at 25°C and pH 6.8. Initial H_2O_2/pollutant = 7 mols/mol. Initial pollutant = 0.2 mM.

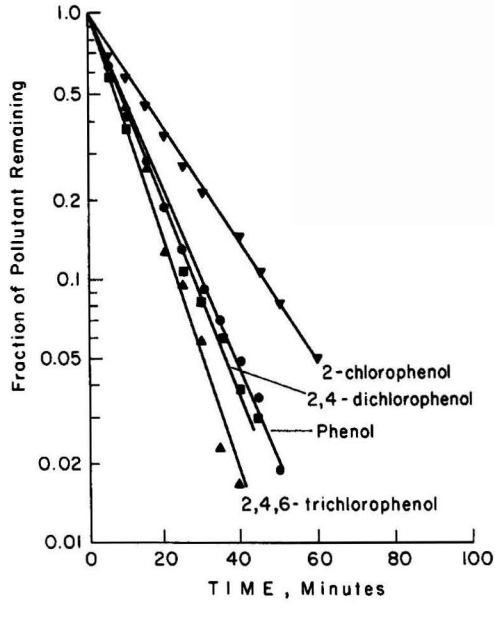

Figure 6. Comparison of rates of reaction of phenol, 2-chlorophenol, 2,4-dichlorophenol, and 2,4,6-trichlorophenol at 25°C and pH 6.8. Initial H_2O_2/pollutant = 7 mols/mol. Initial pollutant = 0.2 mM.

and 3, the combination of UV light and hydrogen peroxide was much more effective than UV only in destroying phenol. However, the presence of hydrogen peroxide had little effect on the reaction rate of 2,4,6-trichlorophenol.

The rates of reaction of dimethyl phthalate and diethyl phthalate were virtually identical at any given set of operating conditions. The phthalates were the slowest reacting compounds studied and were especially unreactive with UV light only (Figure 4).

Comparison of Reaction Rates

Most of the semi-log plots of pollutant concentration were nearly linear over the initial 20 to 30 minutes of reaction, suggesting first order reactions. The decreasing slopes at later times might result from decreasing hydrogen peroxide concentrations and from increasing reaction intermediates that absorb UV light and compete for hydroxyl radicals.

TABLE 1. PSEUDO FIRST ORDER RATE CONSTANTS FOR DESTRUCTION OF AROMATIC POLLUTANTS BY UV ALONE AND BY UV PLUS 7 MOLES HYDROGEN PEROXIDE PER MOLE OF POLLUTANT.

Pollutant	k, min^{-1} UV Alone	k, min^{-1} UV+H_2O_2	$\frac{k(UV+H_2O_2)}{k\ (UV\ alone)}$
Benzene	0.015	0.085	5.7
Chlorobenzene	0.025	0.063	2.5
Toluene	0.023	0.094	4.1
Phenol	0.0035	0.082	26
2-chlorophenol	0.015	0.050	3.3
2,4-dichlorophenol	0.043	0.081	2.0
2,4,6-trichlorophenol	0.078	0.100	1.3
Dimethyl phthalate	0.001	0.045	45
Diethyl phthalate	0.001	0.047	47

TABLE 2. RATE CONSTANTS AND REACTION ORDERS FOR DESTRUCTION OF AROMATIC POLLUTANTS.

Pollutant	k_u	k_p	a	b	c
Benzene	7.6×10^{-6}	3.0×10^{-4}	2.4	1.0	0.82
Chlorobenzene	2.3×10^{-3}	2.5×10^{-6}	1.5	1.2	1.3
Toluene	2.2×10^{-4}	2.0×10^{-3}	1.9	1.1	0.45
Phenol	3.5×10^{-3}	9.7×10^{-4}	1.0	1.0	0.62
2-chlorophenol	1.5×10^{-2}	5.0×10^{-7}	1.0	0.74	1.7
2,4-dichlorophenol	4.3×10^{-2}	1.1×10^{-3}	1.0	0.96	0.51
2,4,6-trichlorophenol	7.8×10^{-2}	3.5×10^{-5}	1.0	0.93	0.92
Dimethyl phthalate	6.5×10^{-4}	7.8×10^{-5}	1.0	0.96	0.94
Diethyl phthalate	8.6×10^{-4}	2.8×10^{-6}	1.0	0.80	1.5

First order rate constants were calculated from the initial linear regions of the semi-log plots. Table 1 lists the rate constants for reactions with UV only and with UV plus 7 moles of peroxide per mole of aromatic. Since reaction mechanisms are complex and reaction intermediates interfere, these values should be considered as pseudo or apparent first order rate constants. The last column in Table 1, which gives the ratio of the rate constant for UV plus peroxide to the rate constant for UV only, provides a measure of the degree of enhancement due to hydrogen peroxide.

The rate constants show that the phthalates were the slowest reacting compounds and that 2,4,6-trichlorophenol had the fastest reaction rate. The synergistic effect of UV light and hydrogen peroxide was most pronounced for phenol and the phthalates. With UV light only, the addition of substituent chlorine atoms to phenol enhanced the susceptibility of the aromatic ring to attack by UV photons. In the presence of both UV light and peroxide, the effect of the hydrogen peroxide on reaction rates became less significant as chlorine atoms were added to the phenol. The last column in Table 1 shows that the reaction rate for phenol is about 26 times greater with peroxide present, whereas the reaction rate of 2,4,6-trichlorophenol is only increased about 30% by hydrogen peroxide.

Correlation of Results

The rates of reaction were correlated by an empirical rate expression because rate laws based on postulated reaction mechanisms were not able to predict the rate behavior.

$$r_p = k_u C_p^{\,a} + k_p C_p^{\,b} C_h^{\,c} \qquad (1)$$

where r_p = reaction rate of pollutant, μ mol/l-min
k_u = rate constant with UV light only
k_p = rate constant with both UV light and hydrogen peroxide
C_p = pollutant concentration, μ mol/l
C_h = hydrogen peroxide concentration, μ mol/l
a, b, c = reaction orders

The first term in this expression gives the reaction rate caused by UV light only. The second term represents the increase in reaction rate in the presence of hydrogen peroxide. The rate constants and reaction orders found by multiple linear regression analysis are listed in Table 2.

The curves predicted by this rate equation are in good agreement with the data obtained in this study. Although the rate expression is empirical in nature, it provides information on concentration dependence that is useful for design.

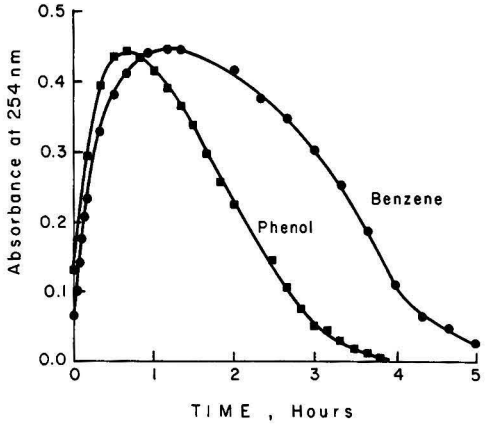

Figure 7. Change of absorbance at 254 nm with time at 25°C and pH 6.8. Initial H_2O_2/pollutant = 7 mols/mol. Initial pollutant = 0.2 mM.

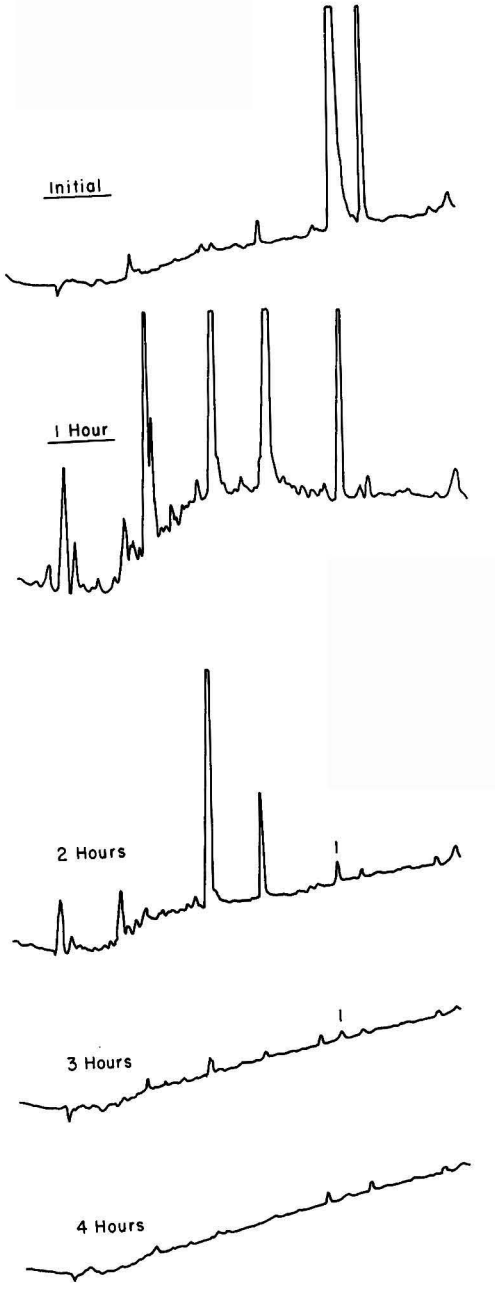

Figure 8. Liquid chromatogram traces for 2,4,6-trichlorophenol samples at start of run and after 1, 2, 3, and 4 hours of treatment. Peak 1 = 2-chlorophenol.

Reaction Intermediates

During the treatment of aromatic pollutants with UV light and hydrogen peroxide, reaction intermediates were formed, shown by the appearance of a brown color in solution and by a large increase in the absorbance of the solution at 254 nm. The changes in absorbance with time during treatment of benzene and phenol with UV and peroxide are shown in Figure 7. The reaction intermediates are as potentially undesirable in the environment as the original pollutants.

The initial rapid increase in absorbance is caused by the formation of intermediates that absorb UV light more strongly than benzene or phenol alone. The buildup of strongly-absorbing reaction intermediates may decrease the reaction rate of the parent compound through competition for available UV light and hydroxyl radicals. By adding hydrogen peroxide periodically and extending the treatment time, both the brown color and the absorbance at 254 nm can be eliminated.

To verify the existence of reaction intermediates, samples taken during the treatment of benzene and 2,4,6-trichlorophenol were analyzed by HPLC. Treated benzene samples were also analyzed by GC/MS. The HPLC results for a four-hour run with 2,4,6-trichlorophenol are shown in Figure 8. Although several intermediate peaks were observed, the only peak identified was 2-chlorophenol. Of more practical significance than the identities of the peaks are their disappearance as reaction time is extended. Some possible intermediates, such as short chain aliphatic acids, are difficult to detect by the analytical procedures used and might still be present at the end of the run. However, the aromatic intermediates most likely to be hazardous are readily detectable at low levels. The absence of peaks by HPLC and GC/MS analyses after extended treatment suggest that the aromatic structures have been eliminated.

CONCLUSION

The combination of UV light and hydrogen peroxide was effective in destroying a wide variety of hazardous aliphatic and aromatic compounds present in water at low levels. The rates of reaction were up to 50 times faster with UV light plus hydrogen peroxide than with UV light alone. For the aromatic compounds studied, reaction rates were fastest for 2,4,6-trichlorophenol, and slowest for dimethyl phthalate and diethyl phthalate. The aromatics formed many chemical intermediates that could be destroyed by extending the treatment time. An empirical expression, with two terms, was developed to correlate the concentration dependence of reaction rates.

ACKNOWLEDGMENT

This research was supported by the U.S. Department of the Interior under grant number 14-08-0001-G-1064.

LITERATURE CITED

1. Prengle, H. W., C. W. Mauk, R. W. Legan, and C. G. Hewes, *Hydrocarbon Proc.*, **54** (10), 82 (1975).
2. Prengle, H. W., and C. E. Mauk, *AIChE Symp. Ser.*, **74** (178), 228 (1978).
3. Zeff, J. D., *AIChE Symp. Ser.*, **73**, (167), 206 (1977).
4. Peyton, G. R., F. Y. Huang, J. L. Burleson, and W. H. Glaze, *Environ. Sci. Techn.*, **16**, 448 (1982).
5. Fletcher, D. B., *Waterworld News*, May/June, 25–27, 1987.
6. Koubek, E., *Ind. Eng. Chem. Proc. Res. Dev.*, **14**, 348 (1975).
7. Ogata, Y., K. Tomizawa, and K. Takagi, *Can. J. Chem.*, **59**, 14 (1981).
8. Clarke, N. and G. Knowles, *Effluent and Water Treatment J.*, **22**, 335 (1982).
9. Ho, P. C., *Environ. Sci. Techn.*, **20**, 260 (1986).
10. Sundstrom, D. W., H. E. Klei, T. A. Nalette, and B. A. Weir, *Hazardous Waste and Hazardous Mat.*, **3**, 101 (1986).
11. Weir, B. A., D. W. Sundstrom, and H. E. Klei, *Hazardous Waste and Hazardous Mat.*, **4**, 165 (1987).
12. Hager, D. G. and C. G. Loven, "On-Site Destruction of Organic Contaminants in Water," presented at Hazardous Wastes Hazardous Materials National Conference, Washington, D.C., Mar. 16–18, 1987.
13. Hager, D. G. and C. G. Loven, "Purification of Contaminated Groundwater by Chemical Oxidation or Adsorption," presented at Superfund Symposium, Kansas City Section AIChE, Kansas City, MO, Nov. 12, 1987.
14. Hager, D. G., C. G. Loven, and C. L. Giggy, "Chemical Oxidation Destruction of Organic Contaminants in Groundwater," presented at HMCRI National Conference, Washington, D.C., Nov. 16–18, 1987.

Biological Treatment of Leachate from a Superfund Site

Edward J. Opatken, Hinton K. Howard, and James J. Bond
U.S. Environmental Protection Agency, Hazardous Waste Engineering Research Laboratory, Cincinnati, OH 45268

Studies were made on treating a leachate from New Lyme, Ohio. The leachate was transported to Cincinnati, where a pilot-sized rotating biological contactor (RBC) was used for a treatment evaluation. Biomass was developed on the RBC discs with primary effluent from the City of Cincinnati's Mill Creek Sewage Treatment Facility. Experiments were then conducted to determine the effectiveness of treating a hazardous waste leachate and to provide information on: the rate of organics removal; the final effluent quality; the fate of priority pollutants and specific organic compounds; and the loss of volatiles via stripping in the RBC. The results of these experiments and the applicability of an RBC to treat a hazardous waste leachate from a Superfund site are reported.

BACKGROUND

Land disposal of organic wastes is no longer regarded as an ultimate solution for solid wastes because of the potential for leachate formation and/or groundwater contamination. Leachate releases have occurred at waste disposal sites and technology is needed to remedy these conditions.

Biodegradation of the organics in leachates may provide an acceptable and cost-effective alternative for treating leachates. The rotating biological contactor (RBC) was selected as a biological treatment process to study its applicability for converting the organics in leachate into innocuous products. A pilot-sized unit was installed at the U.S. Environmental Protection Agency's Test and Evaluation Facility (T&E) in Cincinnati, Ohio to conduct such an investigation.

NEW LYME SUPERFUND SITE

The New Lyme Superfund site [*1*] was selected as the source for the leachate. New Lyme is located in Ashtabula County, Ohio approximately 40 kilometers (25 miles) north of the city of Youngstown, Ohio. The site consists of 14 to 16 hectares (35 to 40 acres) of landfill and began its operations in 1969. It operated as a combined municipal and industrial waste landfill where approximately 230,000 cubic meters (300,000 cubic yards) of wastes were disposed each year. The industrial wastes included paints, solvents, oils, coal tar distillates, and corrosive liquids. In 1978, the landfill's license was revoked and the site was subsequently placed on the National Priorities List under the Comprehensive Environmental Response, Compensation and Liability Act of 1980 (CERCLA). A remedial investigation [*2*] was conducted in 1983 and concluded that the soils around the site: the groundwater under the site: the sediment adjacent to the landfill, and the leachate emanating from the site had been contaminated by the landfill.

Samples were obtained from several seeps surrounding the landfill. The results showed that the leachate contained up to 2000 mg/L of dissolved organics. The leachate for the treatability study was pumped from a deep depression adjacent to the site into a tank truck and transported from New Lyme to Cincinnati for experimentation using the RBC.

PROJECT DESCRIPTION

Figure 1 shows a pilot-sized RBC that contains 1,000 m^2 (11,000 square feet) of surface area, which is roughly 10% the scale of a full-sized unit (100,000 square feet) located at EPA's T&E Facility [*3*]. The diameter is 3.6 m (12 ft), identical to a full-scale unit, the length is only 1 m (3.3 ft), and a full-scale unit is 7.6 m (25 ft).

The RBC was operated in a batch mode. The leachate was transferred from a storage tank to a mix tank where the volume was measured. The nutrients were then added for specific experiments. The contents were pumped into the RBC, and the RBC was operated at a constant speed of 1.5 rpm. When the reaction was complete, the contents were returned to the mix tank and then fed to the clarifier for solids removal. The overflow went to the receiving tank, where the treated leachate was stored until the analytical results showed that the material was within the allowable discharge limits.

Effluent limitations on the treated leachate were imposed by the City of Cincinnati's Mill Creek Treatment Facility (MCTF) and by laboratory prescribed contaminant levels. Both sets of limitations had to be met before the treated leachate was disposed of in the MCTF sewers. The effluent limitations set by the MCTF were as follows: total organic halides (TOX) $\leq$5 mg/L; vapor space organics (VSO) $\leq$300 ppm (4); and $6 < pH < 10$.

The internally applied limits were based on achieving a soluble gross organics level that would be equivalent to or less than a relatively high strength raw wastewater: soluble biochemical oxygen demand (SBOD) $\leq$100 mg/L;

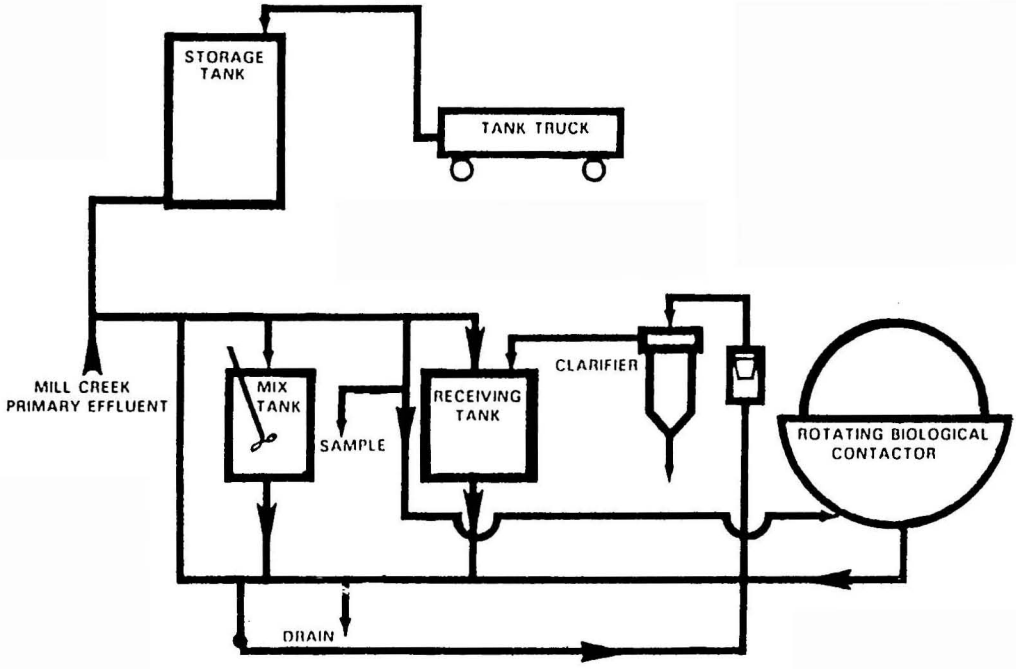

Figure 1. RBC flow schematic.

dissolved organic carbon (DOC) ≤100 mg/L; and soluble chemical oxygen demand (SCOD) ≤300 mg/L.

The underflow from the clarifier was analyzed for priority pollutants and drummed for disposal at a permitted landfill. We did experience a potentially unsafe incident with the drummed sludge. A drum bulged during storage. A gas analysis showed a high concentration of methane, which was probably caused by anaerobic degradation of the sludge. The pH of the sludge was then raised to 12 by adding caustic to deactivate the biomass. This action prevented a recurrence.

RESULTS

Experimental Conditions

The eight experiments conducted with New Lyme leachate varied in the volume of leachate fed to the RBC, the ratio of leachate to primary effluent (L/PE), the nutrient addition to the leachate, and the biomass condition (thickness, appearance, acclimation). The initial runs used a combination of leachate and primary effluent to allow for acclimation of the biomass, which was formed with primary effluent from the MCTP [5]. The initial runs also used 2800L (750 gal) instead of 3800L (1,000 gal) to conserve leachate. Nutrients were added to the leachate for experimentation to study this effect on the reaction. A fixed ratio of carbon (C)/nitrogen (N)/phosphorus (P) of 100/5/2 was used in three of the runs. These experimental variations are summarized in Table 1.

Reaction Rate

The reaction rate was determined by following the drop in the DOC with time [6]. A plot of experiments 1 and 4, are shown in Figure 2, and experiments 3 and 5 are displayed in Figure 3. Experiments 2 and 7 are shown in Figure 4. Experiment 6 is not included in the figures because its purpose was to determine the mass of volatile organics that was stripped by the RBC without any biomass. Experiment 8 is omitted because the leachate had undergone spontaneous biodegradation in the storage tank and was not representative of New Lyme leachate. The DOC at the start of experiment 8 had dropped to 280 mg/L, whereas the DOC for experiment 6 was 1780 mg/L.

Table 1. Experimental Conditions

Runs	Total Vol. Gal.	Ratio Leachate/PE Gal/Gal	Nutrient Addition	Ratio C/N/P	Biomass	Comments
01	750	250/500	No	—	No Acclimation	
02	750	500/250	No	—	Poor	
03	750	500/250	Yes	100/5/2	Satisfactory	
04	750	500/250	No	—	Satisfactory	
05	1,000	1,000/0	Yes	100/5/−2	Satisfactory	
06	1,000	1,000/0	No	—	None	Volatile organics stripping run
07	1,000	1,000/0	Yes-N/No-P	100/5/0	No Acclimation	
08	1,100	1,100/0	Yes	100/5/2	No Acclimation	

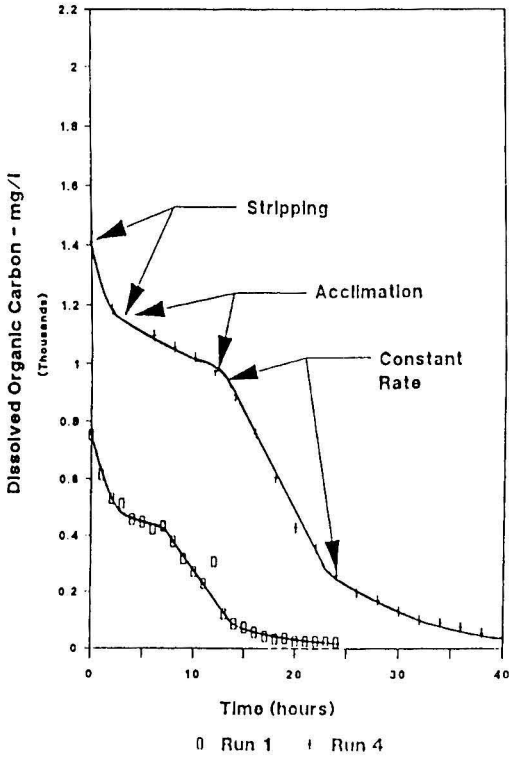

Figure 2. Disappearance of DOC with time experiment 1 and 4.

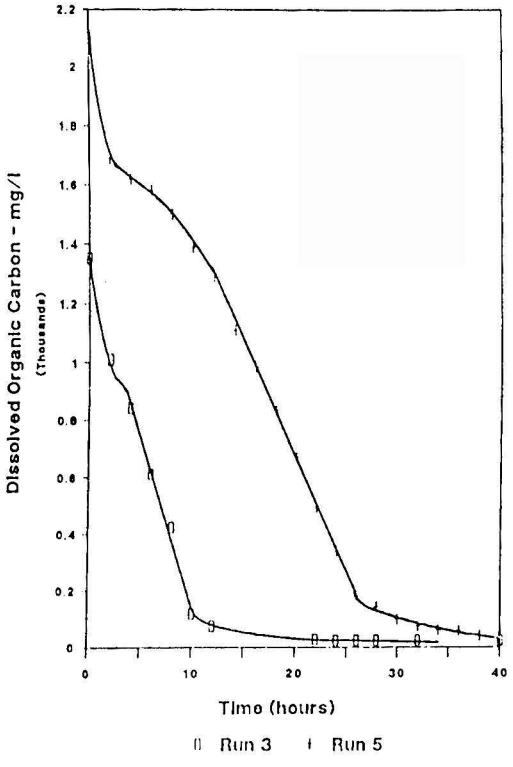

Figure 3. Disappearance of DOC with time experiment 3 and 5.

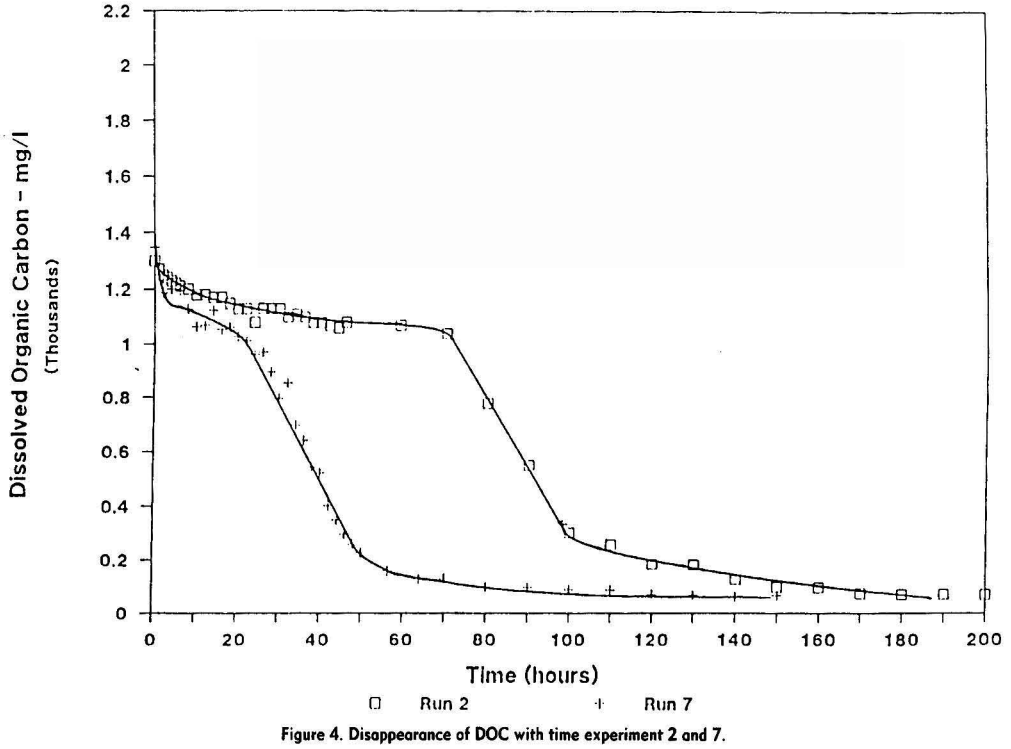

Figure 4. Disappearance of DOC with time experiment 2 and 7.

TABLE 2. GAS ANALYSES OF VOLATILE ORGANICS

Time h	Acetone mg/L	MEK mg/L	Toluene mg/L	Ethyl Benzene mg/L
0	—	—	—	—
0.5	61	320	14	2.1
2.5	500	1900	4.0	4.1
4.5	87	270	<1.2	<1.2
6.5	38	110	<1.2	<1.2

The figures show an initial drop in the DOC concentration. This is attributed to the volatile organics being stripped from solution (see Figure 2, experiment 4). There is evidence of this drop-off in each of the experiments. To verify this assumption, experiment 6 was operated without biomass and the exhaust from the RBC was measured to determine the air flow rates. Samples were withdrawn by inserting a 10 ml syringe in the exhaust line and analyzing for specific organics; acetone methyl ethyl ketone, toluene, and ethyl benzene. The gas analyses data are shown in Table 2. The data show a maximum concentration after 2.5 hours for all compounds, except toluene, followed by a significant drop in concentration at 4.5 hours and a gradual drop at 6.5 hours. The lower concentrations of organics in the gas stream with time is attributed to the lower mol fraction of the volatile organics within the leachate as the material is stripped from solution.

TABLE 3. MATERIAL BALANCE FOR MEK

	Leachate		Gas			Leachate
Time h	MEK conc mg/L	MEK wt g	flow L/h	MEK conc mg/L	MEK wt g	MEK wt* g
0	180	680	130,000	—	—	680
0.5	160	600	130,000	.32	10	670
2.5	110	420	130,000	1.88	280	390
4.5	100	400	130,000	.27	280	110
6.5	55	210	130,000	.11	50	60

* Based on subtracting the mass of MEK removed by stripping from the mass of MEK originally in the liquid.

TABLE 4. RATES OF REACTION AND NUTRIENT RATIOS

Expt.	Reaction Rate gDOC/h	Ratio C/N/P
1	140	100/5.5/<.2
2	82	100/1/<.2
3	350	100/5.5/1.4
4	180	100/1.1/<.2
5	300	100/5/2
7	120	100/6.7/<.2

Note: The C/N/P ratios shown are different from the earlier values given when describing the experimental conditions. The values in this Table reflect the contribution of the primary effluent and the leachate.

TABLE 5. REMOVAL OF POLLUTANTS FROM NEW LYME LEACHATE

	Experiment No. 1 L/PE = 1L/2L			
	L* mg/L	PE mg/L	INF mg/L	Cl EFF mg/L
SBOD	3400	120	1200	<2.0
BOD_T	—	—	1600	—
DOC	2100	100	760	17
TOC	—	—	830	19
SCOD	5900	290	2100	66
COD_T	—	—	2200	69
NH_3-N	8.1	43	32	0.3
TKN-N	14	54	42	2.6
NO_3-N	<1.0	—	1.7	—
PO_4-P	<0.2	2.6	—	<0.2
SS	1200	140	590	170
VSS	380	110	220	110
Volatile PP				
Benzene	0.26	—		<0.025
1,1-Dichloroethane	0.22	—	—	<0.013
Chloroform	0.066	—	—	<0.013
Ethylbenzene	0.50	—	—	<0.025
Methylene Chloride	11	—	—	12
Toluene	1.7	—	—	<0.025
Trichloroethylene	0.023	—	—	<0.013
Additional Volatiles				
Cis 1,2-Dichloroethene	3.9	—	—	0.011
Xylenes	0.22	—	—	—
Acetone	13	—	—	0.35
Methyl Ethyl Ketone	65	—	—	1.1
Methyl Isobutyl Ketone	12	—	—	0.49
2-Hexanone	1.0	—	—	—
Additional Acid				
Benzoic Acid	5.9	—	—	—
4-Methyl Phenol	2.9	—	—	—
2-Methyl Hexanoic Acid	2.9	—	—	—
TOX	0.46	—	—	0.77

* L = Leachate
PE = Primary Effluent
INF = Influent to RBC
Cl EFF = Clarifier Effluent
ND = Not Detected
— = Not Analyzed
TOX = Total Organic Halides

TABLE 6. REMOVAL OF POLLUTANTS FROM NEW LYME LEACHATE

	Experiment No. 2, 3, 4 L/PE = 2L/1L				
	L mg/L	PE** mg/L	INF mg/L	Cl EFF mg/L	Sludge mg/L*
SBOD	4800	140	3000	4.4	—
BOD_T	5000	230	3300	8.4	—
DOC	2200	82	1400	19	—
TOC	2200	102	1500	20	—
SCOD	5200	220	3700	50	—
COD_T	5600	370	4100	78	—
NH_3-N	8.0	15	32	2.3	—
TKN-N	14	22	—	4.3	—
NO_3-N	<1	<1	<1	—	—
PO_4-P	<0.2	2	<0.2	2.6	—
SS	920	260	860	56	—
VSS	200	140	210	35	
Volatile PP					
Benzene	0.26	<0.002	—	<0.002	<0.050
1,1-Dichloroethane	0.22	<0.001	—	<0.001	<0.025
Chloroform	0.066	<0.001	—	<0.001	<0.025
Ethylbenzene	0.50	<0.002	—	<0.002	<0.050
Methylene Chloride	11	0.066	—	<0.002	<0.050
Toluene	1.7	<0.002	—	<0.002	3.7
Trichloroethylene	0.023	<0.001	—	<0.001	<0.025
Base Neutral					
Bis(2-Ethylhexyl) Phthalate	—	<0.026	—	<0.0025	0.043
1,2,4-Trichloro Benzene	—	0.51	—	<0.0025	<0.016
Additional Volatiles					
Cis 1,2-Dichloroethene	3.9	—	—	—	—
Xylenes	0.22	—	—	—	—
Acetone	13	—	—	—	—
Methyl Ethyl Ketone	65	—	—	—	—
Methyl Isobutyl Ketone	12	—	—	—	—
2-Hexanone	1.0	—	—	—	—
Additional Acid					
Benzoic Acid	5.9	—	—	—	—
4-Methyl Phenol	2.9	—	—	—	0.47
2-Methyl Hexanoic Acid	2.9	—	—	—	—
Phenol (PP)	—	<0.026	—	<0.0025	0.060
TOX	0.46	—	—	0.14	—
TTO	—	0.51	—	<0.010	4.2

* Sludge Sample accumulated after Experiment 2.
** Primary pollutants from Experiment 3.
TTO = Total Toxic Organics

A material balance was calculated for MEK in the leachate by analyzing the RBC tank contents at specific time intervals. The calculated leachate values shown in Table 3 were obtained by multiplying the gas flow in the exhaust line by the concentration of MEK in the gas stream after various time intervals and subtracting this value from the MEK originally contained in the leachate. The MEK remaining in the batch after 6.5 hours of operation was higher, based on the leachate analysis method as compared to subtracting the MEK accounted for in the gas stream from the MEK originally present in the leachate. However, both methods show continual drop-off of MEK and the gas analyses proves that MEK was stripped from solution. Provisions may be necessary to capture the volatile organics from an RBC to prevent air contamination when treating leachates with an RBC.

After stripping, there was a period with a reduced reaction rate that was attributed to acclimation of the biomass to the leachate (see Figure 2, experiment 4). There was only a slight drop in DOC during this time interval. The acclimation period varied, but it was especially evident in experiments 2 and 7 where the acclimation period lasted for 20 and 40 hours, respectively. The lengthy acclimation period for experiment 2 was attributed to an inadequate biomass. Prior to the start of experiment 2, the biomass was observed to be reddish-brown and spotty with a noticeable decrease in thickness, indicating that considerable sloughing-off of the biomass had occurred. The extended acclimation period for experiment 7 was attributed to the fact that it followed the volatile organics stripping run where the biomass had been removed from the discs. There was therefore no prior acclimation of the biomass to the leachate.

Following the acclimation period, the reaction progressed at a constant rate, as shown in Figure 2, experiment 4 by the disappearance of DOC, with time. The reaction rate varied for each experiment, ranging from a high of 350g DOC converted per hour to a low of 82 grams per hour. The two experimental runs that had rates equal or greater than 300 grams per hour contained adequate levels of both nitrogen and phosphorus, and had an adequate acclimation period from previous runs. It appears that the nutrient addition for experiments 3 and 5 may have contributed to the high organic removal rate. However, additional cause and effect experiments are needed to verify that nutrients may influence the reaction rate. The reaction rates for the six experiments and the ratios of C/N/P are shown in Table 4.

TABLE 7. REMOVAL OF POLLUTANTS FROM NEW LYME LEACHATE

	Experiment No. 5		Sludge	7	
	L mg/L	EFF mg/L	mg/L*	L mg/L	CL EFF mg/L
SBOD	2700	4	—	2000	3.2
BOD_T	3000	6.6	—	2600	21
DOC	2000	17	—	1400	45
TOC	2100	19	—	1400	52
SCOD	5200	33	—	3800	190
COD_T	—	—	—	4000	220
NH_3-N	100	—	—	84	33
TKN-N	110	—	—	92	42
NO_3-N	<1	60	—	<1	21
PO_4-P	—	1.4	—	<0.2	0.4
SS	1400	6600	51000	1100	88
VSS	240	2600	19000	270	58
Volatile PP					
Benzene	0.28	<0.002	<0.010	<0.002	<0.001
Toluene	4.9	<0.002	0.018	4.3	<0.001
Acid PP					
Phenol	—	—	—	1	—
Additional Volatiles					
Cis 1,2-Dichloroethene	0.94	ND	—	—	—
Xylenes	2.8	ND	0.025	1.9	—
Acetone	140	ND	0.012	27	—
Methyl Ethyl Ketone	470	ND	0.021	200	—
Methyl Isobutyl Ketone	—	—	—	46	—
Methyl Disulfide	—	—	—	1	—
Dimethyl Disulfide	—	—	—	1	—
Dimethyl Trisulfide	—	—	—	1.2	—
Additional Acid					
4-Methylphenol	—	—	—	1	—
2 Methylpentanoic Acid	—	—	—	4.6	—
2 Methylhexanoic Acid	—	—	—	10	—
Hexanoic Acid	—	—	—	5.2	—
Nonanoic Acid	—	—	—	3.1	—
Decanoic Acid	—	—	—	2.1	—
TOX	—	1.2	—	—	0.72
TTO	<0.250	<0.010	0.018	5.4	<0.010

* Sludge sample accumulated after Experiment 5.
EFF-Effluent from RBC.
ND = Not Detected.
— = Not Analyzed.

Pollutant Removals

The experiments with New Lyme leachate were analyzed for typical biological parameters and priority pollutants. The removal of gross organics was determined by analyzing the influent and effluent for DOC, SBOD, SCOD, TOC, total BOD $(BOD)_T$, and COD_T. Other biological parameters analyzed included suspended solids (SS) and volatile suspended solids (VSS), as well as the nutrient chemicals, both the nitrogen series, and phosphorus [7]. The results show good removals of organics, except for experiment 7, which operated without benefit of prior acclimation runs. The clarified effluent had SBOD levels well below the normal discharge limits for a municipal treated secondary effluent (30 mg/L). The results also indicated that nitrification had occurred by the drop in ammonia-nitrogen.

The priority pollutant levels for untreated New Lyme leachate were compared with the effluents from the RBC after each experiment and, on occasion, were compared with the sludge from the clarifier. Several volatile organics that were present in measurable quantities were identified during the priority pollutant analyses. Their removals were occasionally followed during the RBC experiments.

The summary charts shown in Tables 5, 6, and 7 list the analytical data for the experiments with New Lyme leachate. The data for the biological parameters in experiments 2, 3, and 4 were averaged, since they were all run at the same leachate/PE ratio. These results indicate that the removal of the pollutant by the RBC was effective for all the contaminants. The gross organics as represented by DOC, SBOD, and SCOD were reduced to levels approaching a treated municipal secondary effluent. Only in the effluent from experiment 1 was a priority pollutant, methylene chloride, detected. Otherwise, the biological treatment was effective for converting the priority pollutants into innocuous products.

Sludge samples were analyzed following experiments 2 and 5. Toluene was the only priority pollutant identified both times as present in the sludge. It was not determined whether the toluene was present in the liquid or solid phase. However, since toluene was not detected in the effluent, it is assumed that the toluene was associated with the solids in the sludge.

CONCLUSIONS

The study on treating the New Lyme leachate with an RBC showed effective removals at satisfactory reaction

rates. The RBC was an effective treatment process for reducing the organics in New Lyme leachate. Priority pollutants were converted and/or stripped from the leachate during treatment. The effluent quality is equivalent to a secondary treated effluent from a municipal wastewater treatment plant. Nutrient addition, at ratio of C/N/P of 100/5/2, showed evidence of favorably influencing the reaction rate. Volatile organics were stripped from the leachate by the RBC action when operated in a batch mode. Finally, the RBC experienced a period of inactivity near start-up, which is assumed to be caused by the need for the biomass to acclimate to the leachate.

The RBC offers a high degree of treatment for processing leachates from a hazardous waste site. Additional research is needed to determine the degree of organic stripping while the biodegradation reaction is occurring, and to validate the rapid reaction rate kinetics when the nutrients are controlled at their theoretical levels.

LITERATURE CITED

1. Draft Report of "Treatability Testing and Field Investigation Report New-Lyme Landfill," U.S. Army Corps of Engineers, Omaha District, January 1987.
2. Final Remedial Investigation New Lyme Landfill Site, Ashtabula County, Ohio, CH_2M-Hill, February 6, 1985.
3. Brenner, R. C., J. A. Heidman, E. J. Opatken, and A. C. Petrasek, "Design Information on Rotating Biological Contactors," EPA-600/2-84-106, June 1984.
4. "Vapor Space Organics," In-house method developed by the Metropolitan Sewer District of Greater Cincinnati, Industrial Waste Section, Cincinnati, Ohio.
5. Opatken, E. J., K. H. Howard, J. J. Bond, "Biological Treatment of Hazardous Aqueous Wastes," Paper presented at Second International Conf. on New Frontiers for Hazardous Waste Management, September 1987.
6. Opatken, E. J., *Envir. Prog.*, **5**, 1, February 1986.
7. Antonie, R. L., *Fixed Biological Surfaces—Wastewater Treatment*, CRC Press, 1976.

Modeling and Analysis of Moving-Bed Hot-Gas Desulfurization Processes

Raul E. Ayala and Bang Mo Kim
General Electric Company, Corporate Research and Development, Schenectady, NY 12301

Removal of sulfur compounds from hot coal gas is a necessary step during power generation operations. Zinc ferrite has been identified as a promising absorbent material. A mathematical model describing the kinetics of zinc ferrite during absorption and regeneration as it applies to a steady-state moving-bed concept, where the solids are continuously transferred between absorber and regenerator vessels has been developed. Model predictions, based on experimental data, are presented for various flow configurations and operating conditions, including multistage operation of regeneration, where the effect of diffusion mechanisms, temperature, gas concentrations, and flow rates on conversion are presented.

INTRODUCTION

The integrated gasification combined cycle (IGCC) has been identified as a viable approach for the generation of electricity from coal in the next generation of utility plants [*1*]. The removal of sulfur compounds from hot coal gas is now the critical element in the commercial development of the IG-STIG (integrated gasification steam injected gas turbine) concept. The raw gas exiting the gasifier at 482–593°C goes through a particulate removal system before entering the hot desulfurization system, where sulfur compounds such as H_2S and COS are removed. Further particulate removal occurs after the hot desulfurization system and before the gas enters the fuel gas turbine where the gas is burned to produce electricity.

Zinc ferrite is a promising absorbent material for hot gas desulfurization, capable of removing sulfur-containing species from coal gas at gasifier exit temperatures. It is also capable of being regenerated for continuous use [*2*]. For IG-STIG operating temperatures and gas compositions, zinc ferrite is capable of reducing H_2S concentrations down to a few parts per million, much lower than iron oxide can, on a single-stage process, as a result of its very low H_2S partial pressure.

A key issue in the development of a commercial hot desulfurization process is the configuration of the absorption/regeneration system. The conventional approach in solid sorption processes is to utilize multiple sorbent beds, with each bed being cycled between sorption and regeneration mode. This approach minimizes sorbent damage since no movement of the sorbent is required. However, for a hot H_2S scrubbing process, this requirement for cyclic operation has major drawbacks. The most important of these is that the product gas and regenerator exit gas compositions will vary with time.

In the absorption process, H_2S reacts with the sorbent to form metal sulfides (FeS and ZnS from zinc ferrite). In the regenerator, the metal sulfides are converted back to the oxides and the sulfur oxidized, nominally, to SO_2. In cyclic operations, which would be characteristic of a fixed-bed reactor, the regenerator off-gas composition has been found to vary considerably with time, both in sulfur concentration and sulfur species. This variation of outlet gases makes it difficult to design an effective sulfur recovery process.

To counterbalance these potential problems associated with the operation of a fixed-bed cyclic system, a moving-

bed concept in which sorbent slowly moves downward by gravity, countercurrently to the upward flowing fuel gas, has been considered. Spent sorbent is removed from the absorber and fed to the top of the regenerator, which is also a slowly moving bed. Regenerated sorbent is then transported to the top of the absorber and fed via a lock-hopper. The moving bed design has the advantages of having nearly steady-state operation, of minimizing sorbent damage (compared to fluidized beds), and of having "self-cleaning" properties in that coal dust, which may be carried over from the gasifier that deposits in the absorber, is constantly transferred to the regenerator for oxidation.

It is important to be able to understand, predict, and specify such operating parameters as compositions, temperature profiles, gas flow, and sorbent circulation rates before undertaking equipment design, construction, and operation of the H_2S removal system. It is necessary to develop a mathematical model to aid in the calculation of thermal and chemical effects, and that will also allow a prediction of the best operating conditions.

SORBENT CHEMISTRY

During absorption of hydrogen sulfide, zinc ferrite is isothermally converted to zinc and iron sulfides with evolution of water. In regeneration, the sulfided metal sorbent reacts exothermally with oxygen and converts back to the oxides. Sulfur is then oxidized to SO_2. These two processes can be ideally described by the following reactions

$$ZnFe_2O_4 + 3H_2S + H_2 \rightarrow ZnS + 2FeS + 4H_2O \quad (1)$$

$$ZnS + 2FeS + 5O_2 \rightarrow ZnFe_2O_4 + 3SO_2 \quad (2)$$

Sulfur absorption in Reaction (1) is accompanied by a 13.3% increase in solid weight, while regeneration in Reaction (2) results in an equivalent decrease in solid weight. Consequently, the rates of absorption and regeneration in a single sorbent pellet can be measured using thermogravimetric analysis (TGA), where the weight of solid reactant is monitored against time. Models for gas absorption by single pellets have been described in the literature [3, 4, 5]. The unreacted core model has been found to apply to absorption of H_2S over zinc ferrite pellets at high temperature [6]. Other side reactions may occur, depending on reactant concentrations and temperature, as shown by the following:

- Further reduction of zinc ferrite during absorption

$$3ZnFe_2O_4 + H_2 \rightarrow 3ZnO + 2Fe_3O_4 + H_2O$$

$$Fe_3O_4 + H_2 \rightarrow 3FeO + H_2O \quad (3)$$

- Sulfate formation during regeneration

$$Fe_2O_3 + 3SO_2 + \frac{3}{2}O_2 \rightarrow Fe_2(SO_4)_3$$

$$ZnO + SO_2 + \frac{1}{2}O_2 \rightarrow ZnSO_4 \quad (4)$$

- SO_2 formation from sulfate reduction during absorption

$$4FeSO_4 + 10H_2 \rightarrow 3Fe + FeS + 3SO_2 + 10H_2O$$

$$2ZnSO_4 + 5H_2 \rightarrow ZnO + ZnS + SO_2 + 5H_2O \quad (5)$$

TGA single-pellet rate data by Kim and Ayala [7] have been analyzed according to the unreacted core model, which may include gas phase, pore diffusion, intrinsic kinetics, or any combination of the three, as the controlling resistances to the overall rate of absorption. A comparison is reproduced in Figure 1. Conversion x is defined in terms of the fraction of solid reactant converted into products. Predictions of the rates of conversion based on gas phase resistance and chemical reaction resistance alone show significant deviations from experimental data. Those based on pore diffusion alone or pore diffusion coupled with gas phase resistance and chemical reaction provided very good agreement. Since the overall resistance was not significantly affected experimentally by variations in flow rate, and because it was also known that chemical reaction is fast as temperatures of approximately 550°C and 650°C, it was concluded that pore diffusion is the dominant resistance in the overall absorption rate for single pellets. Observations for the regeneration reaction also agree with the previous conclusions.

REACTOR MODEL DEVELOPMENT

The mathematical model of a moving bed comprises two modules: the absorber model, where hydrogen sulfide is removed from the coal gas by absorption onto zinc ferrite sorbent material; and the regenerator model, where the sulfided sorbent is regenerated back to its original oxide form. The present model is able to handle chemical reactions both isothermally as well as adiabatically, with physical property data adjusted for temperature variations along the reactor length.

In general, the global rate of reaction in a reactor bed will incorporate the three resistances encountered in the unreacted core model (gas phase, pore diffusion, and intrinsic kinetics). Based on the work by Fotch, et. al. [6] using cylindrical pellets, the global rate can be written as

$$\frac{dx}{dt} = \frac{1}{\frac{1}{N_k} + \frac{1}{N_p} + \frac{1}{N_g}} \quad (6)$$

where

$$N_k = \frac{2b\,(1-\epsilon_x)\,k_i C_g\,(1-x)^{1/2}}{R} \quad (7)$$

$$N_p = -\frac{4bD_e\,(1-\epsilon_x)\,C_g}{R^2 C_{so} \ln\,(1-x)} \quad (8)$$

$$N_g = \frac{2b\,(1-\epsilon_x)\,k_g C_g}{RC_{so}} \quad (9)$$

N_k, N_p, and N_g are the rate expressions when intrinsic kinetics, pore diffusion, or gas phase diffusion, respectively, are the only reaction controlling mechanisms.

When exothermic reactions are considered, such as the regeneration of sulfided zinc ferrite, the heat generated can be high enough to alter the temperature profile and operating conditions inside the reactor bed. In the reactor model for regeneration, the energy balance equation was developed and coupled with the mass balance to determine the solid conversion, taking into account temperature variations in the diffusion rate under adiabatic operation. The assumptions made in the energy balance equations for regeneration are

- Steady-state operation
- No radial temperature gradients (one-dimensional model)
- No axial dispersion of heat
- No heat losses to the surroundings (adiabatic operation)

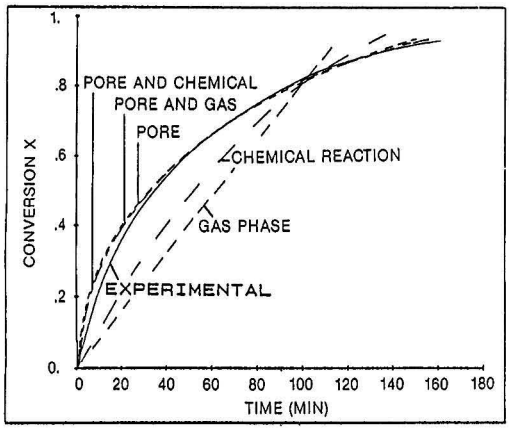

Figure 1. Comparison of rate-controlling mechanisms in the unreacted core model with experimental TGA rate data for absorption (2% H_2S, 550°C).

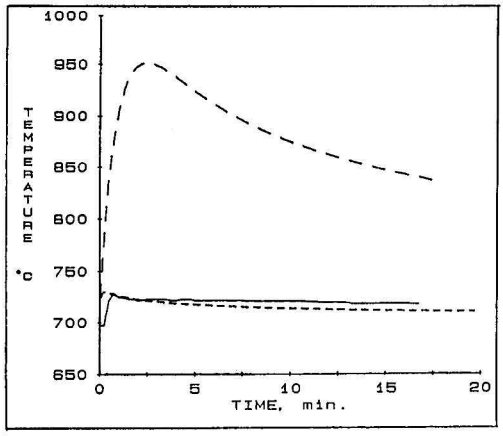

Figure 3. Pellet temperature profile for TGA regeneration (4% O_2, 96% N_2, 700°C); (——) experimental, (----) model with radiation term, and (— —) model with convection term only.

- Thermal equilibrium between solids and gases leaving a differential volume element
- No temperature gradients inside the solid pellet

Based on Figure 2, where the reactor diagram is shown, and the above assumptions, the differential equation describing the heat balance in the reactor bed including conduction, convection, and heat generation, is given by

$$-KA\frac{d^2T}{dZ^2} + \delta\frac{dT}{dZ} + \xi\frac{dx}{dZ} = 0 \qquad (10)$$

where

$$\xi = n_s\Delta H \ (\Delta H < 0) \qquad (11)$$

$$\delta = n_s c_s \pm n_g c_g \qquad (12)$$

Depending on the chosen flow configuration (cocurrent, countercurrent, or multistage), Equations (10) to (12) can be solved subject to various initial conditions. The positive sign is chose in Equation (12) when the flow of reactants is cocurrent and the negative sign chosen when the flow is counter current. Rate of conversion (Equation (6)) and energy balance (Equation (10)) are coupled by the equality

$$v_s\frac{dx}{dZ} = \frac{dx}{dt} \qquad (13)$$

Simultaneous solution of Equations (6) and (10) is necessary when dealing with nonisothermal operation of the reactor such as in regeneration. The Runge-Kutta-Verner method using fifth and sixth order approximations was used to solve numerically and simultaneously the differential conversion and energy rate expressions. When only pore diffusion is considered in the global rate expressions, the difference between the analytical and the numerical solutions of the conversion profile was less than 0.1% over the whole range $x = 0$ to $x = 1$.

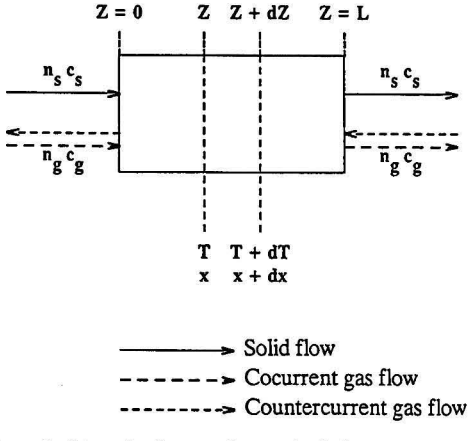

Figure 2. Schematic diagram of a moving-bed reactor system for cocurrent and countercurrent flows.

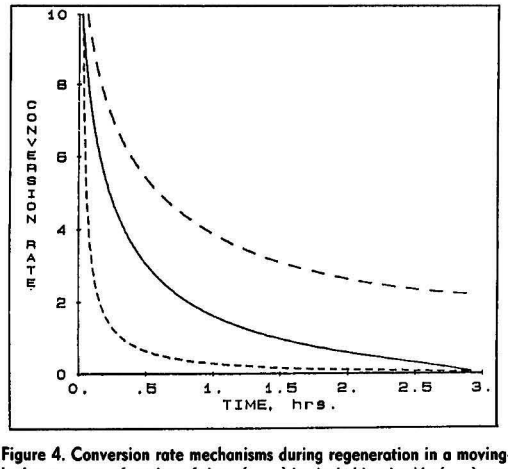

Figure 4. Conversion rate mechanisms during regeneration in a moving-bed reactor as a function of time; (——) intrinsic kinetics N_k; (- - -) pore diffusion N_p; and (— —) gas phase resistance N_g.

TABLE 1. BASE CASE OPERATING CONDITIONS FOR ADSORBER AND REGENERATOR MODELS.

Parameter	Absorber	Regenerator
Inlet temperature	538°C	538°C
Pressure	2068 kPa	211 kPa
Gas superficial velocity	592.5 m/hr	592.5 m/hr
Solid velocity	3.05 cm/hr	3.05 cm/hr
Reactive species mole fraction	0.005 H_2S	0.05 O_2
Solid reactant	$ZnFe_2O_4$	(2FeS + ZnS)
Pellet porosity	0.67	0.45
Average pellet pore radius	903 Å	1180 Å
Effective pore diffusivity	0.09 cm^2/s	0.18 cm^2/s
Intrinsic reaction coefficient	1×10^3 $cm^4/mol/s$	1×10^3 $cm^4/mol/s$
Pellet diameter	0.476 cm	0.476 cm
Pellet length	1.27 cm	1.27 cm
Bed axial conductivity	4.14×10^{-4} cal/cm/s/K	4.14×10^{-4} cal/cm/s/K

MODEL RESULTS

Comparison of theory and experiment for single pellets was done by solving the numerical model at constant gas composition and bulk gas temperature (e.g., simulating TGA experiments) and comparing with actual TGA data. Figure 3 shows a comparison for regeneration at 704°C and 5% O_2 for a single pellet TGA. Heat transfer parameters in the model were calculated from correlations of flow past single cylinders [8]. Good agreement is obtained between the experimentally observed solid temperature and the predicted pellet temperature when radiative heat dissipation is also included in the model calculations, along with the convective and diffusive heat transfer mechanisms. The theoretical temperature curves were generated using the TGA option of the reactor model with and without radiative heat transfer. It is evident that radiation is an important mechanism of heat dissipation in single pellet experiments where bulk gas temperature remains constant.

The following analysis of moving bed systems is based on pore diffusivity data from TGA experiments [7], gas phase parameters from semi-empirical correlations for packed beds [8], and numerical solution of the relevant differential equations. Solution of the rate expressions predicted by each mechanism (N_k, N_p, N_g) for a moving bed (Equations (7) to (9)) is presented in Figure 4. Overall, the rate of conversion determined by the pore diffusion resistance is the lowest of all three. Hence, pore diffusion can be taken as being the dominant, although not necessarily the only, controlling mechanism during reaction in a moving bed. These reactor predictions are in qualitative agreement with results from TGA single-pellet experiments (Figure 1), in that pore diffusion is the dominant resistance to the overall rate of conversion.

Moving Bed Systems Analysis

The absorber model assumes isothermal operation of the system under steady state. Calculations were performed based on 95% removal of H_2S from the incoming gas, which is equivalent to reducing the inlet H_2S concentration from 5000 ppmv down to 250 ppmv. Baseline operating conditions for absorption and regeneration are presented in Table 1.

Gas diffusion inside porous media is assumed to be determined by collisions between gas molecules in the bulk gas (molecular diffusion) and by gas-pore wall collisions (Knudsen diffusion), the two acting as resistances in series to the effective overall diffusion rate. Correlations have been used to estimate the relative importance of each mechanism in the effective overall rate [8]. Figure 5 presents the relative importance of bulk molecular and Knudsen contributions to diffusion during absorption as a function of reactor length. For typical zinc ferrite cylindrical pellets having an average pore radius of 1,000 Å, the reaction rate inside the pores is controlled primarily by bulk molecular diffusion. Consequently, reaction rates should be nearly independent of operating pressure. For much smaller pore sizes, a strong pressure effect on the rate would be expected, since Knudsen diffusion would be in control.

Solid conversion and H_2S concentration profiles for absorption in cocurrent and countercurrent flow are presented in Figures 6 and 7. Under the given operating conditions, cocurrent flow shows faster hydrogen sulfide removal rate than countercurrent flow at low solid conversions (x less than 0.60). For other gas flow rates, cocurrent flow performed at least as well as countercurrent for low solid conversions. As absorption progresses, the driving force for reaction (proportional to gas concentration gradients and inversely related to resistance through the solid product layer) decreases dramatically for the cocurrent case. Near the solids exit, the countercurrent case is now more efficient. Hence, when low solid conversions are expected, cocurrent flow is at least as efficient as, if not better than, the equivalent countercurrent case.

The regeneration reaction was also analyzed using the corresponding regenerator model under atmospheric conditions. The choice of cocurrent or countercurrent flow affects the solid conversion and the temperature profiles along the reactor length. Fractional solid conversion

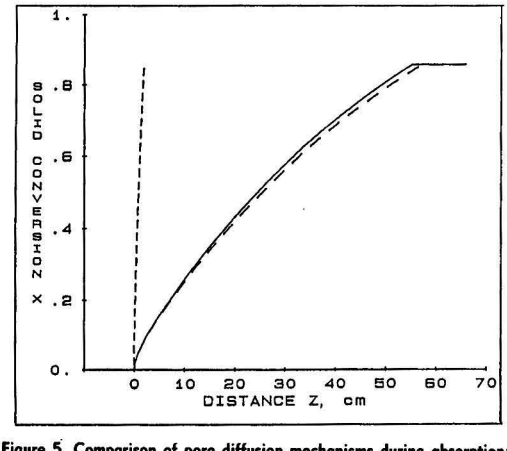

Figure 5. Comparison of pore diffusion mechanisms during absorption; (——) molecular; (- - -) Knudsen; and, (— —) effective diffusivity.

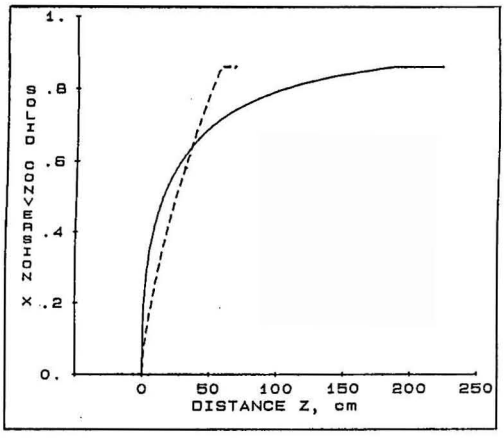

Figure 6. Solid conversion x versus reactor distance as a function of flow configuration during absorption; (——) cocurrent flow; and (- - -) countercurrent flow.

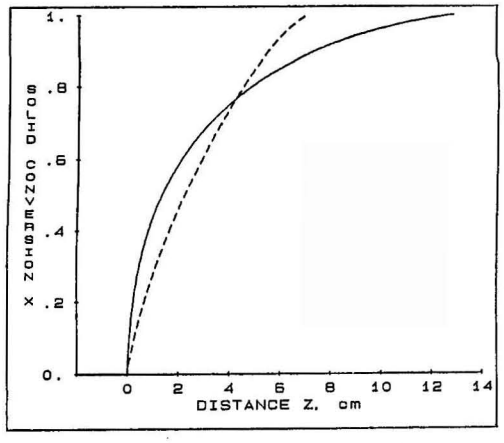

Figure 8. Effect of flow configuration on solid conversion during regeneration; (——) cocurrent flow; (- - -) countercurrent flow.

x versus distance Z as a function of the flow configuration is shown in Figure 8. As before, cocurrent flow performed at least as well as countercurrent for low solid conversions. Above 80% conversion, the reverse is true and countercurrent outperforms cocurrent. The transition point where countercurrent flow is more efficient was found in general to be dependent on the gas-to-solid ratio.

The heat of reaction released during adiabatic operation of the regenerator results in a temperature increase of the system, which may result in sintering and degradation of the sorbent material. High gas flow rates need to be used to dissipate the heat of regeneration (407 Kcal/mol). The corresponding steady-state temperature profile is presented in Figure 9. Major differences in the temperature profile exist between cocurrent and countercurrent flow. On the one hand, in cocurrent flow the lowest temperature is at the solid entrance and the highest temperature is at the solid exit with a concave-down monotonically increasing temperature profile. On the other hand, countercurrent flow presents the highest temperature at the solid entrance that gradually decreases in a concave-up fashion throughout the reactor bed until it finally reaches its lowest temperature at the solid exit. The most important observation is that the average bed temperature is much lower for countercurrent flow, and this is an important factor to consider when other side reactions may be significant within a given temperature interval.

Controlling Bed Temperature

The maximum bed temperature during regeneration can be controlled by gas conditions in one or two distinct ways: by adjusting the ratio of total gas flow to solid flow W, keeping the oxygen concentration constant; or by adjusting the oxygen concentration keeping the excess oxygen constant.

The effects of using the first method on solid conversion and temperature are shown in Figures 10 and 11 during countercurrent flow. Here the concentration of O_2 has been kept constant at 5% and the ratio of total gas flow to solid flow W has been increased from $W = 120$ to $W = 400$. The stoichiometric amount of oxygen ($O_2/ZnS = 5.0$) for 5% O_2 in the gas stream corresponds to $W = 100$.

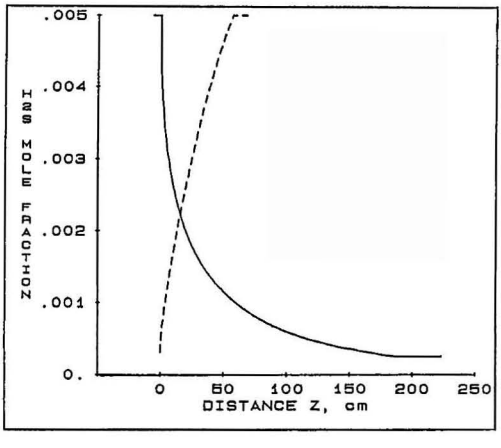

Figure 7. Hydrogen sulfide concentration during absorption for cocurrent and countercurrent flows; (——) cocurrent flow; and (- - -) countercurrent flow.

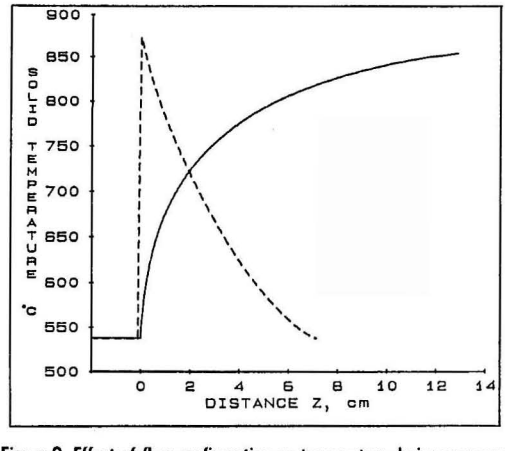

Figure 9. Effect of flow configuration on temperature during regeneration; (——) cocurrent flow; (- - -) countercurrent flow.

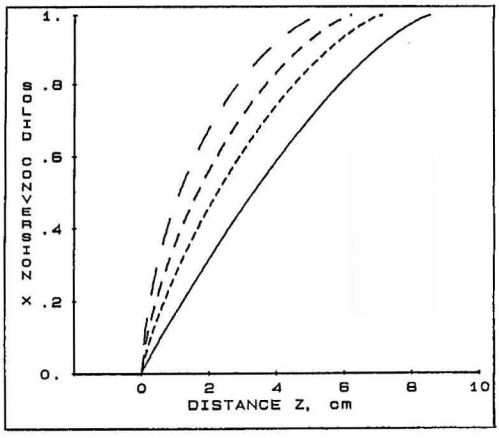

Figure 10. Effect of gas-to-solid ratio, W, on solid conversion during countercurrent regeneration; (——) $W = 120$; (- - - -) $W = 150$; (- - -) $W = 200$, and (— —) $W = 400$.

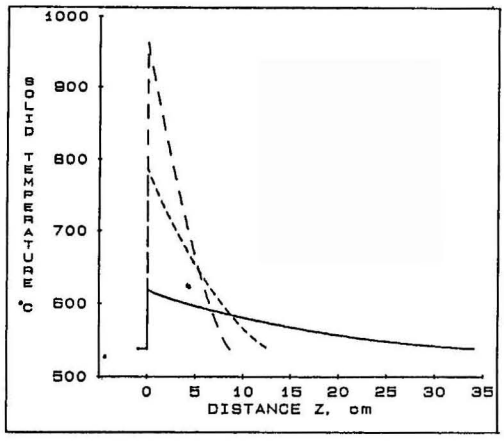

Figure 12. Effect of oxygen concentration at 20% excess O_2 on solid temperature during countercurrent regeneration; (——) 1% O_2; (- - -) 3% O_2; and (— —) 5% O_2.

Hence, all curves presented in Figures 10 and 11 correspond to excess oxygen. Although some reduction in the length of the minimum reaction zone is achieved by using high values of W, the effect is not dramatic. The shape of the conversion profiles moves slightly towards higher conversions as the total amount of gaseous species increases. Figure 11 shows the corresponding temperature profiles where the maximum bed temperature can be reduced from 982°C ($W = 120$) to 649°C ($W = 400$) by increasing the gas flow 3.3 times. The advantage of this method is that the reaction zone remains almost constant.

The second approach of controlling bed temperature is to change the O_2 concentration while keeping the total excess oxygen constant (Figure 12). A reduction in oxygen concentration from 5% to 1% requires a fivefold increase in gas flow rate (to keep the total excess oxygen constant), which results in more than a sixfold increase in the required reactor length to accomplish the same task. Hence, reduction of flowrate and reduction of oxygen concentration produce different results in terms of reactor length.

Sulfate Formation and Water-Gas Shift

In addition to the desired reactions during hot gas cleanup, sulfidation of zinc ferrite and oxidation of the zinc and iron sulfides, sulfate formation during regeneration and water-gas shift reaction during absorption have been considered. Metal sulfates formed during regeneration are undesirable because they decompose in the presence of hydrogen during absorption, liberating sulfur dioxide. Experimental TGA data on sulfate formation as a function of temperature were used in the reactor model predictions. Figure 13 shows the expected relative amount of sulfate formed across the reactor length during cocurrent flow. It is expressed as the ratio (molar rate of sulfate formation)/(total molar rate of sulfide disappearance), e.g., the fraction of sulfide that is converted into sulfate instead of oxide. Even though countercurrent flow is generally chosen as the most effective flow configuration for solid conversion, it has the disadvantage that lower temperatures near the solids exit during regeneration may result in sulfate formation. From this point of

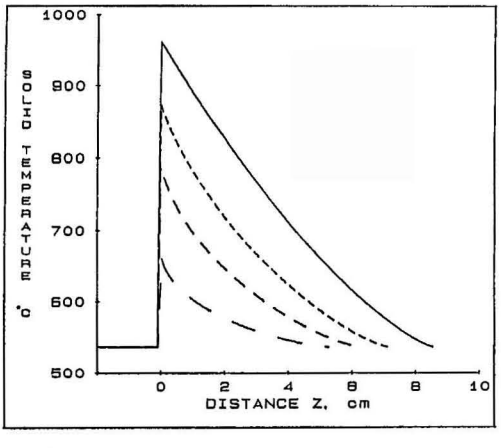

Figure 11. Effect of gas-to-solid ratio, W, on temperature during countercurrent regeneration; (——) $W = 120$; (- - - -) $W = 150$; (- - -) $W = 200$; and (— —) $W = 400$.

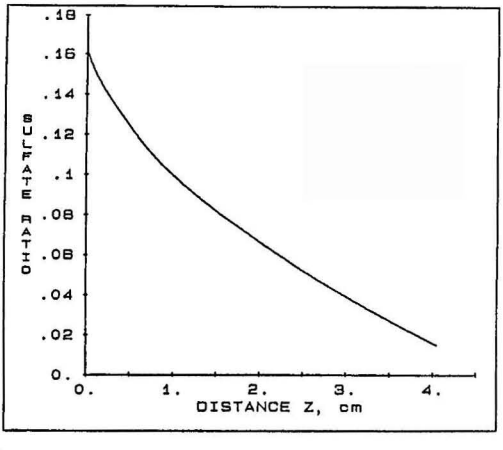

Figure 13. Sulfate ratio versus reactor distance during cocurrent regeneration.

view, cocurrent flow may even be more desirable in some aspects during regeneration since higher temperatures in the bed occur toward the end of the reactor, resulting in thermal decomposition of any previously formed sulfate.

The regenerator algorithm also has added features to handle multistage operation of the reactor. Here, multiple gas inlet and outlet locations in the vessel allow the user to choose various combinations of cocurrent and countercurrent flow configurations in series. Stagewise operation of regeneration allows control of the initial fast rate of heat generation and maintenance of thermal equilibrium between solid and gas, thus avoiding heat accumulation in the solid that may cause sintering. Also, greater control can be obtained on secondary reactions having temperature-dependent yields of undesired products (e.g., sulfate formation).

An example of the three-stage regenerator is presented in Figure 14, where regeneration is carried out in two cocurrent stages followed by a final countercurrent stage, all in series. The reactor vessel shows the first stage is cocurrent flow, where 20% of the total gas (2.5% O_2) is introduced below the stoichiometric ratio to accomplish only a predetermined 11% conversion of the solid. This controlled final solid conversion puts a ceiling on the maximum amount of heat generated and maximum temperature increase in that section. Stage two introduces approximately 75% of the total inlet gas (4% oxygen) at a lower temperature, 316°C, to cool down the solids and carry out the reaction even further at a slower rate than in the first stage. Finally, the third stage "polishes" the regeneration with air in countercurrent flow to guarantee completely regenerated sorbent leaving the regenerator vessel and at lower temperatures.

SUMMARY

A mathematical one-dimensional model has been developed that simulates steady-state operation of a moving-bed process for absorption of H_2S from coal gas and regeneration of the sulfided zinc ferrite back to its original oxide form. Both absorber and regenerator models predict the minimum length of the reaction zones required to achieve a given task, e.g., 95% removal of hydrogen sulfide and 100% regeneration of the sulfided material, and the expected temperature profile during adiabatic operation. Physical property data estimation and secondary reactions, e.g., sulfate formation during regeneration, are also calculated and updated as functions of temperature.

Analysis of various flow configurations revealed the advantage of multistage operation of the regenerator over single-stage regeneration, resulting from the exothermic nature of the oxidation reaction and the undesirability of sulfate formation at low temperatures.

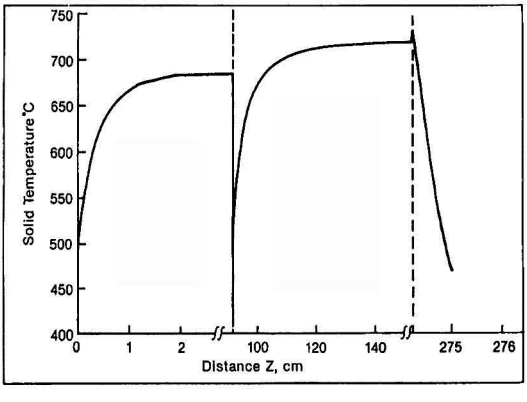

Figure 14. Temperature profile of a multistage regenerator having two cocurrent and a final countercurrent stages.

Acknowledgments

This project was sponsored in part by The Niagara-Mohawk Power Company. The authors wish to thank K. Marley and T. Ellingwood for their assistance in the computer encoding of the model. They also wish to thank A. Vesey for Niagara-Mohawk Power Company for his support and E. Gal from General Electric Environmental Services, Inc. for technical discussions.

NOTATION

- A Reactor cross-sectional area, cm^2
- b Stoichiometric coefficient (moles of solid reaction per mole of gas), dimensionless
- c_g Gas heat capacity, cal/mol/°C
- c_s Solid heat capacity, cal/mol/°C
- C_g Reactant species gas phase molar concentration, mol/cm^3
- C_{SO} Solid reactant molar concentration in the pellet, mol/cm^3
- D_e Effective pore diffusivity, cm^2/s
- K Bed axial thermal conductivity
- k_g Gas phase mass transfer coefficient, $mol/cm^2/s$
- k_i Intrinsic kinetics rate coefficient, $cm^4/mol/s$
- n_g Gas molar flow rate, mol/s
- N_g Gas phase diffusion rate, s^{-1}
- N_k (Intrinsic) kinetic rate, s^{-1}
- N_p Pore diffusion, rate, s^{-1}
- n_{sx} Solid molar flow rate, mol/s
- R Pellet radius, cm
- t Time, s
- T Temperature, °C
- v_s Solid velocity, cm/s
- W Ratio of molar gas flow rate to molar solid flow rate, dimensionless
- x Solid fractional conversion, dimensionless
- Z Axial distance, cm
- δ Enthalpy of reactants defined by Equation (12), cal/°C/s
- ϵ_x Bed void fraction (external to pellet), dimensionless
- ξ Maximum rate of heat generation defined by Equation (11), cal/s
- ΔH Heat of reaction (less than zero for exothermic reactions), cal/mol

LITERATURE CITED

1. Corman, J. C., "System Analysis of Simplified IGCC Plants," Topical Report for the Department of Energy, Contract No. DE-AC21-80ET14928, 1986.
2. Grindley, T., and G. Steinfeld, "Development and Testing of Regenerable Hot Coal Gas Desulfurization Sorbents," Second Ann. Contractor's Mtg. on Contaminant Control in Hot Coal-Derived Gas Streams, Report DOE/METC/82–47, 1982.
3. Levenspiel, O., *Chemical Reaction Engineering*, John Wiley and Sons, New York, 1972.
4. Szekely, J., J. W. Evans, and H. Y. Sohn, *Gas-Solid Reactions*, Academic Press, New York, 1976.
5. Gibson III, J. B., and D. P. Harrison, *Ind. Eng. Chem. Proc. Des. Dev.*, **19**, 231 (1980).
6. Fotch, G. D., L. N. Sa, P. V. Ranade, and D. P. Harrison, "Structural Property Changes in Metal Oxide Hot Coal Gas Desulfurization Sorbents," Final Report, Department of Energy Contract DE-AC21-84MC21166, 1986.
7. Kim, B. M., and R. E. Ayala, "Hot Hydrogen Sulfide Removal Process Modeling and Experimental Analysis," Final Report for Niagara-Mohawk Power Corporation, General Electric Company, 87SRD006, 1987.
8. Welty, J. R., C. E. Wicks, and R. E. Wilson, *Fundamentals of Momentum, Heat, and Mass Transfer*, John Wiley and Sons, New York, 1976.

Testing of Novel Sorbents for H_2S Removal from Coal Gas

S. K. Gangwal, J. M. Stogner, and S. M. Harkins
Research Triangle Institute, Research Triangle Park, NC 27709

and

S. J. Bossart
Morgantown Energy Technology Center, Morgantown, WV 26507

Application of zinc ferrite, a regenerable mixed metal oxide, for the removal of H_2S from hot coal derived gas streams is limited to a maximum temperature of about 1,250°F (677°C) and to a minimum H_2S concentration of about 5 ppmv in the cleaned gas. Four novel sorbents that have shown potential for overcoming the limitations of zinc ferrite [1, 4] were selected for development and bench-scale testing. Several variations of these mixed metal oxides were prepared, using different amounts of binders. They were tested in the presence of simulated coal gas using a thermogravimetric reactor (TGR) for selection of preparations possessing an adequate combination of reactivity, regenerability, capacity, and strength. Limited bench-scale tests were conducted in the presence of simulated fluidized-bed coal gasifier product gases at pressures from 1 to 2 MPa, temperatures from 525°C to 625°C and space velocities from 1,000 to 3000 $Nm^3/(m^3 \cdot h)$.

INTRODUCTION

Integrated gasification combined-cycle (IGCC) and gasifier/molten carbonate fuel cell (MCFC) power systems employing hot gas cleanup are two of the most promising advanced technologies for producing electric power from coal [9]. These systems feature temperature and pressure matching of system components and modular shop-fabricated construction. Figure 1 shows the IGCC system schematic. The gasifier/MCFC system schematic would be identical to Figure 1, except that the gas turbine block would be replaced with an MCFC power generation system. Matching of the pressure and temperature of the coal gasifier, hot gas cleanup device, and the power generator attempts to eliminate the requirement for expansive heat recovery equipment and efficiency losses associated with coal gas scrubbing.

Use of coal for power generation is generally considered to have a greater environmental impact than other fuel feedstocks such as oil and natural gas. This is primarily due to the high levels of contaminants in coal, which may be released to the atmosphere or deposited on the land. The air emissions of primary concern are particulates, sulfur dioxides, and nitrogen oxides. Advanced IGCC systems, using hot gas cleanup, are targeted toward reducing contaminants to very low levels so that environmental considerations are eliminated from the choice of using coal versus natural gas or oil as a fuel feedstock.

Sulfur has received more attention than any other coal contaminant. Power generation facilities release sulfur to the atmosphere primarily in the form of sulfur dioxide, which is a precursor to "acid rain" formation. Sulfur removal is important for protection of MCFC components and compliance with environmental regulations. The gasification/MCFC system has much more stringent sulfur removal requirements than those for the IGCC system, due to the sensitivity of the fuel cell. Sulfur removal to less than 1 ppmv may be required to ensure fuel cell operability.

The development of hot gas desulfurization technologies has focused on solid metal-oxide sorbents that can remove reduced sulfur species from the coal gas and then be reused for further sulfur removal after regeneration with air. Zinc ferrite (an iron and zinc compound with a spinel structure) is presently the leading candidate sorbent [2]. It has a high sulfur removal capability at temperatures up to 1,250°F (677°C) and is easily regenerated with air [5, 6, 7, 8]. The sulfur content in the cleaned fuel gas exiting the zinc ferrite sorbent is typically less than 10 ppmv. This sulfur level is acceptable for fuel gas specifications to the gas turbine and is far below the level prescribed by current environmental regulations. For gasi-

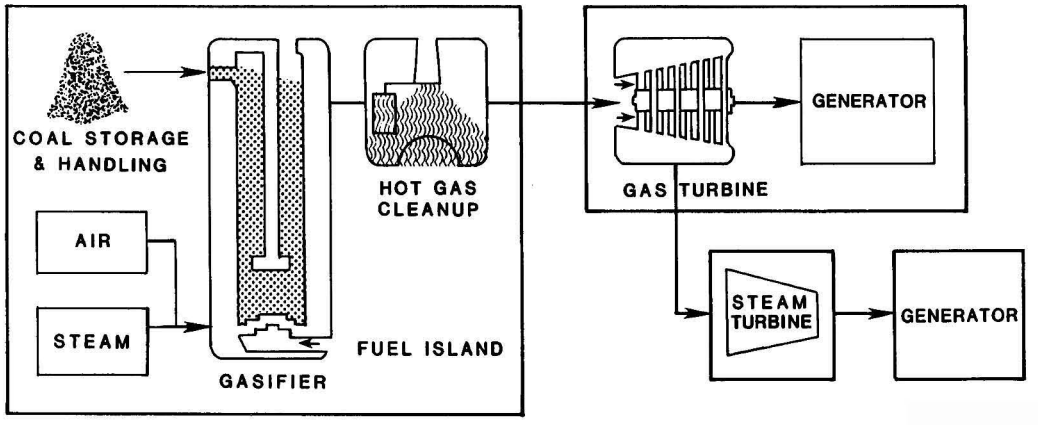

Figure 1. Integrated gasification combined-cycle system for power generation.

fier/MCFC applications, a polishing sulfur sorbent such as nickel oxide would be required after bulk sulfur removal by zinc ferrite.

The sulfur dioxide produced during regeneration of the zinc ferrite can be treated with one of several processes available for sulfur dioxide control. The objective is to recover the sulfur in an environmentally acceptable, resaleable, or readily disposable form. Process options include conversion to elemental sulfur suitable for sale, production of sulfuric acid, and conversion to a disposable sodium or calcium sulfate. Another option is the recycle of the sulfur dioxide-containing stream to the coal gasifier for reaction with the dolomite or limestone, which may be incorporated as an in-bed desulfurization sorbent.

There are several potential improvements possible over existing zinc ferrite technology. These include extension of the operating temperature above 1,250°F (677°C), removal of coal-gas sulfur to less than 1 ppmv, simplified handling of regeneration off-gases, increased sorbent capacity, and capability to mitigate other coal-derived contaminants (e.g., chloride and ammonia). Recent laboratory-scale experiments [*1, 3*] have identified novel sorbents that may have the potential for removal of sulfur to less than 1 ppmv and for operation at temperatures above 1,250°F (677°C). Based on these experiments, the following sorbents were chosen for further development and bench-scale testing:

Chemical Formulation	Designation
$(ZnO)_{0.86}$-$(CuO)_{0.14}$-Fe_2O_3	(ZC)F
$(CuO)(Al_2O_3)$	CA
$(CuO)_3(Al_2O_3)(Fe_2O_3)$	(C3)FA
$(ZnO)_{0.8}(TiO_2)$	(0.8Z)T

The (ZC)F formulation is essentially a modification of the zinc ferrite sorbent in which a small amount of the zinc oxide is replaced with copper oxide. The addition of copper oxide to zinc ferrite has been shown to reduce sulfur levels to less than 1 ppmv. It is also capable of converting over 50% of the ammonia in the coal gas to nitrogen and hydrogen. Adding copper to the zinc ferrite formulation may enable this sorbent to be used directly for gasifier/MCFC applications without the need for a polishing sulfur sorbent.

The CA and (C3)FA formulations have the potential of removing sulfur to lower levels and of operating at temperatures higher than the capabilities for zinc ferrite. The addition of aluminum oxide to copper-containing sorbents is thought to stabilize the copper as copper oxide and minimize reduction to copper metal. Based on thermodynamic calculations, lower sulfur levels can be achieved if the coal-gas sulfur reacts with copper oxide rather than copper metal.

TABLE 1. SORBENT SPECIFICATIONS

Form:	Cylindrical extrudate
Diameter:	3/16″ (4.76 mm)
Length:	3/8″ to 1/2″ (9.5 to 12.7 mm)
BET surface area:	≥ 2 m^2/g
Pore volume[a]:	≥ 0.3 cm^3/g
ASTM crush strength[b]:	≥ 1 lb/mm (4.5 N/mm)
Desired X-ray diffraction phases:	(ZC)F—$ZnFe_2O_4$, $CuFe_2O_4$ (0.8Z)T—$ZnTiO_3$, Zn_2TiO_4, $Zn_2Ti_3O_8$ CA—$CuAl_2O_4$ (C3)FA—$CuFe_2O_4$, $CuAl_2O_4$, CuO

[a] Based on mercury porosimeter.
[b] Radial crush strength based on ASTM D-4179.

The (0.8Z)T formulation has the potential to extend the operating temperature range of zinc-based sorbents above 1,250°F (677°C). Addition of titanium to zinc-based sorbents is thought to stabilize the zinc oxide as zinc titanate and minimize vaporization of zinc. Zinc vaporization after reduction of zinc oxide to zinc metal can become a problem for zinc ferrite at temperatures exceeding 1,250°F (677°C).

The ultimate objectives were to evaluate desulfurization performance of novel sorbents using a versatile high-temperature/high-pressure desulfurization reactor system (bench-unit), to develop a conceptual design, and evaluate the economics for commercial-scale (100 MW) desulfurization systems employing these sorbents. The study is in its initial stages. The overall approach is presented, followed by details of sorbent preparation and properties, details of sorbent screening tests, design details of the bench-unit, and limited bench-scale test results.

OVERALL APPROACH

Following the selection of novel sorbent formulations for development and testing, a list of desirable sorbent specifications was prepared, based on prior experience with the zinc ferrite sorbent and the novel sorbents. United Catalyst, Inc. (UCI) of Louisville, Kentucky, who

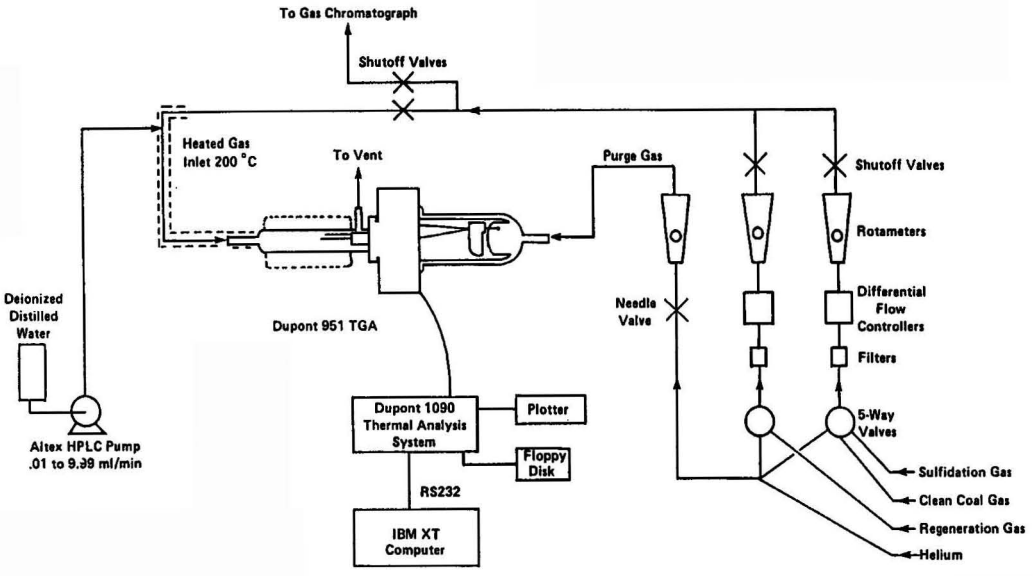

Figure 2. Thermogravimetric reactor system.

TABLE 2. TGR TEST GAS COMPOSITIONS (%)

	Clean Coal Gas	Sulfidation Gas	Regeneration Gas
H_2	10.4	10.4	—
CO_2	4.5	4.5	—
CO	16.0	16.0	—
N_2	42.5	39.9	56.0
H_2O	26.6	26.6	41.0
H_2S	—	2.6	—
O_2	—	—	3.0

had successfully prepared the zinc ferrite and (ZC)F sorbents for Morgantown Energy Technology Center (METC) in the past, was requested to manufacture and supply the sorbents with the desired specifications (Table 1). Before preparing large batches of sorbents for bench-scale testing, small quantities of each sorbent were prepared with varying amounts of binder content. Initial preparations indicated the necessity for 2% inorganic binder (bentonite) to achieve desired crush strength in the sorbents. However, organic binder (methyl cellulose) content was varied from 0–10% to provide a trade-off between porosity and strength. The sorbent preparation consisted of high temperature (1,600°F [871°C]) calcination of stoichiometric amount of the oxides. The differing levels of organic binder that were completely burned off during calcination resulted in the creation of differing levels of porosity and pore structure. At least three variations were prepared for each sorbent in small quantities. These variations were tested in the presence of simulated coal gas using a thermogravimetric reactor (TGR). The TGR tests consisted of two sulfidations and an interim regeneration. The tests gave a measure of the sorbents' reactivity and regenerability.

The TGR screening tests of (ZC)F and (0.8Z)T sorbents have been completed and 1 ft^3 (28.3 L) batches of these sorbents have been prepared for bench-scale testing. Sorbents CA and (C3)FA are still undergoing screening because, although reactivity and regenerability of some of the sorbents have been found acceptable, their strength has been found to undergo severe reduction following two sulfidations and one regeneration on the TGR. While sorbent preparation and TGR screening tests were being carried out, a high pressure/high temperature bench-scale test unit was designed, constructed, and commissioned. A limited number of bench-scale tests have been conducted with the (ZC)F and (0.8Z)T sorbents. In the future, each sorbent will be subjected to a series of parametric tests. Pressure, temperature, H_2S concentration, and space velocity will be the variables investigated during testing. Each sorbent will also be tested over multiple cycles and in the presence of other coal gas contaminants (e.g. chloride, ammonia, and tar). Based on these test results, preliminary conceptual design and economic comparison of sorbents for use in commercial-scale (100 MW) desulfurization systems will be carried out. Both IGCC and gasifier/MCFC power plants will be considered in the economic evaluation.

TGR System and Test Procedure

An atmospheric pressure TGR system, based on the Dupont 951 TGA, was used for screening the sorbent variations. A schematic diagram of this system is shown in Figure 2. Each TGR test was carried out with one pellet on the balance arm and four additional pellets in the reaction zone slightly downstream of the balance arm pellet. The additional pellets were necessary to enable a representative measurement of crush strength of the pellets after the test. The general TGR test procedure consisted of the following steps in sequence:

Step 1. 30-minute reduction in clean simulated coal gas at 550°C.
Step 2. 2.5 hour sulfidation in simulated coal gas at 550°C.
Step 3. 2 hour oxidative regeneration at 650°C.
Step 4. 30 minute reductive regeneration in clean simulated coal gas at 550°C.
Step 5. 2.5 hour sulfidation in simulated coal gas at 550°C.

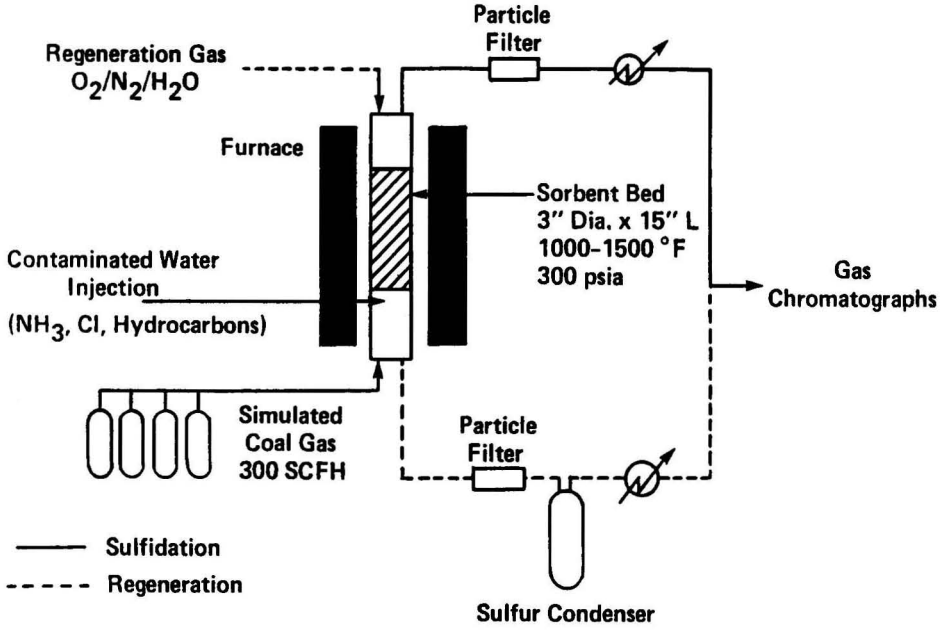

Figure 3. Bench-scale desulfurization reactor system.

The TGR test gas compositions are shown in Table 2. Following the test sequence, the BET surface area of the used balance arm pellet and the average crush strength of the five pellets were measured. The TGR test was designed to crudely simulate the events in a fixed-bed reactor. During initial stages of sulfidation in a fixed-bed, the bottom of the bed would be exposed to sulfidation gas, but a major portion of the bed would be exposed to nearly clean reducing gas. This was the reason for including Step 1 in the test. Step 4 was used to decompose the residual sulfate (as indicated by incomplete regeneration) formed during oxidative regeneration, Step 3. Steps 2, 3, and 5 represented the 1.5 cycles of the test, which provided a measure of the sorbent's reactivity, regenerability, and capacity.

Although the test procedure described above was generally followed for all sorbents, with the CA and (C3)FA sorbents a few tests were also carried out in which the reduction steps were omitted. A few tests were also carried out in which a higher oxidative regeneration temperature of 725°C was used to minimize sulfate formation.

Bench-Scale Unit

A highly versatile bench-scale reactor system was constructed and commissioned for the testing of the novel sorbents at high pressure and temperature. A simplified schematic of the system is shown in Figure 3. The most significant design features of the bench unit are listed in Table 3. The reactor dimensions are shown in Figure 4. The bench unit has been designed for a maximum flow of 300 scfh (8.5 Nm^3/h) of simulated coal gas at a maximum pressure of 300 psia (2 MPa) and a maximum temperature of 1,500°F (816°C). The fixed-bed reactor is 3.06" (7.75 cm) in diameter and the usual height of the test sorbent bed is 15" (38 cm). The sorbent volume tested is typically 1.75 liters. The unit is constructed on a skid so that it can be easily transported to gasifier sites for testing with actual coal gas in the future. The unit is constructed of either 316 or 304 stainless steel. The wetted parts exposed to coal gas have been Alon processed (a high temperature aluminum vapor treatment) to prevent corrosion of the stainless steel by sulfur gases in the presence of steam. This also facilitates accurate measurement of low level sulfur gases. The removable sorbent cage facilitates quick turnaround for changing sorbent in between runs. Bypassing around the cage is prevented by a secondary O-ring, as shown in Figure 4, which is squeezed by the cage, which in turn is pressed by the main reactor flange.

TABLE 3. SIGNIFICANT DESIGN FEATURES OF BENCH UNIT

The sorbent cage is easily removable following runs.
Separate lines, in opposite direction, are provided for regeneration and sulfidation and all exposed stainless steel surfaces above 200°C are Alon processed to prevent corrosion.
Automated on-line gas chromatographs with thermal conductivity and flame photometric detectors allow complete gas analysis and sulfur gas speciation down to 0.1 ppmv.
Sulfur formed during regeneration may be either oxidized to SO_2 using a secondary oxygen line at bed exit or collected in a trap.
A separate line is provided for injecting trace coal gas contaminants directly under the sorbent bed.
Entrained particulates during either regeneration or sulfidation can be captured and measured using removable 5 μm ceramic filters.
Onset of reactor plugging may be detected by an electronic differential pressure monitor.
Precise pressure control is provided by two back-pressure regulators in series.
Temperature is monitored at seven positions along the sorbent bed using an Alon processed thermowell.
Seven high pressure mass flow controllers and two steam generators provide high flexibility in generating desired gas compositions.

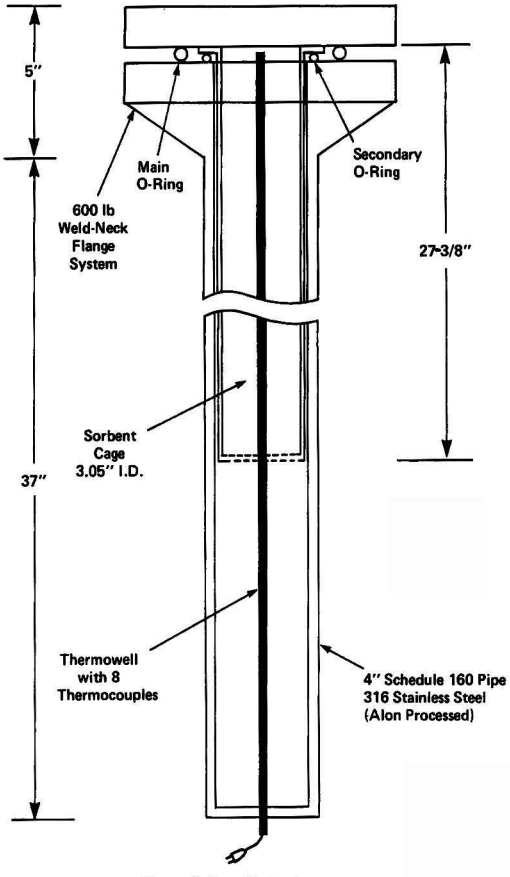

Figure 4. Desulfurization reactor.

RESULTS AND DISCUSSION

Sorbent Screening

The physical properties of selected sorbent variations are shown in Table 4. The corresponding X-ray diffraction phases are shown in Table 5. The CA and (C3)FA sorbents corresponding to 10% burnout had poor crush strength and are omitted from the table. TGR screening tests for (ZC)F, (0.8Z)T, CA and (C3)FA sorbent variations are shown in Figures 5, 6, 7, and 8, respectively. The steps (1 through 5) shown in these figures were discussed earlier with the description of the TGR system and test procedure. The surface area and crush strength of the fresh and TGR sulfided sorbent variations are compared in Table 6. The mercury pore volume of the fresh and sulfided (0.8Z)T sorbent variations are shown in Table 7.

For the TGR test of the (ZC)F sorbents (Figure 5), the rapid initial weight loss is due to the initial 30 minute reduction, resulting in partial reduction of the CuO to Cu and Fe_2O_3 to Fe_3O_4. Approximately 30–50% of the theoretical maximum reduction occurred during this step. Reduction of CuO is undesirable because of significantly higher thermodynamic H_2S removal efficiency of CuO versus Cu. The 30 minute reduction is followed by 2.5 hours of sulfidation during which approximately 12% weight gain occurs (from initial weight). The weight gain corresponds closely to complete formation of FeS, ZnS, and Cu_2S (i.e., nearly complete conversion of Fe_2O_3, ZnO, and CuO to the sulfides). During oxidative regeneration at 650°C, complete regeneration does not occur, presumably due to formation of $CuSO_4$ and $ZnSO_4$. During reductive regeneration at 550°C, this sulfate quickly decomposes and the original weight corresponding to reduced form is quickly achieved. This is followed by a second sulfidation at 550°C.

Although significant differences in TGR performance do not exist between the variations, one interesting observation is that the sample prepared with 0% organic binder maintained a second sulfidation cycle very similar to the first. The other two sorbents show lower reactivity during the second cycle. Based on the TGR test, a clear choice between the variations is not possible, but crush strength results (Tables 4 and 6) indicate L-2868 to be the sorbent of choice. One ft^3 (28.3 L) of this sorbent was prepared for bench-scale testing.

For the TGR test of the (0.8Z)T sorbent (Figure 6) the initial weight loss during reduction of about 0.13% was quite insignificant. There is a much smaller amount of residual sulfate after the 650°C oxidative regeneration than the (ZC)F sorbents. The most striking feature, however, is the significantly higher reactivity of L-2887 prepared with 10% organic binder than the two other (0.8Z)T sorbents. The weight gain during sulfidation is nearly identical during both cycles, and corresponds to nearly complete conversion of ZnO to ZnS (Table 7). The crush strengths of the fresh and sulfided (0.8Z)T samples are quite respectable (Tables 4 and 6). The mercury pore volume reduction of the sorbents appears to correlate with the percent conversion (Table 7). Based on the above results, L-2887 was chosen and 1 ft^3 (28.3 L) was manufactured for bench-scale testing.

TABLE 4. MECHANICAL AND STRUCTURAL PROPERTIES OF SORBENT VARIATIONS

Designation	UCI number	Organic binder (%)	Bulk density (g/cm^3)	BET surface area (m^2/g)	Mercury pore volume (cm^3/g)	Macroporosity (%)	Average pore diameter (μm)	Crush strength (N/mm)	Calcination temperature and time °C (h)
(ZC)F	L-2868	0	1.37	4.0	0.32	65	0.31	15.8	843 (2)
(ZC)F	L-2869	5	1.20	3.1	0.33	59	0.39	4.9	843 (2)
(ZC)F	L-2870	10	0.99	2.5	0.32	51	0.41	3.0	843 (2)
(0.8Z)T	L-2885	0	1.11	3.2	0.32	57	0.29	28.9	871 (2)
(0.8Z)T	L-2886	5	1.09	4.3	0.37	66	0.37	28.9	871 (2)
(0.8Z)T	L-2887	10	1.00	3.3	0.37	60	0.55	20.9	871 (2)
CA	L-2890	0	0.86	69	0.45	63	0.046	3.10	871 (2)
CA	L-2891	5	0.84	48	0.42	55	0.18	4.50	871 (2)
(C3)FA	L-2888	0	1.35	17	0.29	62	0.10	30.7	871 (2)
(C3)FA	L-2889	5	1.25	11	0.35	66	0.24	12.5	871 (2)

TABLE 5. SORBENT XRD CHEMICAL PHASES AND MEAN CRYSTALLITE SIZES[a]

Designation	UCI Number	XRD phases — Percent (crystallite size in angstroms) [1 Angstrom = 0.1 nm]
(ZC)F	L-2868	CuO-4.71; $ZnFe_2O_4$ (1669); CuO (small amount)
(ZC)F	L-2869	CuO-4.52; $ZnFe_2O_4$ (>2,000)
(ZC)F	L-2870	CuO-4.68; $ZnFe_2O_4$ (>2,000)
(0.8Z)T	L-2885	$Zn_2Ti_3O_8$ (1718); α-Zn_2TiO_4[(?)]; Anatase TiO_2-44 (>2000); Rutile TiO_2 — small amount; ZnO — small amount
(0.8Z)T	L-2886	$Zn_2Ti_3O_8$ — 64 (>2000); α-Zn_2TiO_4-36(888); $ZnTiO_3$ — small amount; Rutile TiO_2-56 (>2000); Anatase TiO_2-44 (>2000); ZnO[(?)]
(0.8Z)T	L-2887	$Zn_2Ti_3O_8$-66 (>2000); α-Zn_2TiO_4-34(1000); $ZnTiO_3$-small amount; Anatase TiO_2-61(>2000), Rutile TiO_2-39 (>2000); ZnO[(?)]
CA	L-2890	$CuAl_2O_4$-60(199); CuO-40(228); γ-Al_2O_3-dispersed
CA	L-2891	$CuAl_2O_4$-87(252); CuO-13(408); γ-Al_2O_3-dispersed
(C3)FA	L-2888	$CuFe_2O_4$-40(288); $CuAl_2O_4$-30(328); CuO-30(224); γ-Fe_2O_3[(?)]
(C3)FA	L-2889	$CuFe_2O_4$-42(619); $CuAl_2O_4$-32(790); CuO-26(500); γ-Fe_2O_3

[a] The CuO analysis in (ZC)F sorbents was by wet chemical methods.
[(?)] Tentative identification.

The TGR results for CA sorbent variations (0 and 5 percent organic) are shown in Figure 7. Curves 1 and 3 compare L-2890 performance at 650°C and 725°C oxidative regeneration temperatures; curves 1 and 2 illustrate the effect of the organic binder content. Different times were used for different cycles to allow better visualization because they do not affect conclusion for the sorbent performance. The effect of organic binder content appears insignificant. This may be a direct consequence of the very high surface areas and small crystallite sizes of these sorbents (see Tables 1 and 2). The reduction is very rapid and corresponds to nearly complete CuO reduction to Cu in all cases.

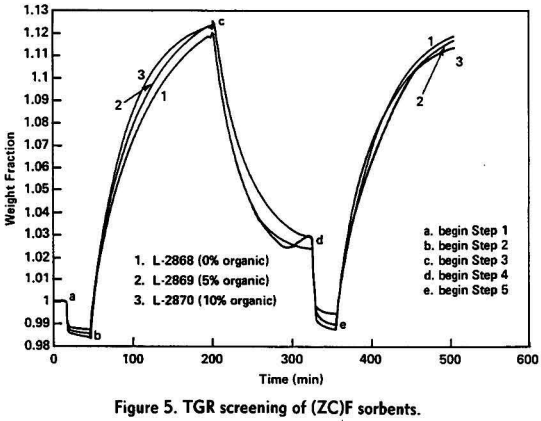

Figure 5. TGR screening of (ZC)F sorbents.

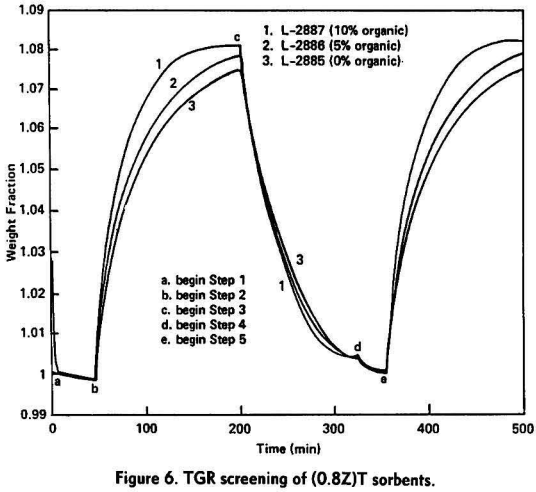

Figure 6. TGR screening of (0.8Z)T sorbents.

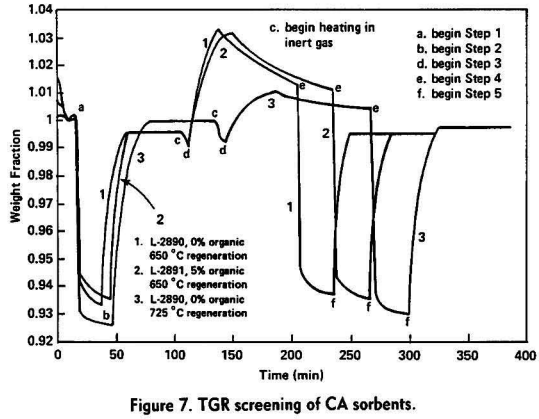

Figure 7. TGR screening of CA sorbents.

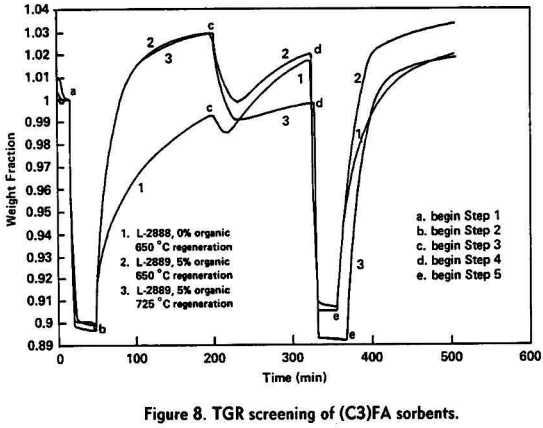

Figure 8. TGR screening of (C3)FA sorbents.

TABLE 6. EFFECT OF 1.5 CYCLES ON SORBENT STRUCTURAL PROPERTIES (550°C SULFIDATION, 650°C OXIDATIVE REGENERATION)

Designation	UCI Number	Crush strength (lb/mm)		Surface area (m^2/g)	
		Fresh	Sulfided	Fresh	Sulfided
(ZC)F	L-2868	3.55	3.81	4.0	14.39
(ZC)F	L-2869	1.10	2.06	3.07	2.46
(ZC)F	L-2870	0.67	1.23	2.53	2.40
(0.8Z)T	L-2885	6.5	6.8	3.18	8.41
(0.8Z)T	L-2886	6.5	>7.0	4.33	8.38
(0.8Z)T	L-2887	4.7	5.5	3.25	12.5
CA	L-2890	0.7	0.9	69	36.6
CA	L-2891	1.0	1.64	48	53.5
CA[a]	L-2890	0.7	0.5	69	54.1
(C3)FA	L-2888	6.9	2.07	17.3	18.5
(C3)FA	L-2889	2.8	2.0	10.8	20.7
(C3)FA[a]	L-2889	2.8	1.28	10.8	17.6

[a] 725°C oxidative regeneration.

TABLE 7. COMPARISON OF PERCENT CONVERSION ON THE TGR AND PERCENT REDUCTION IN PORE VOLUME (cm^3/g) OF (0.8Z)T SORBENTS

Sample number[a]	Mercury pore volume		% Reduction in pore volume	% Conversion of ZnO to ZnS
	Fresh	Sulfided		
L-2885	0.32	0.236	26.3	87.2
L-2886	0.368	0.211	42.7	91.1
L-2887	0.372	0.208	44.1	94.9

[a] For complete specifications, see Tables 4 and 5.

The sulfidation is also very rapid, presumably due to the high surface area and pore volume. Once a constant weight is achieved, it remains stable. The sorbent is then heated to the required regeneration temperature in inert gas during which it loses some weight indicating decomposition of the sulfided sorbent. The oxidative regeneration is then begun, and shows a weight gain followed by a slow weight loss. One hypothesis that may explain this observation is a series reaction of the following type:

$$Cu_2S \xrightarrow{k_1} CuSO_4 \cdot CuO \xrightarrow{k_2} 2CuO$$

The intermediate $CuSO_4 \cdot CuO$ (i.e., Cu_2SO_5) is a compound with established thermodynamic formation data, although its formation in our tests is yet to be confirmed using X-ray-diffraction measurements.

Assuming the above (or similar) hypothesis applies, the peak in the weight curve is much lower at the higher oxidative regeneration temperature, indicating a substantially higher k_2. The first reaction is apparently diffusion-limited, with a low apparent activation energy, whereas the activation energy of the decomposition reaction is high and thus:

TABLE 8. BENCH-SCALE TEST RESULTS FOR (ZC)F AND (0.8Z)T SORBENTS

		(ZC)F sorbent				(0.8Z) sorbent			
		Cycle 1		Cycle 2		Cycle 1		Cycle 2	
Pressure (psia/MPa)		221/1.5		154/1.05		267/1.82		267/1.82	
Average temperature (°F/°C)		1,094/590		1,053/567		1,102/594		1,074/579	
Space velocity $Nm^3/(m^3 \cdot h)$		2809		2120		2120		1060	
Gas composition (volume %)		Inlet	Outlet (average)	Inlet	Outlet (average)	Inlet	Outlet (average)	Inlet	Outlet (average)
	H_2	15.4	18.2	13.9	20.3	13.9	18.6	13.3	21.0
	CO_2	15.6	19.4	11.5	19.7	11.5	18.1	10.5	18.5
	H_2O	10.8	9.5	19.8	13.5	19.8	14.9	23.0	15.4
	H_2S	1.60	—	1.5	—	1.5	—	1.41	—
	N_2	39.5	39.3	37.9	38.8	37.9	38.4	36.9	36.8
	CH_4	0.6	0.6	0.6	0.6	0.6	0.6	0.6	0.6
	CO	16.5	13.0	14.9	7.1	14.9	9.4	15.4	7.7
Gas flow rate (Nm^3/h)		4.92	4.95	3.73	3.64	3.73	3.69	1.87	1.86
Sulfur loaded prior to breakthrough[a]	g/100 g	14.5		13.4		7.0		7.2	
	% of maximum **	44.1		41.4		40.5		41.4	

[a] Arbitrarily defined as 100 ppmv for (ZC)F sorbent and 500 ppmv for (0.8Z)T sorbent.
** Based on complete conversion to ZnS, Cu_2S, and FeS.

$$\frac{k_{2_{725°C}}}{k_{2_{650°C}}} >> \frac{k_{1_{725°C}}}{k_{1_{650°C}}}$$

The important consequence of the data is that the final weight of the oxidatively regenerated sorbent is much closer to the original weight at 725°C versus 650°C. Another important implication of the data is the insignificant deterioration in second cycle performance of the sorbent. We have also tested the CA sorbent omitting the reduction steps (not shown here) and found insignificant deterioration of performance.

Based on the above results, the CA sorbent should be regenerated at higher temperatures than about 725°C to minimize the sulfate formation. The sorbent may be a good candidate for integration with gasifiers with higher gas exit temperatures. However, the problem of low crush strength of the CA sorbent is yet to be resolved and it decreases with higher temperature cycles (See Table 6). We are currently attempting to prepare CA with a higher crush strength using a higher bentonite content and/or a higher calcination temperature.

The results for the (C3)FA sorbent are shown in Figure 8. Curves 1 and 2 show the effect of organic binder content; for curve 3 a higher oxidative regeneration temperature of 725°C (as for CA) was used. The reduction is extremely rapid. Based on stoichiometry of the sorbent, complete reduction of CuO to Cu and Fe_2O_3 to Fe_3O_4 would result in a weight loss of 10.45%. The actual weight loss is very close to this value. The first sulfidation cycles for curves 1 and 2 (i.e., sorbents with 0% and 5% organic binder, respectively) show significant differences, with L-2889 showing a much superior rate and amount of weight gain. The oxidative regeneration at 650°C shows a weight loss followed by a weight gain. This indicates competing reactions, as with the CA sorbent. However, the chemistry may be substantially more complex for (C3)FA than for CA because of the obvious reason of two active ingredients for (C3)FA versus one for CA.

One possible explanation of the oxidative regeneration curves for (C3)FA may be that weight loss due to conversion of FeS to Fe_2O_3 and weight gain due to sulfate formation from Cu_2S and FeS occur simultaneously. The second sulfidation for L-2889 (5% organic) is essentially similar to the first. On the other hand, for L-2888 prepared without organic binder, it is significantly improved. This indicates significant structural changes in L-2888 after one cycle. The fact that structural changes do occur in all (C3)FA sorbents is evident from the crush strength data (Table 6). The only difference between curves 2 and 3 is that a 725°C regeneration temperature was used for curve 3 instead of 650°C. The regeneration is significantly more rapid at 725°C, and the weight gain after regeneration is nearly insignificant showing negligible sulfate formation. The final sorbent weight is nearly the same as the original weight. The second sulfidation cycle for curve 3, however, showed slightly deteriorated performance. The regeneration temperature of 725°C appears to be necessary to prevent sulfate formation. These sorbents may also be good candidates for integration with higher temperature gasifiers.

(ZC)F and (0.8Z)T formulations have already been finalized for bench unit testing. CA and (C3)FA formulations are yet to be finalized because attempts are being made to prepare these sorbents with higher crush strength and better maintenance of crush strength during testing.

TABLE 9. H_2S AND COS PRE-BREAKTHROUGH PROFILES FOR BENCH-SCALE TESTS WITH (ZC)F AND (0.8Z)T SORBENTS (DRY BASIS, SEE TABLE 8 FOR TEST CONDITIONS)

Run time (min)	(ZC)F sorbent, cycle 2		(0.8Z)T, sorbent, cycle 2	
	H_2S (ppmv)	COS (ppmv)	H_2S (ppmv)	COS (ppmv)
10	0.2	N.D.	9	1.2
20	0.24	N.D.	8	0.6
40	0.40	N.D.	8	0.3
60	0.63	N.D.	8	0.3
80	0.9	N.D.	8	<0.3
100	0.9	N.D.	9	0.3
120	1.2	N.D.	8	0.3
140	2.0	N.D.	11	0.3
160	2.7	N.D.	17	0.7
180	14.0	0.3	100	1.8
201	60	1.6	380	5.5
207	80	2.3	530	8
211	100	3	N.M.	N.M.
216	130	4	N.M.	N.M.

N.D. = Not detected; N.M. = Not measured.

Bench-Scale Tests

Limited bench-scale testing has been carried out. Sulfidation conditions and performance for (ZC)F and (0.8Z)T sorbents are presented in Tables 8 and 9. Each of these sorbents was subjected to two sulfidation cycles at the conditions shown, with an interim regeneration.

Considering sulfidation first, (ZC)F demonstrated very high removal efficiency with H_2S staying below 1 ppmv for a significant portion of the test prior to breakthrough. There was a slow, but orderly increase of H_2S from nearly 0 ppm initially to about 2 ppmv in 140 minutes. The low level of H_2S is attributable to reaction of either the copper oxide (CuO) phase or the copper ferrite ($CuFe_2O_4$) phase. Both have very favorable thermodynamics for H_2S removal [4]. The zinc titanate sorbent reduced the H_2S to about 8 ppmv (~7 ppmv on a wet basis) prior to breakthrough. This corresponds approximately to ZnO sulfidation thermodynamics at the temperature of the test. The second cycle performance of the sorbents was nearly as good as the first, indicating good regenerability. The striking feature of the data is the insensitivity of sulfur loading (as a percent of maximum prior to breakthrough) to test conditions and sorbent type. The low sorbent utilization may be caused by increased diffusional limitations at elevated pressure. Significant shift reaction occurred over both sorbents, as evident from the major gas species concentrations in the inlet and outlet gases. Condensate samples were saved from the sulfidation tests and are being analyzed for sulfur content.

The regeneration of both sorbents was carried out in two stages—oxidative regeneration and reductive regeneration. During oxidative regeneration, an air/steam mixture was used in an appropriate ratio (typically 10/90 to 20/80) with an inlet temperature of 538°C (1,000°F). The pressure and space velocity were matched to the second sulfidation cycle for both sorbents. Significant (approximately 20% of the bed sulfur) elemental sulfur was produced during regeneration of (ZC)F. However, attempts to collect elemental sulfur created significant downstream operational problems. For later runs, a secondary oxidation (pure oxygen) past the bed was utilized to convert all of the sulfur formed to SO_2. Maximum bed temperatures of up to 840°C for the (ZC)F sorbent and 760°C for the (0.8Z)T sorbent were achieved during regeneration. Generally, the air/steam ratio was adjusted to prevent temperatures to rise above 750°C. Following completion of oxidative regeneration (when SO_2 fell below 500 ppm in the effluent), a reductive regeneration was

carried out with a mixture of clean reducing gas and steam to rapidly decompose the residual sulfate prior to the second sulfidation cycle. Typically the oxidative regeneration lasted about 4 hours and the reductive regeneration lasted about 1 hour. The condensate from (ZC)F oxidative regeneration was blue to light blue indicating the presence of copper sulfate. It is being analyzed for copper to get an idea of copper loss from the sorbent.

The sorbents were removed from the bed after the second cycle. Representative samples were saved from the top, middle, and bottom portions of the bed. The crush strengths of the sorbents did not decline after the tests. The samples are presently being analyzed for sulfur and carbon.

CONCLUSIONS

Important conclusions from the work to date are that the (ZC)F sorbent (zinc ferrite modified with small amount of copper oxide) successfully reduced the sulfur level in hot simulated coal derived gas to sub-ppm levels, the target for MCFC applications. The percent conversion of the zinc containing sorbents in a pressurized fixed-bed was nearly insensitive to sorbent type or process conditions. The (C3)FA and CA sorbents should be regenerated at temperatures greater than 725°C to minimize sulfate formation.

The crush strength of the (ZC)F and (0.8Z)T sorbents increased after TGR testing, whereas it decreased for the CA and (C3)FA sorbents after TGR testing at a desirable regeneration temperature of 725°C. Surface areas of the sulfided sorbents increased or decreased randomly after TGR tests and do not appear to relate to conversion. The mercury pore volume of the (0.8Z)T sorbents correlated with percent conversion on the TGR. The amount of organic binder in the original sorbent formulation which is burned off during calcination is important in providing a trade-off between porosity and strength.

ACKNOWLEDGMENTS

Financial support for this work was provided by the U.S. Department of Energy, Morgantown Energy Technology Center under Contract No. DE-AC21-86MC23126. Helpful discussions were held with Dr. Douglas P. Harrison of Louisiana State University, Baton Rouge, and Dr. Thomas Grindley of Morgantown Energy Technology Center. The sorbent samples were manufactured and supplied by United Catalysts, Inc., Louisville, Kentucky.

LITERATURE CITED

1. Bossart, S. J., Morgantown Energy Technology Center, Private Communication, 1986.
2. Day, L. Megan, *Modern Power Sys.*, **6** (11), 71, 1986.
3. Flytzani-Stephanopoulos, M., et. al., "Novel Sorbents for High Temperature Regenerative H_2S Removal," DOE/MC/20417-1898 (DE86004261), 1984.
4. Flytzani-Stephanopoulos, M., et al., "Detailed Studies of Novel Regenerable Sorbents for High-Temperature Coal-Gas Desulfurization," 4th Quarterly Report, Contact No. DE-AC21-85MC22193, 1986.
5. Grindley, T., "The Effect of Temperature and Pressure on the Regeneration of Zinc Ferrite Desulfurization Sorbent," Proceedings, Sixth Annual Meeting on Contaminant Control in Coal-Derived Gas Streams, DOE/METC-86/6042, 190–220, 1986.
6. Grindley, T., and G. Steinfeld, "Development and Testing of Regenerable Hot-Coal-Gas Desulfurization Sorbents," *Proc. Sec. Ann. Mtg. on Contaminant Control in Hot Coal-Derived Gas Stream*, DOE/METC/82-47, 332–359, 1982.
7. Grindley, T., and G. Steinfeld, "Zinc Ferrite Hydrogen Sulfide Absorbent," Proceedings, *Third Ann. Mtg. on Contaminant Control in Hot Coal-Derived Gas Streams*, DOE/METC/84-6, 145–171, 1983.
8. Grindley, T., and G. Steinfeld, "Testing of Zinc Ferrite H_2S Absorbent in a Coal Gasifier Sidestream," *Proc. Fourth Ann. Mtg., on Contaminant Control in Hot Coal-Derived Gas Streams*, DOE/METC/85-3, 314–336, 1984.
9. U.S. Department of Energy, "Hot Gas Cleanup for Electrical Power Generation Systems," Morgantown Energy Technology Center, DOE/METC-86/6038 (DE86006607), May, 1986.

Metal Ion Scavenging from Water with Fine Mesh Ion Exchangers and Microporous Membranes

Robert R. Grinstead
Central Research Department, Dow Chemical USA, 2800 Mitchell Dr., Walnut Creek, CA, 94598
and
H. Hunter Paalman
Western Applied Science & Technology Laboratory, Dow Chemical USA, P.O. Box 1398, Pittsburg, CA 94565

The productivity of ion exchange processes is usually limited by the diffusional process. The use of very fine mesh resins (down to 10–25 microns diameter) in very thin (ca 3–9 mm) beds supported on a microfiltration membrane of three micron pore diameter is described. These systems were used to process a simulated wastewater containing 4000 ppm of NaCl, plus some calcium and magnesium chlorides, as well as 0.2 ppm each of the metal ions Cu, Ni, Pb, Zn, and Cr (III). Regeneration with dilute HCl produced a concentrate of 1/1000 the volume of the feedwater treated.

INTRODUCTION

Increasing concern about environmental damage from various constituents of wastewater discharges has led to increasing restrictions on the allowable levels of numerous species. Foremost among these are certain metal ions, such as those of Cu, As, Hg, Pb, and Ni, toxicities of which are well known, and that are frequent constituents of waste discharges.

Innumerable methods exist for the removal of metal ions from water. Among the simplest are alkaline precipitation methods, wherein metal hydroxides are produced by the addition of an alkali. Although generally effective for most metal cations, the finite solubilities of metal hydroxides usually preclude obtaining treated water containing much less than a few tenths of a ppm [*1, 2*]. Use of a flocculant such as ferric chloride can improve the effectiveness of hydrolytic precipitation, and levels as low as 10 micrograms per liter have been reported [*3, 4*]. Such methods are simple and reliable, their chief disadvantages are the large quantities of sludge produced, and the consequent disposal problem.

Reduction of metal ion concentrations below these levels requires increasingly sophisticated methods, such as ion exchange, sulfide precipitation, and chelating absorbents such as starch xanthates. A number of reviews on this subject have recently appeared [*1, 2, 4*], and a further discussion is beyond the scope of this report.

One of the more attractive methods for removing metal ions is ion exchange, particularly using chelating ion exchange resins. Because most chelating agents have a considerably greater affinity for the transition metal ions, which constitute the bulk of the toxic metals of interest, than they have for the more innocuous ions of calcium and magnesium, chelating exchangers are particularly useful in treating natural waters containing considerable amounts of the latter ions. In addition, the use of ion exchangers as beds provides a large number of theoretical contact stages, leading to the ability to produce very low metal ion concentrations in the column effluents.

Because considerable capital is usually involved, ion exchange is a more expensive process than hydrolytic precipitation, and cost reductions are dependent upon developing the ability to process water more rapidly. In most cases, the limiting process is diffusion of the exchanging species, either through the stagnant film surrounding the resin bead, or into the bead itself. While greater processing rates are achievable by using smaller beads than the conventional 20–50 mesh range, the pressure drops rise quickly to impractical levels.

To circumvent this difficulty the concept of powdered resin was developed in the 1960s, in which ground up resin was used as a precoat in a pressure filter system, providing a thin bed of resin on a suitable screen support [*5*]. This type of system has found use in the boiler water polishing industry and in the treatment of nuclear wastes [*6*]. Although they allow high flow rates on a resin volume basis, these systems are not regenerated or reused.

Another approach has been taken by the Ecotec Corporation of Canada, in which thin beds of fine mesh (down to about 100 mesh) beads are displayed in circular beds, and are regenerated much the same as as conventional bed [*7*]. Although this system takes advantage of the smaller resin size, the latter is not greatly smaller than conventional resin systems.

TABLE 1. RESIN CAPACITIES

Polymer	Cu capacity, mmole/ml resin	Final resin mesh size
Biobeads, 200–325 mesh	0.12	200–325
Biobeads −400 mesh	0.09	325–600

TABLE 2. FEED COMPOSITION

NaCl	4000 ppm
Calcium	120 ppm (present as chloride)
Magnesium	24 ppm (present as chloride)
Cu, Zn, Cr(III), Ni, Pb	0.2 ppm each (present as chloride)
pH	6-8 (adjusted with NH_3)

The present study was undertaken with the aim of reducing the cost of regenerable ion exchange processes by extending their applicability down into the 400–500 mesh range, where extremely fast kinetics can be achieved. Data reported here demonstrate the usefulness of this concept for removal of metal ions from a simulated wastewater down to parts per billion levels.

EXPERIMENTAL METHODS

Resins

Chelex 100 is a polystyrene-based gel-type chelating resin containing the iminodiacetate functional group, and was obtained from the Bio-Rad Corp as a 200–325 mesh (40–70 micron) material. Its chelating capacity was given as 0.7 milliequivalents/ml. Chelex 20 contains the same functional group, but is a macroporous resin of 20–50 mesh size.

The ED3A resins were prepared from gel-type chloromethylated polystyrene-based beads, obtained also from Bio-Rad. A normal 200–400 mesh material, Bio-Beads S-X1 was available as a regular product, and a finer fraction of this material was supplied as a special sample for some of the resins. This sample was labeled "−400 mesh", but the resin made from it was in the 10–40 micron range (325–600 mesh).

ED3A was prepared by the addition of 3.5 moles of sodium chloroacetate to one mole of ethylenediamine in aqueous solution, maintaining the pH at 10–11 and the temperature at 60–70°C. The resulting solution, which contained about equal amounts of EDTA and the triacetate, was used directly. It was expected that reaction of the ED3A with the chloromethyl group of the polymer beads would occur through the single unsubstituted nitrogen proton, while EDTA, containing only tertiary amines, would be unlikely to react.

The chloromethylated beads were first reacted with about 25% of the stoichiometric quantity of trimethylamine to partially quaternize the resin, and then with a solution of the ED3A in water.

At the end of the reaction the beads were washed successively with 1*N* NaCl, 1*N* ammonium hydroxide, and finally water. The extent of the reaction with ED3A was determined by shaking a sample with excess $CuSO_4$, determining the residual copper in the filtrate, and also in an eluate of 3*N* HCl. Capacities of the samples are shown in Table 1.

Equipment

Two types of cells were used. Initially, an Amicon 60 ml ultrafiltration cell with a 13 cm^2 filtration area was used. This cell contained a magnetic stirrer, which was not used, since a stable bed was desired. The cell was fed from a pressurized reservoir, and the permeate was collected on a turntable, or delivered to an interval stepping fraction collector.

For smaller flows a second cell was used, consisting of an in-line pressure filter housing. A number of these were examined, but the one finally selected was a Nuclepore Swinlok filter of 25 mm diameter. Sufficient headroom existed over the membrane to allow a resin bed of at least 10–15 mm depth to be placed.

Membranes

All membranes used in this study were from the Millipore Corp., with three micron pore diameter, and were made of polytetrafluoroethylene bonded to polypropylene.

Feed Solutions

A synthetic solution was prepared to resemble a typical wastewater, and had the composition given in Table 2.

Analytical Methods

The metal ion analyses were performed using an ARL 35000 inductively coupled plasma (ICP) atomic emission spectrometer. The ICP compromise conditions were as follows: power, 1.2 kw; reflected power, less than 10w; observation height, 15 mm above load coil; Argon coolant flow, 40 psi (275 kPa); Argon plasma flow, 30 psi (203 kPa); Argon sample flow, 1 L/min; sample uptake rate, 1.2 ml/min. The following analytical wavelengths (in nm) were used for analysis: Cr: 267.72; Cu: 324.75; Ni: 231.6; Pb: 220.35; Zn: 213.86. High purity (Spex Ind.) multielement standards were used for ICP calibration.

Procedure

A known bulk volume of resin was measured, placed in the cell and allowed to settle, whereupon the bed depth was measured. In the case of the UF cells feed was introduced from a pressurized reservoir, while for in-line filter runs a Masterflex pump was used. Samples were collected in glass tubes which had been first cleaned with nitric acid, followed by rinsing with distilled water. Subsequent uses of the tubes were preceded by rinsing with distilled water. Samples to be analyzed were transferred to polyethylene bottles that had been pre-cleaned with detergent, nitric acid, and ASTM Type 1 deionized water (I-Chem Research, Inc., Hayward, CA).

When sufficient feed solution had been treated the feed reservoir was disconnected and a Masterflex pump was used to pass dilute HCl through the bed as an eluant. Because relatively small samples were taken of the eluate, they were diluted prior to submission for analysis.

EXPERIMENTAL DATA

ED3A Resin Runs

Figures 1 and 2 show data for runs with resins containing the ED3A functional group. In Figure 1, satisfactory performance was obtained up thru the highest flow rate, which was about 73 gpm/cu ft (0.16 cu m/cu m × s). For purposes of classifying performance we have categorized those runs in which about 90% removal was obtained as "satisfactory." In Figure 2, where a higher flow was used, removal efficiencies were clearly much lower, and we conclude that a flow somewhere between 73 and 120

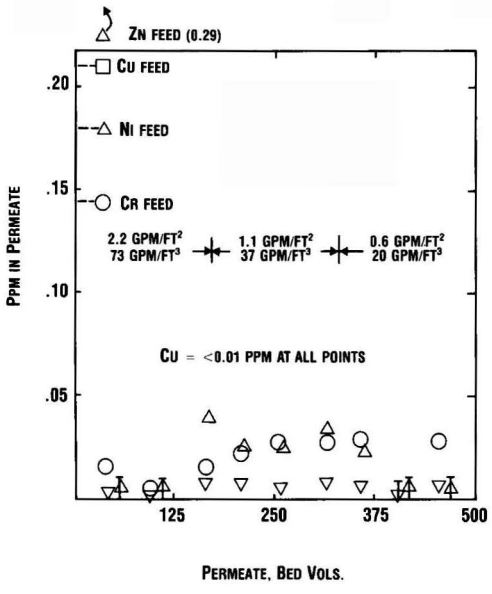

Figure 1. Metal ion scavenging by ED3A resin.

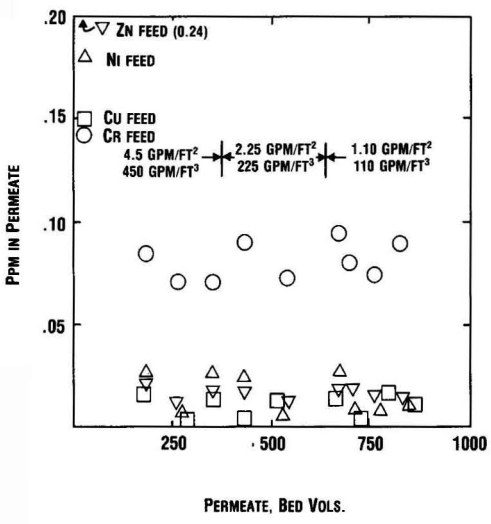

Figure 3. Metal ion scavenging by ED3A resin.

gpm/cu ft (0.16 and 0.27 cu m/cu m × s) would be the limit of satisfactory operation.

Figure 3 presents data for a run with the 325–600 mesh ED3A resin, in which flow rates were varied from 110 to 450 gpm/cu ft (0.25 to 1.00 cu m/cu m × s). Performance in this series was categorized as generally satisfactory, although it is clearly a borderline case for chromium removal.

Chelex 100 Resin Runs

Figure 4 presents data for a set of Chelex 100 runs, in which the flow rate was also varied from 110 to 450 gpm/cu ft (0.25 to 1.00 cu m/cu m × s). Chromium removal was borderline for the slowest flow rate and unsatisfactory for the higher flows; removal of the other metals was quite satisfactory.

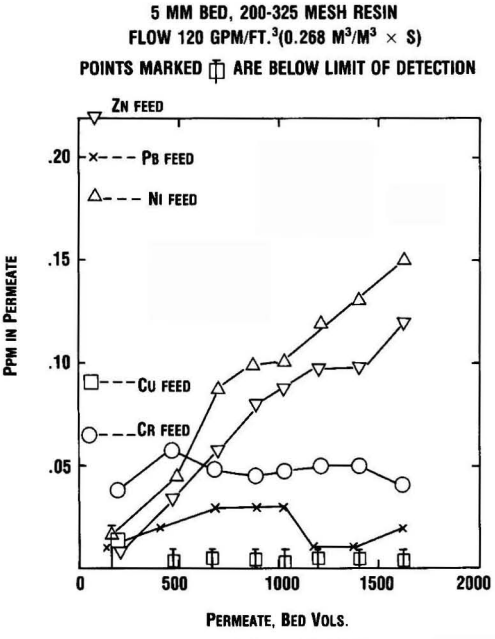

Figure 2. Metal ion polishing with ED3A resin.

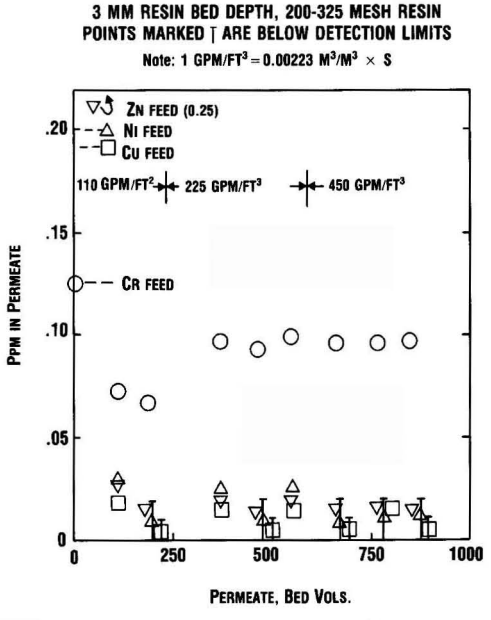

Figure 4. Metal ion polishing by Chelex 100 resin.

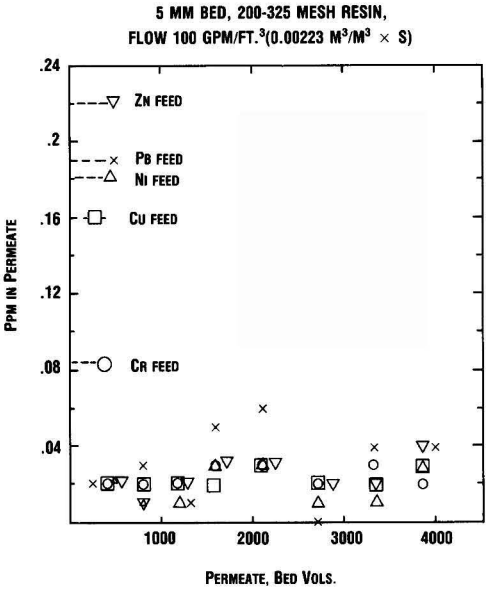

Figure 5. Metal ion polishing with Chelex 100.

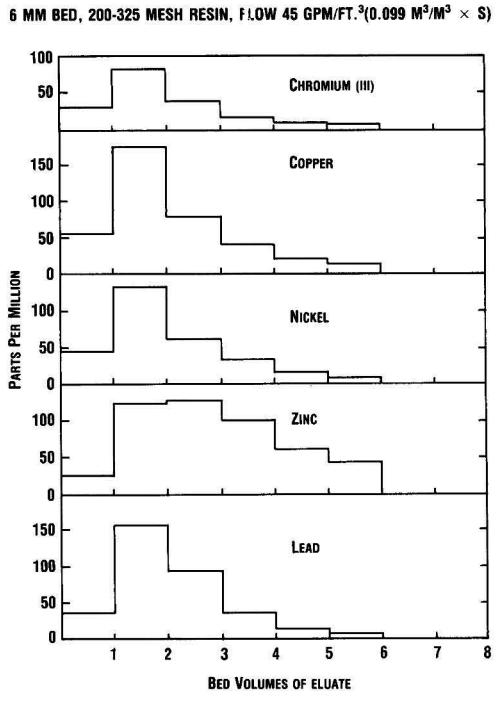

Figure 6. Elution of metals from Chelex 100 with 3*N* HCl.

Figure 5 shows a run that was designed to test resin performance over a rather long cycle time, and at a reasonable upper limit of flow rate for metal ion removal, 100 gpm/cu ft (0.223 cu m/cu m × s). In this run, 0.2 ppm of lead was added to gain some additional data. As the figure shows, except for a few points for lead, removal was generally in the range of 85–90%. The run was discontinued after about 4,000 bed volume had been processed, although in theory the resin capacity was sufficient to absorb all of these ions from about 60,000 bed volumes of solution.

Conditions for the above runs are summarized in Table 3. Pressure drops are shown, and, for the shorter runs, were fairly constant throughout the run, some increase in pressure was noted for the longer runs. In particular for the 4,000 bed volume run the pressure rose from 15 to a final value of 30 psi (206 KPa) during the run.

Elution Runs

Elution of the metal ions from both resins was readily accomplished with dilute (1-3*N*) HCl, and for a given concentration was more rapid from Chelex 100 than from the ED3A resin. Elution of the Chelex 100 resin from the run in which 4,000 bed volumes were processed is shown in Figure 6. Only six bed volumes of 3*N* HCl, flowing at about half the feed processing rate, were used in this test, after this the resin was removed from the bed and shaken overnight, first with an excess of 3*N* HCl, and finally with 0.01*N* HCl. For all of the metals, except zinc and chromium elution was fairly complete in the six bed volumes of 3*N* HCl, less than 5% being found in the overnight contact with 3*N* HCl. The final contact was made to insure complete removal of the zinc, which obviously tails considerably. The tailing here is probably due to the existence of anionic chloro complexes of zinc, which tend to be strongly absorbed in resins with cationic fixed groups. This resin, although a zwitterion, is in fact cationic in acid solution, since the carboxyl groups will be protonated.

About 12% of the zinc was found there, as well as about 12% of the chromium. In the case of the chromium, it is believed that this evidence of incomplete elution is more likely due to the well known sluggish behavior of this ion in reactions involving complex formation and dissociation.

DISCUSSION

The relation between resin bead size and performance is shown in Figure 7. As a basis for comparison the per-

TABLE 3. SUMMARY OF METAL ION ABSORPTION RUNS

Resin Capacities: ED3A (200–325 mesh), 0.12 millimoles/ml; ED3A (325–600 mesh), 0.09 millimoles/ml; Chelex 100, (200–325 mesh), 0.7 millimole/ml.

Resin	Mesh Size	Flow, gpm/cu ft	Bed Depth, mm	Press., psig	Performance*
ED3A	200–325	20	9	9	S
ED3A	200–325	40	9	12	S
ED3A	200–325	80	9	19	S
ED3A	200–325	120	5	7	U
ED3A	200–325	100	3	15	U
ED3A	200–325	220	3	30	U
ED3A	325–600	110	3	2	S
ED3A	325–600	225	3	5	S
ED3A	325–600	450	3	12	S
Chelex 100	200–325	110	3	5	S
Chelex 100	200–325	100	5	15–30	S
Chelex 100	200–325	225	3	13	U
Chelex 100	200–325	450	3	27	U

* S = satisfactory; U = unsatisfactory.
Note: 1 gpm/cu ft = 0.00223 cu m/cu m × s; 1 psi = 6.89 KPa

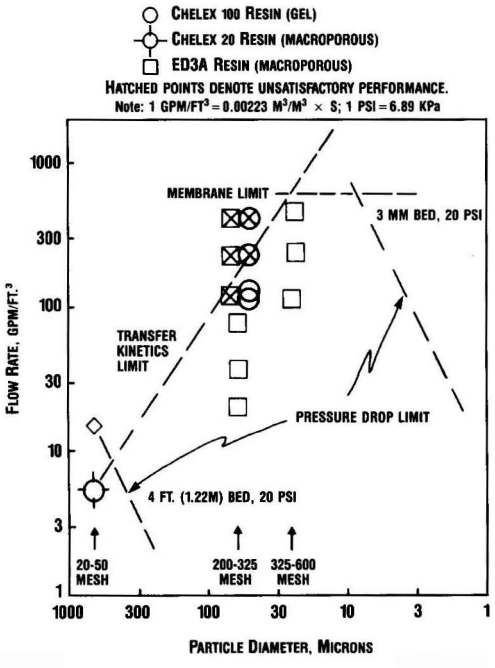

Figure 7. Effect of particle size.

formance of a conventional size resin (Chelex 20) was determined in preliminary tests. From the standpoint of satisfactory performance, a practical limit to flow rate was found to be about 5 gpm/cu ft (0.011 cu m/cu m × s); this is denoted by the open circle in the lower-left corner of the figure. Another limitation to be considered is the pressure drop through the bed. The diamond indicates the flow limit for typical conditions of a four foot deep bed with a 20 psi pressure drop, about 45 gpm/cu ft (0.10 cu m/cu m × s). For this system, the actual limitation on productivity is the kinetics rather than the pressure drop.

For a mass transfer-limited system it can be calculated that the transfer rate, and thus the permissible volume throughput of a system of spherical beads, should increase as the inverse 1.5 power of the bead diameter [8], and this is represented by the line passing through the open circle. Similarly, for a given pressure drop and bed depth the volumetric flow that can be forced through the bed is a direct function of the second power of the bead diameter. This is shown by the diagonal line passing through the diamond. Thus, for these conditions, the maximum flow that can be utilized is at the intersection of these two lines, and is about 8 gpm/cu ft (0.018 cu m/cu m × s), using about 35–40 mesh resin.

One way to circumvent this limitation is to change the parameters, i.e., to reduce the bed depth and/or to increase the applied pressure. Reducing the bed depth to 3 mm gives the parallel line at the top of the figure. Using a resin bed with these characteristics, it should be possible to operate satisfactorily at the intersection of this line with the transfer kinetics limitation line, which is at about 1500 gpm/cu ft. The horizontal line connected to this line represents the flow limitation of the three micron pore size of the membrane. For example, at resin mesh sizes of greater than about 400–500 mesh it is the membrane, not the resin bed, which provides the limiting pressure drop.

Against this background are displayed points representing the performance of the several systems of Table 3. For each resin the open points denote runs judged satisfactory (ca 80–90% metal ion removal), while the filled points denote unsatisfactory runs.

If the model described fit precisely, we would expect the "transfer kinetics" line to be the boundary between the regions of unsatisfactory and satisfactory runs. This is, in fact, nearly the situation, and the lack of agreement is very likely the result of the fact that the 20–50 mesh point represents a macroporous resin, while the other points all represent gel resins. The latter generally exhibit significantly smaller transfer kinetics, and it should not be surprising that the limiting flow rates for gel resins are somewhat lower than predicted. Another qualifying factor is the reality that the resins are not composed of uniform size beads, but cover a range of sizes, the plotted position representing the mid-range of the sizes.

The important conclusion to be realized is that the smaller beads, displayed in very shallow beds, do in fact provide performance, characterized by allowable volume flow rates, considerably greater than the conventional 20–50 mesh fraction. For the 200–325 mesh resin, the improvement is a factor of about 20, while for the 325–600 mesh resin the factor is about 100.

The primary advantage to be realized from resin systems incorporating the concept of very thin beds of fine resin is a much smaller volume of resin and a corresponding smaller equipment size. Although smaller it must be expected that the equipment that would evolve to fit these systems will be somewhat different, the probably somewhat more expensive than conventional ion exchange equipment. For example, although the size of the equipment will be smaller, it must have a substantially greater support area, which focuses on the properties of the membrane or screen system, and may lead to devices similar to those used by ultrafiltration and reverse osmosis systems. Nevertheless, it seems likely that the overall capital costs should be lower than for conventional systems.

Finally, since flows can be very high, leading to relatively shorter cycle times, the most promising types of applications may be polishing operations, i.e., those involving removal or exchange of small amounts of materials. Many ion exchange applications, however, are of this sort (boiler water deionization, softening of low hardness water, or waste cleanup of streams containing metal ions).

ACKNOWLEDGMENT

Analytical support was provided by Don Burns of the Western Division analytical group, who carried out the metal ion analyses. We also wish to acknowledge the help of Frances Chang, who carried out some of the initial experiments with conventional resins.

LITERATURE CITED

1. Beszedits, S., and A. Netzer, "Removal of Heavy Metals from Wastewaters," *B & L Information Services*, Toronto, Canada, 1986.
2. Peters, R. W., Y. Ku, and D. Bhattacharyya, *AIChE Symp. Series 81*, #243, 165 (1985).
3. Electric Power Research Institute, Technical Brief TP.CCS.12.7.87, Palo Alto (1987).
4. Clifford, D., S. Subramanian, and T. J. Sorg, *Env. Sci. and Tech.*, **20**, 11, 1072 (1986).
5. Levendusky, J. A., U.S. Patent 3,250,703, May 10, 1966.
6. Frederick, K. H., *Ultrapure Water*, **4**, 9, 58 (1987).
7. Brown, C. J., U.S. Patent 4,673,507, June 16, 1987.
8. *Perry's Chemical Engineer's Handbook, 6th Ed.*, Section 16, D. W. Green, Ed., New York: McGraw Hill Co., 1984.

Process Selection Criteria for the Biological Treatment of Industrial Wastewaters

W. W. Eckenfelder, Y. Argaman, and E. Miller
AWARE Incorporated, Nashville, TN

This paper illustrates some of the principles that lead to a rational selection of a biological treatment process for industrial wastewaters.

INTRODUCTION

Over the years, biological treatment has been established as a cost-effective solution in a wide variety of industrial wastewater management problems. It should, therefore, be considered whenever an industrial waste exists that is amenable to biodegradation or can be rendered biodegradable. Once the biotreatability of the waste has been established, the most appropriate biological treatment scheme must be selected. The available biotreatment alternatives differ from one another in many respects such as nature of electron acceptor (aerobic, anoxic, or anaerobic), biomass state (suspended or fixed growth), hydraulic regime (plug flow or completely mixed), and others. Selection of the process will be based primarily on the wastewater characteristics and the treatment goals.

FACTORS AFFECTING PROCESS SELECTION

The main factors affecting process selection for biological treatment are the raw wastewater characteristics and the treatment objectives. Additional factors such as climatic conditions, plant location, land availability, etc., also impact process selection but are not discussed in detail herein.

Wastewater Characterization

For the screening of process alternatives, it is convenient to partition the organic content into various fractions based on amenability to biological treatment. A possible partition scheme is shown in Figure 1.

The insoluble organics are relatively more easily removed in any biological process since they are enmeshed in the biomass and either degrade or physically separate from the liquid. The soluble organics are generally more difficult to remove since portions of these compounds are not readily available to the biomass. Those soluble organics which are sorbed to biomass are also removed with relative ease although part of such organics may degrade rather slowly. Of the non-sorbable soluble organics a portion may degrade through the activity of extracellular enzymes, while the non-degradable portion will be left in the effluent.

Other wastewater characteristics of concern in process selection are the organics concentration, the presence of nutrients, toxicants or inhibitory compounds.

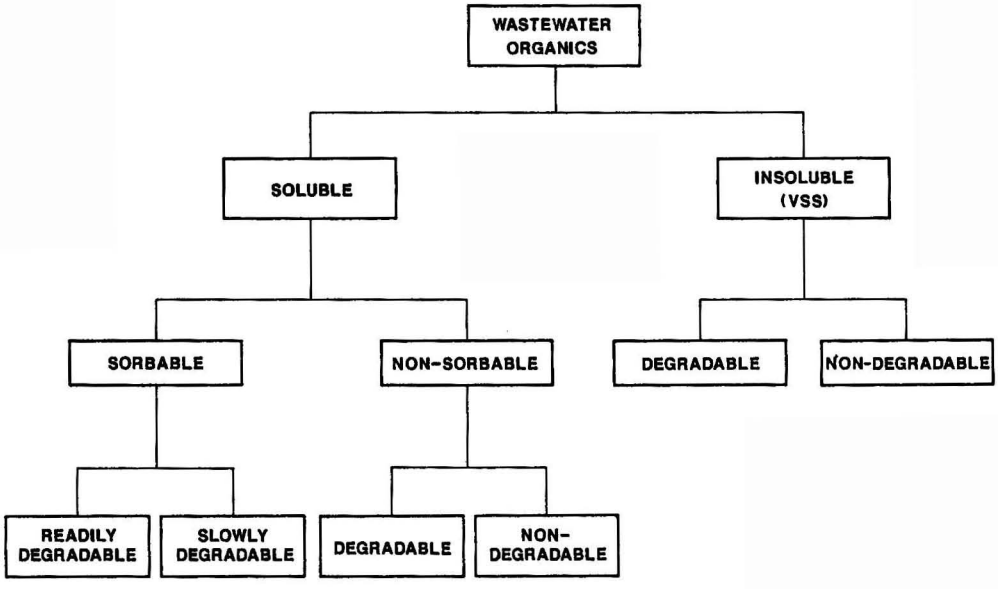

Figure 1. Partition of organic constituents of a wastewater.

Treatment Objectives

Treatment objectives also play a crucial role in process selection. The primary treatment objective in biological systems is removal of biodegradable organics to levels specified by regulatory agencies. Different treatment process can be tailored to achieve the desired level of organic removal. Additional objectives can include nutrient removal, toxicity reduction, and non-degradable organics removal.

AVAILABLE BIOLOGICAL TREATMENT PROCESSES

The essence of biological treatment is the utilization of organic pollutants by microorganisms for growth and maintenance. This can be represented by the following simplified equation:

$$\text{Organics} + \text{Nutrients} + \text{Electron Acceptor} \xrightarrow{\text{Biomass}} \text{New Biomass} + \text{End Products} + \text{Energy}$$

Biological processes differ from one another by the nature of the electron acceptor and by the system configuration. A schematic illustration of the most common biological treatment processes currently available is presented in Figure 2.

Based on the nature of the electron acceptor, all biological treatment processes can be generally categorized as aerobic or anaerobic. In the former, molecular oxygen must be present and serve as the electron acceptor. In the latter, molecular oxygen is absent and some forms of carbon or sulfur can serve as electron acceptors. In anoxic systems, oxidized nitrogen serves as an electron acceptor and is reduced to nitrogen gas.

Both aerobic and anaerobic processes can further be classified as fixed growth or dispersed growth systems. The most common aerobic fixed-growth systems are the trickling filters and the rotating biological contactors (RBC). The aerobic dispersed growth systems are the aerated lagoons and activated sludge processes. The latter may assume different forms in terms of hydraulic configuration such as plug flow, completely mixed, intermittent process, or the selector type. In special cases, pure oxygen, PACT®, or nitrification/denitrification systems are used.

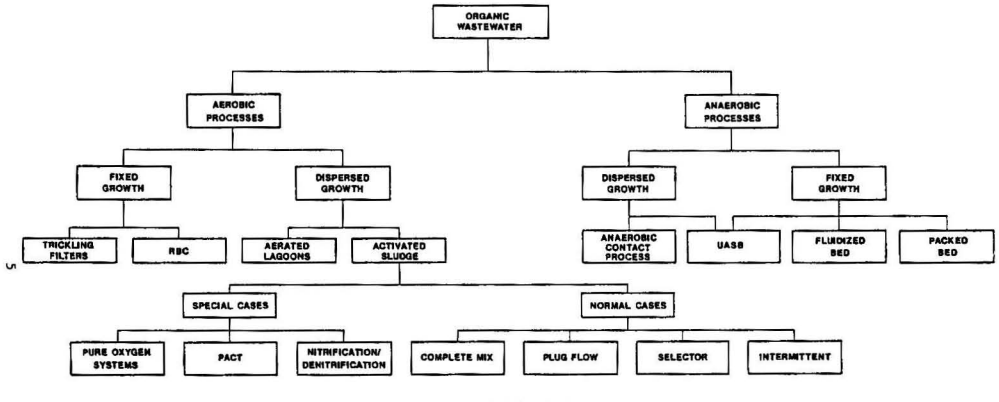

Figure 2. Major currently available biological treatment processes.

TABLE 1. COMPARISON OF ANAEROBIC AND AEROBIC TREATMENTS

Parameter	Anaerobic	Aerobic
Energy Requirements	Low	High
Degree of Treatment	Moderate (60–90%)	High (95%+)
Sludge Production	Low	High
Process Stability (to toxic compounds and load changes)	Low to moderate	Moderate to high
Startup Time	2 to 4 months	2 to 4 weeks
Nutrient Requirements	Low	High for certain industrial wastes
Odor	Potential odor problems	Less opportunity for odors
Alkalinity Requirements	High for certain industrial wastes	Low
Biogas Production	Yes (net benefit is contingent on the need for reactor heating)	No

The anaerobic treatment can also be divided into fixed and dispersed growth processes, as shown in Figure 2. The dispersed growth system is also known as the anaerobic contact process and is similar to activated sludge, except it does not use oxygen. The fixed growth anaerobic systems include fluidized beds and packed beds. A hybrid of fixed- and dispersed-growth system is the upflow anaerobic sludge blanket (UASB) process.

The diagram shown in Figure 2 represents the major types of biological treatment processes that are currently available. Various additional processes, modifications, and process combinations are also encountered. Examples of process combinations include the two-stage and anaerobic-aerobic system, and the trickling filter solids contact process that combines trickling filters with activated sludge.

PROCESS SELECTION CRITERIA

Once the wastewater characteristics and treatment objectives have been established, the engineer can proceed with process screening and selection. Some of the criteria and rationale behind this procedure are discussed below.

Aerobic versus Anaerobic Treatment

A general comparison of aerobic and anaerobic treatment processes is presented in Table 1. The difference between the two processes results primarily from the different terminal electron acceptor used by the microorganisms. In the aerobic process, where oxygen is the electron acceptor, the growth process is more efficient. It therefore results in higher sludge yields and energy requirements, but is less likely to produce odors. The anaerobic process is more sensitive to environmental conditions (pH, temperature, toxic shocks) and requires longer startup times.

One major limitation of the anaerobic process is that it cannot economically achieve high performance levels, such as an effluent BOD of 20 mg/l or 95% BOD removal, as often required by regulatory agencies. I can be cost effective, however, if employed as pretreatment before aerobic polishing of high-strength industrial wastewater. The cost curve shown in Figure 3 illustrates this point. This figure compares the overall cost, expressed in relative net present value (NPV), for treating a hypothetical high-strength wastewater by an all-aerobic system with an anaerobic pretreatment followed by aerobic polishing. The results clearly show the economic benefits obtained by the combined anaerobic/aerobic system and its dependence on raw wastewater strength. In the example shown in Figure 3, the cost advantage of the combined system starts at an influent BOD of 1,000 mg/l. Obviously, in other situations the transition point may shift in either direction, but the general trend should be similar.

Dispersed Growth versus Fixed-Bed Reactors

It is convenient to divide biological reactors into dispersed growth and fixed-bed reactors. In the dispersed growth reactors, biodegradation is carried out by biomass that is suspended in the liquid phase of the reactor. In the fixed-bed reactor, the biomass is attached to a fixed medium within the reactor.

Compared to the dispersed growth reactors, the primary merit associated with the fixed-bed reactors stems from their simplicity and ease of operation, thus making them ideal for remote and small industrial streams. Furthermore, because of the relatively high concentration of the biomass attached to the surface of the fixed media these reactors can handle higher loads per unit volume of reactor. Therefore, they are a better choice whenever land is limited. In addition, the dense nature of the microbial film, which sloughs off the media, produces sludge of relatively constant nature that can readily be removed by sedimentation. This is particularly important whenever sludge settling problems are expected in an alternative suspended growth reactor. Evidence was also found that fixed bed reactors are less affected by shock loads compared to dispersed growth systems.

The major disadvantages of the fixed-bed reactors compared to the dispersed growth systems are their lesser flexibility in operation, difficulty to achieve very high removal efficiencies, and greater sensitivity to cold weather

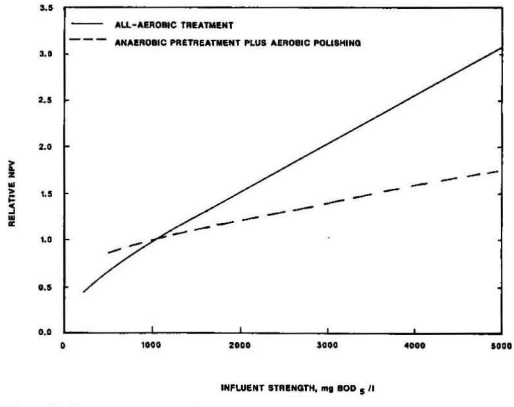

Figure 3. Cost comparison for aerobic and anaerobic + aerobic treatment system.

conditions. Another important drawback of fixed-bed systems is that they are less understood, thus modeling and process design procedures are not as rigorous and advanced as for the dispersed growth systems. This drawback has two important implications. First, in many cases the fixed-bed reactors are improperly designed, which leads to either over- or under-design. Second, it is more difficult to estimate prototype performance based on bench-scale experiments. This kind of drawback is of particular importance in cases where the nature of the wastewater is unknown.

Since the achievement of high removal efficiencies in fixed-bed systems is economically prohibitive, these system are often utilized as a roughing stage preceding a dispersed growth polishing stage.

Aerobic Dispersed Growth Systems

These are the most common biological treatment systems for industrial wastewater. The discussion of these systems will be divided into three parts based on the following wastewater characteristics and treatment requirements:

1. degradable and non-inhibitory wastes;
2. partially non-degradable or inhibitory wastes; and,
3. wastewater requiring nitrogen removal.

Degradable and Non-inhibitory Wastes: Wastewater that contain degradable organics with no bioinhibitory compounds can be treated in any of several activated sludge process configurations shown in Figure 4. The primary key to activated sludge process selection is the rate and extent of biological breakdown of the soluble organic content. This is because soluble and readily degradable organics may serve as a primary food source for filamentous organisms. Wastewater from the food processing industry, distilleries, paper mills, and some synthetic fiber manufacturing facilities fall in this category.

The reason for filamentous bulking development lies in the different growth rate curves of the filamentous and floc forming microorganisms shown in Figure 5. This figure shows that under low substrate concentrations the filaments will outgrow the floc formers, whereas under high concentrations the reverse will occur. Hence, in a complete mix system where the substrate concentration in the reactor is low (as it must equal the effluent concentration), filaments are likely to predominate. To overcome this problem, a treatment system must be devised whereby the raw wastewater come in contact with the biomass under conditions that favor floc-forming bacteria, i.e., high ambient substrate concentrations. These conditions are achieved in the inlet zone of a plug flow reactor, or the initial phase of a batch or intermittent operation. The floc formers will predominate in such systems, even though the final substrate concentration drops to levels favoring filaments because the majority of the substrate has been consumed by the floc formers.

The alternative approach to achieving a favorable species distribution is to employ a selector. In the selector, a rapid sorption of degradable organics by the floc formers occurs, thus depriving the filaments of a food source. While the data base on a variety of wastewaters is not available, it would appear that 40–70% removal or sorbable organics is required for a well-balanced culture, i.e., floc formers versus filaments. The sorption of organics can be related to the floc load ((mg BOD sorbable)/gvss), as shown in Figure 6. This figure provides the basis for the selector design. The selector is usually designed to operate with a 15 minute detention time. In most cases, sorption is close to complete within this time period.

Partially Non-degradable or Inhibitory Wastes: Wastewaters containing a non-degradable fraction or that exhibit inhibition to biological treatment can be treated biologically in combination with physical adsorption. During the last decade, the addition of activated carbon to activated sludge reactors and the conversion of these reactors into PACT® systems has been studied extensively in experimental and full-scale units. These studies have

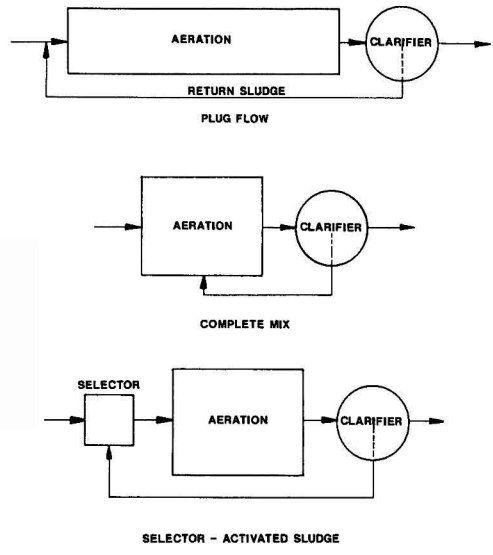

Figure 4. Types of activated sludge processes for industrial wastewater treatment.

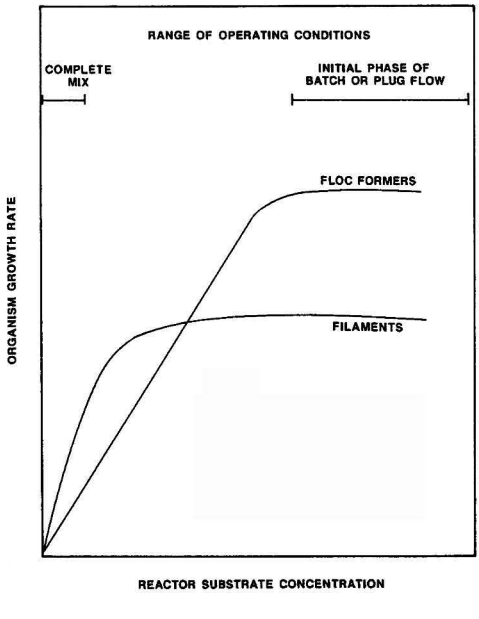

Figure 5. Organism growth rate as related to substrate concentration and reactor configuration.

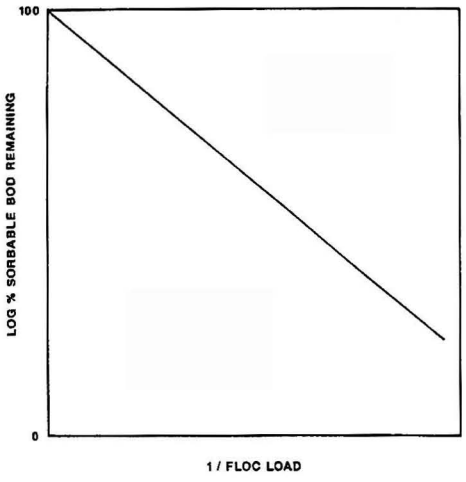

Figure 6. Biosorption relationship for soluble degradable wastewaters.

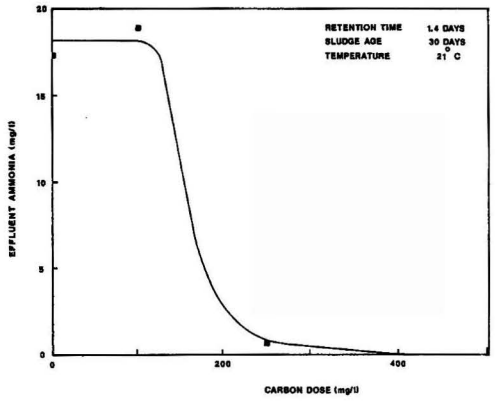

Figure 7. Effect on carbon dose on effluent ammonia concentration.

TABLE 2. EFFECT OF POWDERED CARBON ADDITION ON ACTIVATED SLUDGE PERFORMANCE

Parameter	Influent	Control	PACT®
Carbon Dose, mg/l		0	1,500
HRT, day		16.7	16.8
SRT, day		50	50
Biomass MLSS, mg/l[a]		2,430	6,070
Biomass MLVSS, mg/l[a]		2,054	5,388
Carbon MLSS, mg/l		—	3,196
COD_s, mg/l	10,207	1,992	920
Percent Removal		80	91
BOD_5, mg/l	5,734	57	43
Percent Removal		99	99
TOC_s, mg/l	3,281	565	192
Percent Removal		83	94
SVI, ml/g		157	65

[a] Includes organics adsorbed to the PAC.

revealed that the PACT® reactors have several advantages over the conventional systems.

One of the major advantages of the PACT® system, compared to a conventional activated sludge reactor, is its capability to reduce the effluent non-biodegradable organic load. A typical example of this case is shown in Table 2. A control reactor, which simulated the operation of a full-scale activated sludge reactor, was fed with pharmaceutical wastewater containing an average BOD of 5,734 mg/l and an average COD of 10,207 mg/l. After treatment, the BOD was reduced to 57 mg/l and the COD was reduced to 1,992 mg/l. In comparison, an identical reactor dose with 1,500 mg/l of powdered activated carbon was capable of reducing the influent BOD to approximately the same level (43 mg/l) and the COD to below 1,000 g/l. The increased removal of COD was due to adsorption of non-degradable organics. Table 2 emphasizes another merit of the PACT® reactor: improving the ability of sludge to settle. As can be seen from this table, under identical operational conditions, the SVI of the control reactor is 157 ml/g while the SVI of the PACT® was 65 ml/g.

Another important feature of the PACT® process is its capability to adsorb bioinhibitory compounds present in some industrial wastewater, thus alleviating the bioinhibition effect. For example, it is well known that nitrifiers can be inhibited by a variety of organic chemicals, even at low concentrations. In PACT® systems, carbon adsorption can eliminate this inhibition and consequently enhance nitrification. To illustrate this point, the effluent ammonia concentration of five identical activated sludge reactors dosed with different amounts of carbon is

TABLE 3. COMPARISON OF PACT® AND ACTIVATED SLUDGE IN REMOVING PRIORITY POLLUTANTS

Priority Pollutant	Feed Concentration ppb	% Removal by Activated Sludge	% Removal by PACT® 300 ppm*
Benzene	81	98.5	99.6
Chlorobenzene	3,660	99.1	99.8
Chloroethane	667	99.8	>99.9
Chloroform	72	96.7	96.9
Methyl Chloride	138	98.5	>99.7
Tetrachloroethylene	33	>99.5	>99.5
1,2-Dichlorobenzene	18	90.6	>99
2,4-Dinitrotoluene	1,000	31	90
2,6-Dinitrotoluene	1,100	14	95
Nitrobenzene	330	94.5	>99.9
1,2,4-Trichlorobenzene	210	99.9	>99.9
2,4-Dichlorophenol	19	0	93
2,4-Dinitrophenol	140	39	>99
4,-Nitrophenol	1,100	25	97

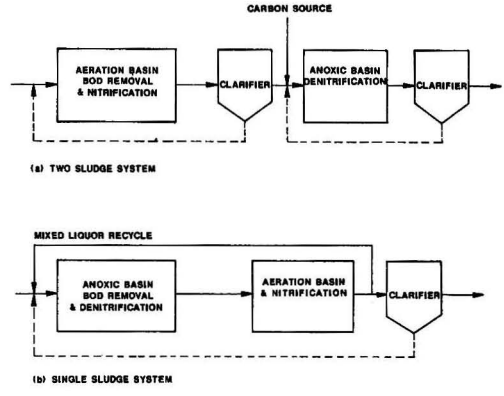

Figure 8. Alternative systems for total nitrogen removal.

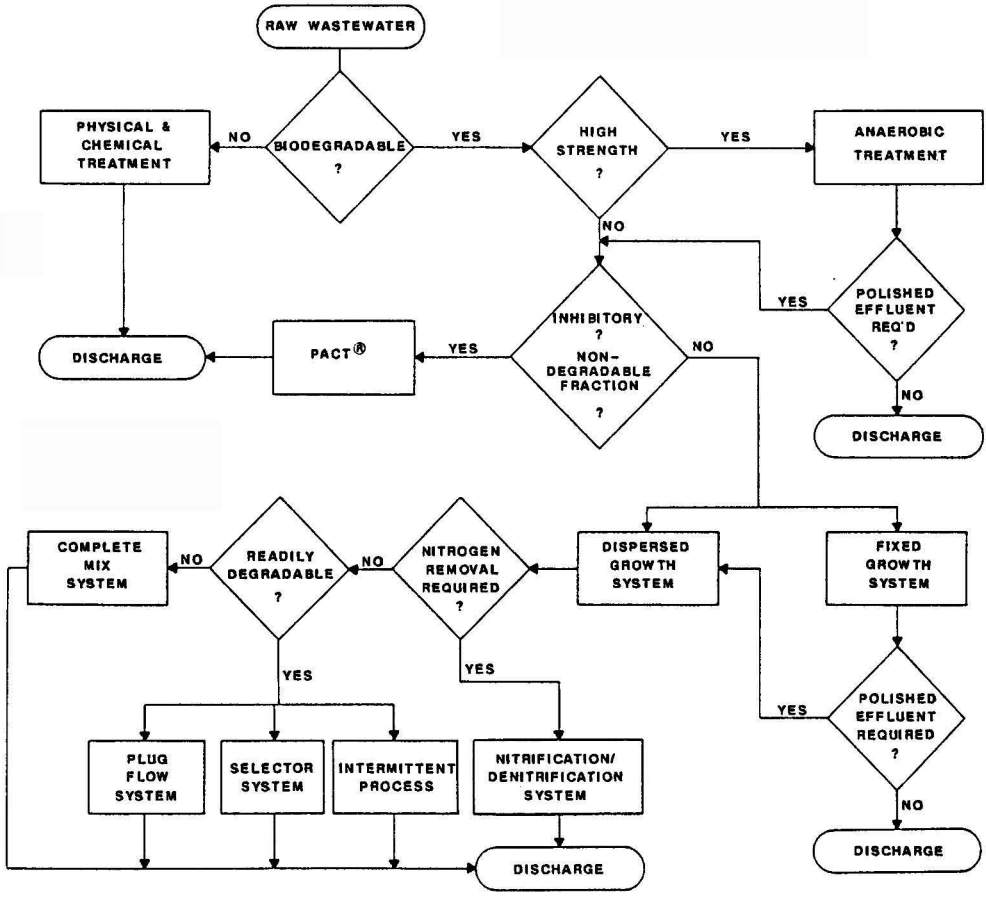

Figure 9. Simplified process selection flowsheet for biological treatment.

shown in Figure 7. The operating conditions of the reactors were such that, without inhibition, nitrification would take place in all the reactors. However, as can be seen from this figure, only those reactors that were dosed with more than approximately 200 mg/l of carbon were capable of achieving complete nitrification.

A PACT® system can also be useful when priority pollutants removal is required. As illustrated in Table 3, a PACT® reactor out-performed activated sludge with respect to priority pollutants removal. The advantage of PACT® was most pronounced in removing compounds such as dinitrotoluene, dinitrophenol, nitrophenol, and dichlorophenol.

Wastewater Requiring Nitrogen Removal: Wastewater containing nitrogenous compounds may need system designed to meet specific nitrogen removal requirements. In most cases, the raw wastewater contains nitrogen in the organic or ammonium forms. Discharge permits may limit the ammonia or total nitrogen levels. In the first case, a biological system can be designed that will achieve nitrification; i.e., conversion of all nitrogen compounds to the nitrate (NO_3^-) form. This can be achieved in any type of activated sludge system, provided that the solids retention time (SRT) exceeds a critical value. This value is dependent on both the nature of the wastewater and the operating temperature.

Two-stage systems for BOD removal and nitrification are sometimes used in industrial waste plants. The major advantage of such systems lies in the protection of the nitrifiers from shock loads, toxicity, or inhibitory effects afforded by the first-stage BOD removal system.

Complete removal of nitrogen can be accomplished through denitrification of nitrified wastewater. For industrial wastewater, the process can take one of two basic forms: a two-sludge system (Figure 8a); or, a single-sludge system with mixed liquor recycle (Figure 8b). Several additional modifications of these basic processes have been developed. The single-sludge system offers several economical advantages over the two-sludge system in that it uses only one clarification step, no external carbon source, lower neutralization chemical requirements, and lower oxygen requirements.

SUMMARY

Some of the considerations for selecting biological treatment processes for industrial wastewater have been discussed. A simplified diagram summarizing these considerations is presented in Figure 9. Needless to say, many actual cases encountered in practice will be considerably more complex. However, it would be an impossible task to try and cover all possible cases in one paper. It is believed, however, that the principles presented herein could help the practicing engineer in arriving at a rational process selection for any particular case.

Two Strategies for PCB Soil Remediation: Biodegradation and Surfactant Extraction

John B. McDermott, Ronald Unterman, Michael J. Brennan, Ronald E. Brooks, David P. Mobley, Charles C. Schwartz, and David K. Dietrich

General Electric Co., Corporate Research and Development, Schenectady, NY 12301

Two strategies for the cleanup of PCB-contaminated soils are being developed: biodegradation by selected bacteria and extraction with aqueous surfactant solutions. Extensive biodegradation has been demonstrated by Pseudomonas putida *strain LB400 in studies with Aroclor-spiked laboratory soil and soil from a New York State site containing 525 ppm of transformed Aroclor 1242 (depleted of di- and trichlorobiphenyls). Solutions of sodium dodecylbenzenesulfonate can extract PCB from soils. A bench-scale process with four countercurrent stages effected the cleanup of a heavy clayey soil. The PCB was recovered from the surfactant solution by precipitation with calcium chloride, reducing the mass of contaminated material to 3% of the original soil mass.*

INTRODUCTION

The excavation, shipment, and placement in a secure landfill of PCB-contaminated soil is no longer favorably viewed by regulatory agencies and the public. Permanent destruction of the PCB is the ultimate goal of any remediation activity. We are developing two strategies for the cleanup of PCB-contaminated soil: biodegradation by selected bacteria and extraction with aqueous surfactants solutions. The biodegradation strategy has progressed from microbe selection and small laboratory-scale experiments to an actual site test. The extraction with aqueous surfactant solutions has been demonstrated with soil contaminated in the laboratory and actual site soil using a bench-scale process.

BIODEGRADATION

Over the past several years, we identified many bacteria with the ability to aerobically degrade PCBs. These bacteria were isolated from various PCB-contaminated sites in and around New York State by enriching cultures using biphenyl as the sole carbon source. As can be seen from Figure 1, the ability to degrade PCB ranges from very poor for the bacteria on the left to outstanding for the bacteria on the right. The bacteria used for a majority of the biodegradation•studies are all excellent PCB degraders: MB1 (Corynebacterium), H850 (Alcaligenes eutrophus), and LB400 (*Pseudomonas putida*). The biochemistry displayed by these bacteria can differ considerably. This difference is manifested in the ability of MB1 to readily degrade PCB congeners chlorinated in the 4,4′ positions while LB400 has some difficulty with those congeners. Conversely, LB400 can degrade 2,5,2′,5′-tetrachlorobiphenyl but MB1 cannot. This congener specificity is the hallmark of PCB biodegradation and distinguishes it from other chemical and physical transformations.

Laboratory Experiments

Resting cell assays were used to determine the ability of the bacteria to degrade PCB that was adsorbed to soil. The cells were grown in a buffer solution with biphenyl as the sole carbon source (cells grown on Luria broth were less effective at degrading PCB), harvested, washed, and resuspended in buffer to a concentration of approximately 10^9 cells/ml. These resuspended cells were then shake-incubated with PCB contaminated soil; the cell suspension to soil mass ratio was approximately 10:1. The assays were performed with both laboratory contaminated soils and an actual site soil.

Rapid degradation occurred with the three laboratory contaminated soils. With soil spiked to 50 ppm Aroclor 1242, MB1 and LB400 both degraded in excess of 95% of the PCB in one day. When the concentration was increased to 500 ppm Aroclor 1242, LB400 degraded 85% of the material in two days. When the soil was spiked to 50 ppm Aroclor 1254 (a more highly chlorinated Aroclor mixture), LB400 degraded greater than 65% of the PCB in one day.

The site soil came from a former racing drag strip in New York State that had been contaminated with Aroclor 1242. The contamination resulted when oil containing PCB was used for dust control. The sample of soil obtained was homogenized by tumbling and had a PCB concentration of 525 ppm. A gas chromatogram of the PCB no longer resembled a commercial Aroclor 1242; it had been depleted of di- and trichlorobiphenyls, probably by evaporation of these more volatile congeners, and resembled an Aroclor 1248. When LB400 was assayed with this soil using the same experimental procedures above, it de-

graded 15% of the PCB in one day and 51% in three days. This is slower than exhibited with the laboratory contaminated soils, but is still quite favorable.

In order to take these bacteria into the field for a site test, a suitable experimental protocol had to be developed. Reflecting the constraints of a field experiment, these *in situ* protocol experiments were conducted with 3–4% of the cells used in the shake assays, unwashed cells, less water, 8°C cooler temperature, no agitation, and less aeration. The soil was the same dragstrip soil previously used, but with much larger samples—1 to 5 kg, and the bacterium used was LB400. The variables investigated were frequency of bacterial application, periodic soil mixing, and temperature. Control experiments were conducted using several different soil applications, *e.g.*, water, buffer solution, Hg^{+2} poisoned LB400, and a mutant strain of LB400 unable to grow on biphenyl.

In approximately 30 days, the first signs of biodegradation were detectable in an unstirred soil sample dosed with bacteria three times weekly. The degradation occurred primarily in the top centimeter of soil. In 15 weeks, 50% of the PCB had been degraded in the top centimeter with much less degradation at the lower depths (10%). The cell count at the lower depths was approximately one-tenth of that at the surface. A soil sample that had been exposed to the same dosing regimen was mixed after three months and then maintained with the same thrice weekly dosing. After some time, the redistributed soil once again displayed the greatest degradation in the top centimeter. Since the rate of biodegradation is a strong function of soil depth, the frequency of soil mixing is an important consideration.

In another experiment, a 5 kg soil sample was dosed three times weekly and then mixed after each application. After 23 weeks the PCB had been degraded 35% at all depths (down to 15 cm). This 35% degradation at all depths represents a much greater amount of PCB destruction than the 50% degradation in the top centimeter obtained in the unstirred sample.

The rate of biodegradation exhibited in these *in situ* protocol experiments was much lower than that displayed in the shake assays. It is probably the result of trying to match conditions experienced during a field test such as lower cell counts, less water, and cooler temperatures.

There was an interesting result in one of the control experiments. In the sample that was inoculated three times weekly with heat-killed LB400, a small amount of biodegradation was observed. When the bacteria responsible for this biodegradation was isolated, it was not LB400. Also, the congener specificity of the degradation did not match that of LB400. The pattern of degradation more closely matched that of DS100, a poor PCB-degrading bacterium isolated from the drag strip much earlier in the investigation. It appears that the thrice weekly dosing with heat-killed bacteria (*i.e.*, nutrients) resulted in the proliferation of a native PCB-degrading bacterium.

Drag Strip Site Test

The site used for this test was the former racing drag strip discussed earlier. The Aroclor 1242 contamination was limited to the top 15 centimeters of a relatively sandy soil. This shallow contamination with a lower chlorinated Aroclor mixture on a soil with moderately good percolation made this an ideal site for a biodegradation test using LB400.

The site for the test was prepared by rototilling a 5 m × 12 m area to a depth of approximately 20 cm in an effort to vertically homogenize the PCB concentration, which ranged from 50ppm to 500ppm. A transparent tent was

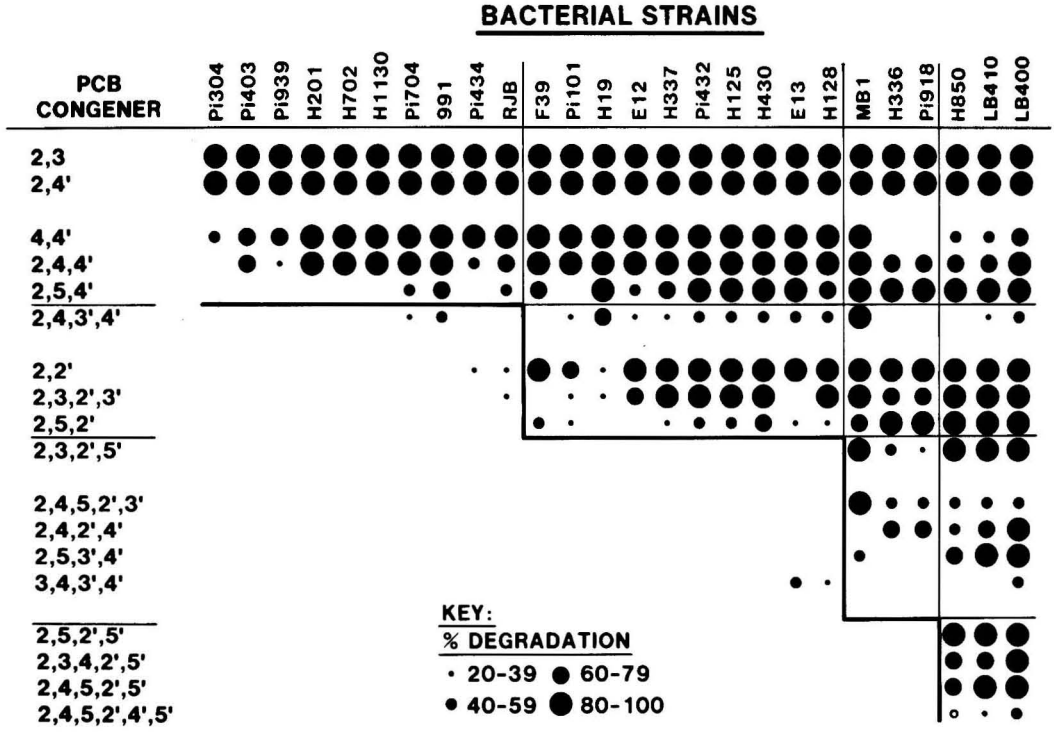

Figure 1. PCB-degrading bacteria.

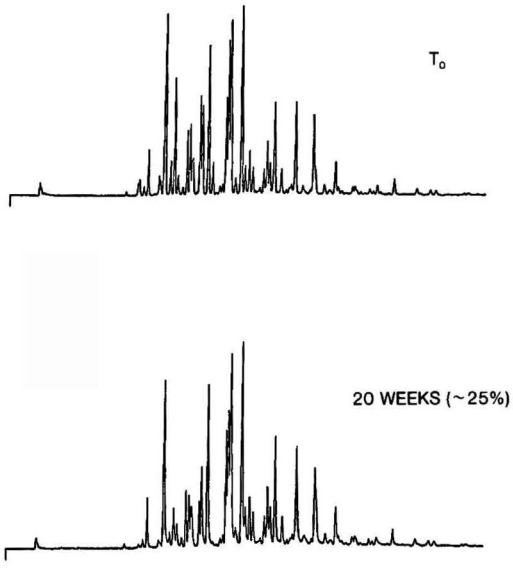

Figure 2. Gas chromatograms from drag strip site test indicate 25% biodegradation.

erected over the area to protect the site from the elements and provide some solar heating. This tent later proved to be as much of a handicap as an asset. Two 3m × 3m test plots were marked off for the test, one for the biodegradation trial, the other for a control. The experimental and control plots were thrice weekly dosed with 200 l of LB400 (2×10^9 cells/ml) and 200 l of buffer solution, respectively. Prior to each dosing, one half of each plot was rototilled. Progress was monitored by weekly collection of soil samples.

The test began in June, 1987 and the last dosing occurred on October 21, 1987. Before the test began, the soil was sampled using a 30 cm × 30 cm grid configuration throughout the entire tent area; a final soil sampling in November was configured similarly. While the analysis of these grid samples (plus some test borings) is not yet complete, the analysis of the weekly samples has been completed.

PCB biodegradation was first detectable after 8 to 10 weeks. After 13 weeks, the soil in the top 3 cm of the unstirred portion of the test plot showed approximately 20% biodegradation of the PCB. The soil from the lower depths of the unmixed soil and the mixed soil from the other half of the plot displayed lesser, but still significant PCB destruction. After 18 weeks, approximately 25% of the PCB had been degraded from the top 3 cm of the unmixed portion. The mixed half showed approximately 10% destruction. Example gas chromatograms are provided in Figure 2 for a t_0 sample and a 20 week sample from the unmixed portion of the test plot (there was little activity between week 18 and week 20 as a result of the cool autumn weather). There was no evidence of any PCB destruction in any of the soil samples from the control plot.

The rate of biodegradation at the drag strip was about 50% of the rate seen in the laboratory experiments. A large portion of the rate reduction can be attributed to the poor control of soil temperature and moisture content and the fragile nature of LB400. This was particularly a problem during very hot weather experienced during July. The air temperature in the tent often exceeded 50°C and the soil temperature exceeded 43°C at the surface, thus rapidly drying the soil and desiccating the bacteria. LB400 cell counts on the soil two days after dosing were virtually zero during this exceptionally hot weather.

This site test was the first *in situ* PCB biodegradation field test ever conducted. The results were modest by comparison to laboratory tests, but still very encouraging. A great deal has been learned about the difficulties likely to be encountered during a field test of this nature. We hope to go back to the drag strip to continue our studies, possibly using a different bacterium whose congener specificity complements that of LB400. Laboratory studies using mixed bacterial cultures with complementary specificities have shown 90% PCB destruction.

Ultimately, the best biodegradation strategy would involve a microorganism that remains viable for an extended period of time in the environment and has a very high level of activity. Toward this goal, we have isolated the genes responsible for the PCB-degrading capabilities of LB400 and have introduced them into *E. coli*. This clone has recently demonstrated PCB activity similar to LB400. With the genes isolated from LB400, there now is the possibility of engineering the ideal bacterium for *in situ* treatment of PCB-contaminated soil.

SURFACTANT EXTRACTION

Another PCB soil remediation strategy under development at GE Corporate Research and Development is the use of aqueous surfactant solutions for the extraction and separation of PCB from the soil. Unlike the biodegradation strategy above, this is a mass reduction process where the PCB is concentrated into a precipitate that is 2–3% of the original soil mass.

Figure 3 is a conceptual schematic of the process. The soil would be excavated, followed by mechanical breakup and size separation to remove large stones and debris. This oversize material, with its low specific surface area, could be returned to the site after minimal treatment. The bulk of the soil would then go on to the countercurrent washing operation where the PCB is extracted using an aqueous surfactant solution. The soil could be subjected to a water wash, following the extraction operation to remove the surfactant if deemed necessary. After dewatering, the soil would be returned to the site. The aqueous process stream exiting the washing operation with PCB, would then be mixed with $CaCl_2$ to precipitate the surfactant, PCB, and any soil fines. The waste water would be a brine solution with a minimal (<2 ppb) amount of PCB. This waste stream could be treated with activated carbon to further reduce the PCB content. The products of the process would be soil suitable for returning to the site and a concentrated PCB and surfactant precipitate that could be incinerated for final PCB destruction.

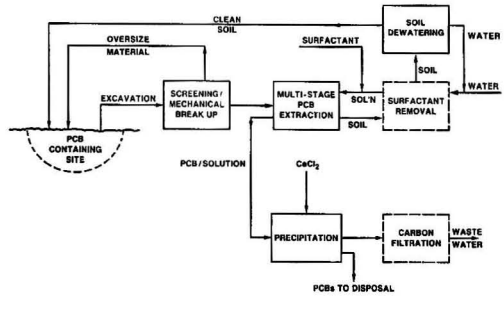

Figure 3. PCB extraction process concept.

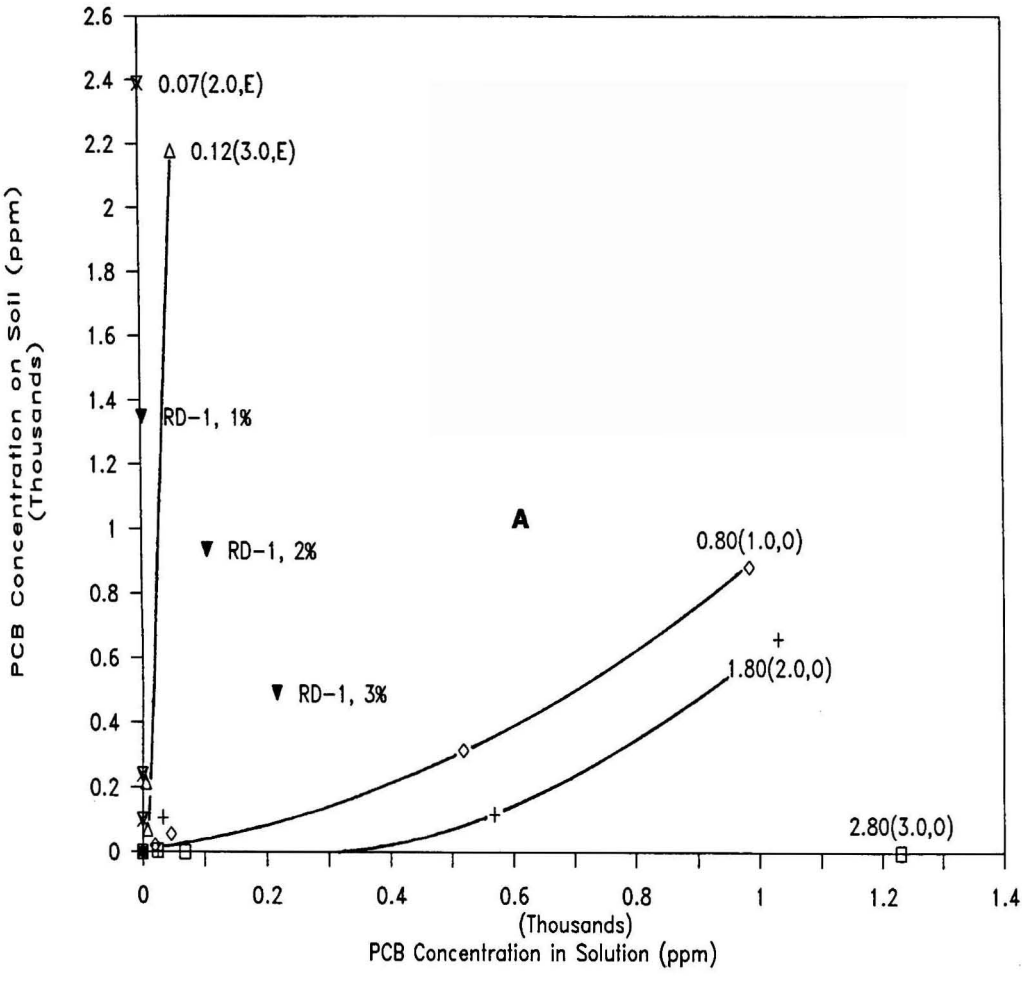

Figure 4(A). PCB extraction isotherms for Triton X-100.

Preliminary Studies

Our studies have concentrated on the soil washing operation and the PCB/surfactant precipitation. The objectives of the early engineering studies were to characterize the interactions of the PCB/soil/surfactant system and to collect data allowing the selection of unit operations. A brief discussion of the selections and the experimental reasons for them follows:

Several factors were considered in the selection of a surfactant for the process. The surfactant had to have a good capacity for solubilizing PCB and allow some type of PCB separation from the process stream to occur. In addition, the surfactant had to be biodegradable. After screening several surfactant systems, two were selected for further study: 1. Triton X-100, a nonionic surfactant manufactured by Rohm & Haas, and 2. Surco 233, an anionic surfactant manufactured by Onyx Chemical Company. Both of these surfactants, at concentrations ranging from 1 to 3% in water, could increase the solubility of Aroclor 1260 in water from 2–3 ppb to several thousand ppm.

The adsorption/desorption behavior of these two surfactants with various soil systems was studied to determine how many stages might be required to remove the surfactant from the soil at the end of the process if it was desirable to do so. The Triton X-100 and the Surco 233 behaved quite differently. When contacted with heavy clay soils, particularly montmorillinite clays, the Triton X-100 would adsorb onto the soil to a maximum level of 15–20% by weight. The Surco 233, when exposed to the same soils never adsorbed to a level exceeding 1%. In both cases, the soil surfactant concentration monotonically increased with solution concentration and reached its maximum when in contact with fairly dilute surfactant solutions (<0.2%). This difference in the maximum level of adsorption between these two surfactants, particularly with clays, ultimately resulted in very different PCB extraction performances.

The extraction behaviors of Triton X-100 and Surco 233 were studied using various soils contaminated in the laboratory with Aroclor 1260 and an actual site soil from Oakland, CA with an Aroclor 1260 concentration of 1350 ppm. This information is compiled and presented in Figures 4(A) and 4(B) as two series of isotherms, one for each surfactant. An isotherm depicting complete removal of the PCB would lie horizontally along the x-axis, while an isotherm depicting no removal would be vertical along the y-axis. Next to each isotherm is a label configured x . xx (y . y,z) where x . xx is the equilibrium surfactant concen-

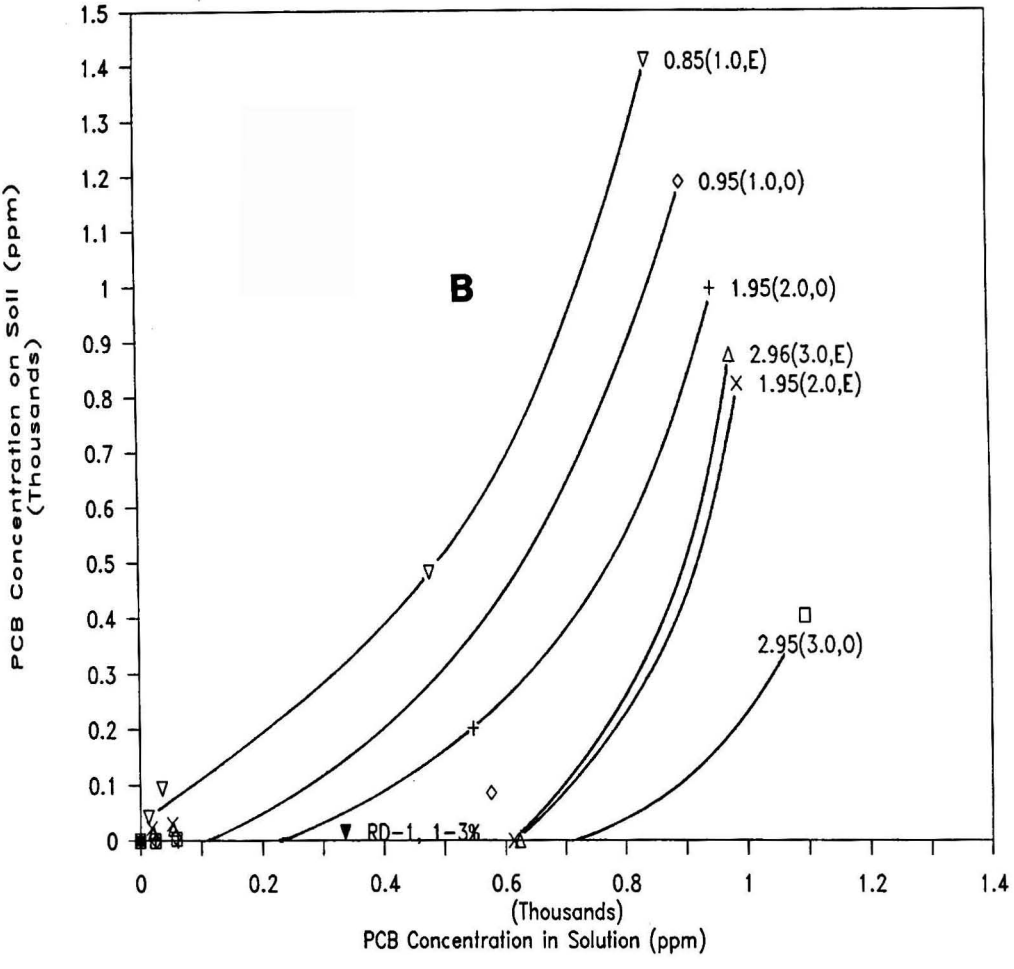

Figure 4(B). PCB extraction for Surco 233.

tration (weight percent) after adsorption onto the soil, y . y is the feed concentration of the surfactant before adsorption, and z is the soil type—O, a sandy/silty surface soil from Oakland or E (Emathlite 600), a refined montmorillonite clay. The extractions of the actual site samples are labeled RD-1; the feed concentration of the surfactant is noted next to the label. The RD-1 soil is an Oakland subsurface soil largely composed of montmorillonite clay.

The effect of the adsorption of the Triton X-100 onto the montmorillonite clay is obvious from the nearly vertical isotherms and the low equilibrium surfactant concentrations. This phenomenon renders the Triton X-100 very ineffective when used with certain clays. Extractions of RD-1 soil with Triton X-100 resulted in poor removal, though not as poor as the cases with Emathlite.

The Surco 233, on the other hand, performed rather well with all soils studied. This can be attributed to the low adsorption of Surco 233 onto any of the soils, thus leaving most of the surfactant in solution to solubilize the PCB. This ability to perform well even with difficult clay soils makes Surco 233 or a similar anionic surfactant the best choice for soils with a high clay content.

The performance of the solid/liquid separation process has a large impact upon the efficiencies of the extraction stages. If the separation is poor, with either large amounts of solids in the overflow or large amounts of liquid in the underflow, the number of real stages required to perform the same cleanup as a few ideal stages will be large. Three separation processes were explored. The first was the use of thickeners or settlers. Unfortunately, the settling rate of clays, particularly when dispersed in a surfactant solution, is rather low. For the Oakland subsurface soil, the settling mass flux was measured to be 12.5 lbs/ft^2/day. This settling rate would result in thickener areas that were unmanageable. Fine clay particles are also difficult to filter. The fine platey particles form nearly impermeable filter cakes at minute thicknesses. The pressure drop increases rapidly once any filter cake has formed. This leaves centrifugation as the only option for separation of fine clay particles from surfactant solutions. Centrifugation at 1000 × g effects satisfactory separation.

While the equilibrium behavior discussed above determines the maximum possible performance of the process, the kinetics of the extraction are equally important in determining the overall effectiveness of an actual process. The rate of extraction was measured for Oakland surface soil spiked with 1000 ppm Aroclor 1260 using a 2% Surco 233 solution as the extraction liquid. The rate was modest, with an 80% approach to equilibrium after 20 minutes of contact.

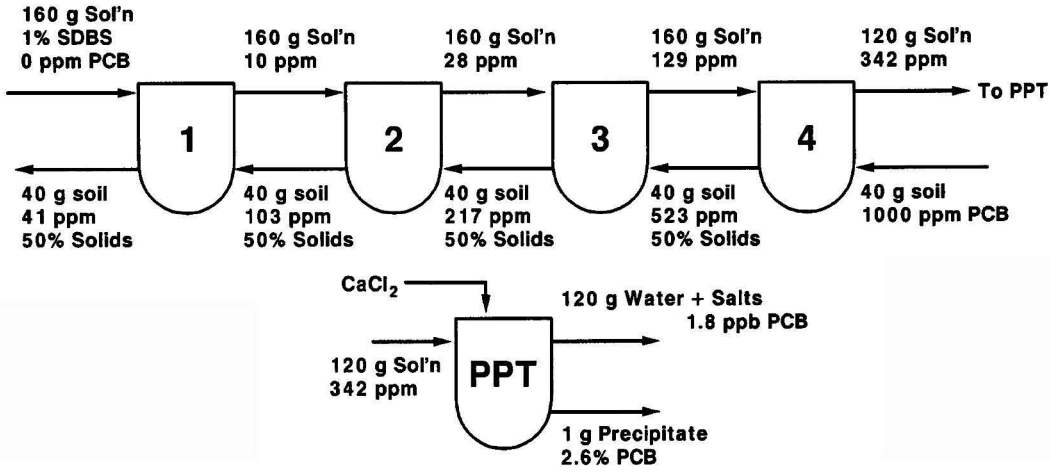

Figure 5. Flow diagram of four stage bench-scale extraction process with performance data for laboratory-spiked Oakland soil.

Up to this point, the discussion has been of items that are directly involved in the extraction operation. The other half of the process is the separation of the PCB material from the process stream leaving the extractor. Ideally, one would like to separate the PCB from the surfactant solution allowing the surfactant to be recycled to the extractor. Selective adsorption was investigated, but no adsorbent could be identified with both a high selectivity for PCB and a large capacity for adsorbed material. Liquid/liquid extraction was considered but was dismissed because of a concern about extraction of the organic solvent into the surfactant stream and deposition of that organic onto the soil when recycled. Biodegradation is possible for some Aroclor mixtures, but no Aroclor 1260 degrading biosystem is currently available for use in a process such as this. The treatment finally settled upon was precipitation of the surfactant with a divalent ion such as Ca^{+2} to remove both the anionic surfactant and the PCB. Unfortunately, the surfactant is lost and can not be recycled. This loss of surfactant and the incineration of the precipitate, which is primarily surfactant, are the major costs of this process.

Surco 233 is a surfactant formulation consisting primarily of sodium dodecylbenzenesulfonate plus lime soap dispersing agents. These other ingredients of Surco 233 give the mixture some resistance to water hardness. Since the process stream treatment calls for the precipitation of the surfactant with Ca^{+2} ions, any resistance to water hardness is undesirable. For this reason we chose to use the primary active ingredient of Surco 233, sodium dodecylbenzenesulfonate (SDBS), as the surfactant in the extraction process. With this precipitation, the PCB can be concentrated in a solid that has a mass 2–3% of the original soil. The resulting waste water is a brine solution with 1–2 ppb PCB.

Bench-Scale Process

The surfactant extraction and precipitation portions of the soil washing process have been demonstrated with a small bench-scale process comprising four mixing stages, a laboratory centrifuge, and a precipitation vessel. The process was demonstrated with Oakland subsurface soil spiked with 1,000 ppm Aroclor 1260 and an actual site soil from Oakland of similar mineralogy contaminated with 100–200 ppm Aroclor 1260.

The process was operated batch-wise and countercurrently. The stage capacity was 40 g of soil and 200 g of 1% SDBS surfactant solution. The mixing contact time was 20 minutes at 300 rpm and solid/liquid separation was effected by 20 minutes at 1000 × g, resulting in an underflow of 50% solids. The solid:liquid feed ratio was 1:4.

Figure 5 is the schematic of the process and contains the performance data for each stage. The soil, initially at 1,000 ppm PCB, was cleaned to approximately 40 ppm. This represents a twenty-five-fold reduction in PCB concentration. The PCB balance around the extraction process is 100%. There is some PCB unaccounted for in the precipitation process, resulting from the difficulty of extracting PCB from the precipitate material. The precipitate PCB concentration was higher than the 2.6% reported here. The waste water exiting the precipitation unit had a PCB concentration of 1.8 ppb, approximately the solubility of Aroclor 1260 in water.

The performance of the extraction process with the actual site soil was rather different. The contamination of the feed soil ranged from 100 to 168 ppm Aroclor 1260 (only ranges can be given as a result of the heterogeneity of the site soil); the product soil exiting the process had a PCB concentration ranging from 18 to 24 ppm. While this represented a cleanup to well under 50 ppm PCB, the degree of extraction was not nearly as good as that for the laboratory spiked soil.

The actual site soil differs from the laboratory spiked in three ways; the level of contamination, the age of contamination, and the mode of contamination. The work with actual site soils has only recently begun; further studies are necessary to determine which, if any, of the factors above strongly influence the behavior of the process. Other issues to be addressed are the influence of other contaminants and the effect of various soil constituents (*e.g.*, humic material) on the efficiency of the extraction.

SUMMARY

Two strategies for the remediation of PCB contaminated soil are presented. The biodegradation with naturally-occurring bacteria has been tested in the field with modest results and the surfactant extraction has been demonstrated on a small scale with both laboratory contaminated soil and actual site soil. These strategies require further study before implementation, but both show promise for being safe, economical routes for the remediation of PCB-contaminated sites.

Design Considerations for Natural Draft Landfill Gas Incinerators

Joseph Colannino
Sur-Lite Corporation, 8124 Allport Avenue, Santa Fe Springs, Cal 90670

A consistent methodology regarding major facets of enclosed landfill flare design is presented. A natural draft landfill gas (LFG) incinerator is an enclosed flare consisting of three parts: burner, damper, and stack. Such an incinerator will burn LFG at temperatures up to 1800°F without the need for support gas, or fans to provide draft. Modeling of actual heat release, draft, and stack velocity is a function of many parameters including stack height, incinerator temperature, ambient conditions, stack and damper area, frictional losses, flue molecular weight and heat capacity, among others. The involved variables are simplified to three dimensionless groups that depend on temperature and damper area alone. Graphs are presented for reference, along with a full analytical treatment for those who wish to develop comprehensive modeling.

INTRODUCTION

As the name implies, a natural draft incinerator is any device for burning a combustible vapor or gas, including LFG, utilizing the phenomena of natural draft. The term "incinerator" is used to distinguish the unit from open flares or "candle" flares that emanate visible flames and are not enclosed. The term, however, is far from universal. Economics dictate the use of a natural draft device (as opposed to forced or induced draft) in the case of landfills. For the purposes of this article a natural draft incinerator is a device enclosed on four sides (and often the bottom), open on the top, and having damper controls to regulate air draw and temperature. A view of such an LFG incinerator is given in Figure 1.

Joseph Colannino is presently at Energy Systems Assoc., 15991 Red Hill Avenue, Tustin, CA 92680.

All natural draft incinerators share the same essential features: a natural draft chimney, proprietary burners to anchor the flame at the bottom of the stack, and a damper arrangement or other means for regulating draft air to control temperature and support combustion.

WHY LFG INCINERATORS?

As a landfill ages, buried biodegradable waste is consumed by common bacterial species. Close to the surface, where oxygen is available, the decomposition is aerobic, producing the familiar respiration products carbon dioxide and water. However, not far below the surface, oxygen is unavailable as diffusing air is consumed by the aerobic species. Thus, for the bulk of the landfill, oxygen is unavailable and the decomposition must proceed anaerobically, producing methane. Although methane is odorless, it is flammable. Other gas products are also produced or introduced by the landfill environment, includ-

ing trace concentrations of powerful odorants such as hydrogen sulfide and mercaptans. Trace levels of known carcinogens such as some halogenated hydrocarbons, e.g., vinyl chloride, perchloro- and trichloroethylene and aromatics such as benzene are often present.

The resulting LFG can and does migrate beyond landfill boundaries and may collect in surrounding buildings producing both nuisance and hazard. In an effort to curtail such fugitive emissions, an expanding list of States require the use of LFG collection systems, whereby a series of wells are operated under negative pressure to collect the LFG. LFG so collected, has a heating value of 10 to 20 million J/m^3 (300 to 600 BTU/ft^3). Central to most collection schemes is autothermal incineration—the burning of waste gas without additional fuel. Such practices are mandated in several states including California, and are likely to increase as air and water quality standards become more stringent.

Depending on the location, the gas may be flared with a simple candle flare—a scaled down version of the common refinery flare. However, more controlled conditions are required for effective destruction, e.g., a uniform temperature for a specified residence time, especially when carcinogens are present, or as required by legislation.

Incinerator design varies with local codes. Many enclosed flares are required to meet 1,033 K (1,400°F), with a minimum retention time of 0.3 seconds and overall heights of six meters (twenty feet) or more. However, in special cases higher temperatures and residence times are required, e.g., 1,144 K (1,600°F), 2 seconds. In other areas of the country, incinerators should be 5 meters (16 feet) tall, while many other localities have few restrictions.

DESIGN OF NATURAL DRAFT INCINERATORS

Once a natural draft waste gas incinerator is chosen, the first design parameter addressed is the ability of the stack to generate draft. Perry's, et. al. [1] gives the following formula relating the height and temperature to theoretical draft:

$$\Delta P = 0.0342\, Ph(1/T - 1/T_f) \qquad (1)$$

where ΔP is the theoretical draft, Pa; P is the absolute pressure, Pa; h is the stack height above the burner, m; T is the ambient temperature K; and T_f is the average temperature of the flue, K.

The formula is derived by equating the potential energy of the stack at temperature, to the pressure-volume work that the stack can perform. Thus, an equivalent formulation of Equation (1) is:

$$\Delta P = \rho_f \cdot gh \cdot \frac{\Delta T}{T} \qquad (2)$$

where ρ_f is the density of the flue at temperature, kg/m^3 (lbm/ft^3); g is the acceleration due to gravity, 9.8066 m/s (32.174 ft/s^2); and ΔT is the difference between the flue temperature and the ambient temperature, K.

Equation (2) suggests a dimensionless parameter of the form:

The actual formulation given by Perry, et. al. is expressed in British units as:

$$P = 0.256\, Ph(1/T - 1/T_f)$$

where ΔP is the theoretical draft, in. water column; P is the absolute pressure, in. Hg @60°F; h is the stack height above the burner, ft; T is the ambient temperature, °R; and T_f is the average temperature of the flue, °R.

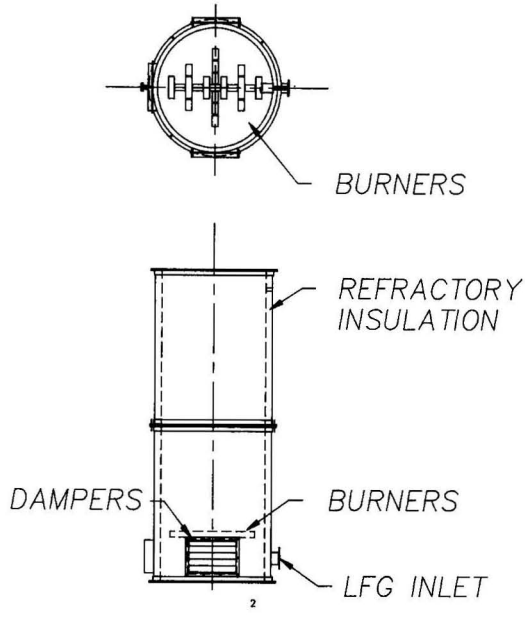

Figure 1. A natural draft waste gas incinerator.

$$\frac{\Delta P}{\rho_f gh} = T' - 1 \qquad (3)$$

where T' is the dimensionless incinerator temperature (T_f/T).

An advantage of Equation (3) is that any consistent set of units may be used. (When using British units, the left hand side of Equation (3) should be multiplied by g_c (32.174 ft/s^2 · 1lbm/lbf), to maintain dimensional consistency.) Equations 1 through 3 are all theoretical draft equations in that they do not consider frictional stack losses, entrance and exit losses through the dampers, or other forms of entropy. Entropy losses are correlated below.

From a mechanical energy balance, the maximum velocity through the stack may be calculated by:

$$\frac{\Delta P}{\rho_f} = \frac{v^2}{2} \qquad (4)$$

where v is the theoretical velocity of the stack [2].

Equating (4) with (3), a dimensionless equation of the following form is derived:

$$\frac{v^2}{2gh} = T' - 1 \qquad (5)$$

As in Equation (3), the velocity represented in Equation (5) is the theoretical stack velocity, an upper limit that neglects stack and damper losses. Equations (3) and (5) may be grouped along with dimensionless temperature as a series of Equalities:

Group I Equalities

$$N_I° = \frac{\Delta P}{\rho_f gh} \qquad (Ia)$$

$$\frac{v^2}{2gh} = \quad \text{(Ib)}$$

$$T' - 1 \quad \text{(Ic)}$$

The Group I Equalities ($N_I°$) relate draft, velocity, and temperature in a consistent form that will be convenient for later usage. The superscript ° denotes an ideal value that does not account for friction and other losses. Term Ia represents the energy ratio of draft to the potential of the stack at temperature. Term Ib is the ratio of kinetic or inertial forces to the gravitational force, and in fact is the Froude number. Term Ic expresses a dimensionless thermal driving force $\Delta T/T$.

MAXIMUM HEAT LOAD

In the preceding draft, velocity, and temperature were related in a non-dimensional form. We aim to do the same for the maximum heat load that the incinerator can provide under natural draft conditions. From a heat balance:

$$\dot{Q} = \dot{m}\, C_p\, \Delta T \quad (6)$$

where $\dot{m}$ is the mass flow of flue, kg/s; $\dot{Q}$ is the maximum heat load (power) that can be supported by natural draft, W; and C_p is the heat capacity of the flue, 1050 J/(kg · K) [0.25 BTU/(1bm · F)] is reasonable [3].

From a mass balance on the stack

$$\dot{m} = \rho_f A_f v_f \quad (7)$$

where A_f is the cross-sectional area of the incinerator, and v_f is the velocity of the flue.

Under ideal conditions, v_f is related to the stack parameters by Equation (5). ρ_f may be substituted with PM/RT_f, where R is the gas constant, and M is the molecular weight of the flue—29 kg/kgmol is suitable as the flue is mostly air. (Landfill incinerators operate at about 30/1 volumetric air/methane ratio.) Doing this and substituting Equation (5) and (7) into Equation (6), and rearranging terms leading to the following non-dimensional form:

Group II Equality

$$N_{II}° = \frac{\dot{Q}}{PA_f\sqrt{(2gh)}} = \quad \text{(IIa)}$$

$$\frac{C_p M}{R} \cdot \frac{(T' - 1)^{3/2}}{T'} \quad \text{(IIb)}$$

Group II ($N_{II}°$) is comprised of thermal-energy/pressure-volume-work ratios. Again, the superscript ° is used to denote an ideal value that takes no account of losses.

It is instructive to note that if P in term IIa is replaced by ΔP, the ratio of draft energy to heat is obtained. For reasonably sized stacks the ratio of stack-draft-energy/heat is .05% or less. In other words, the heat used to heat the flue typically represents more than 2,000 times the energy of natural draft.

Group I and II terms are plotted against dimensionless temperature (T') in Figure 2. Group I relates velocity and draft pressure to stack height in a single correlation. Group II relates the maximum heat load that a natural draft can support for a given temperature, incinerator cross-sectional area, and stack height. Group II shows Q directly proportional to stack area and the square root of height and temperature.

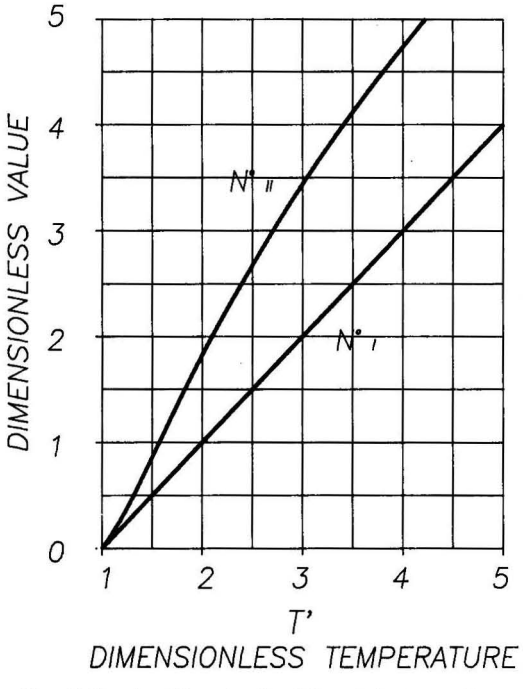

Figure 2. Group I and II as a function of dimensionless temperature.

ENTROPY LOSSES

Actual draft and permissible heat load is usually much lower than predicted by Group I and II correlations. This is due to two primary sources: stack loss due to friction, and damper loss due to the sudden contraction and subsequent expansion of influent air passing through the dampers. If the burners themselves occupy a significant area inside the flare stack, their resistance to flow must also be accounted for. In principle, these losses could be largely eliminated by streamlined air inlet passages and smooth interior stack walls. However, it is not economically justified to go to such lengths if the main objective is merely to incinerate LFG. Thus, lost work estimates are essential. It is rarely economical to recuperate thermal energy, even though many landfill incinerators produce 50 million BTU/hr or more of heat.

A factor that will reliably account for entropy losses with as simple a modification to the theoretical equations as possible is needed. We define such a factor, K, such that:

$$N_I = N_I° \cdot K \quad (8)$$

where N_I (sans superscript) denotes Group I parameters for which losses have been accounted.

It follows from this definition and the derivation of the Group II equalities that

$$N_{II} = N_{II}° \cdot \sqrt{K} \quad (9)$$

where N_{II} denotes Group II parameters for which losses have been accounted.

Presenting these variables in similar fashion to the ideal correlations we have:

Group I Equalities
(with losses accounted for)

$$N_I =$$

$$\frac{\Delta P_{net}}{\rho_f g h} = \quad (8a)$$

$$\frac{v_{act}^2}{2gh} = \quad (8b)$$

$$(T' - 1) \cdot K = \quad (8c)$$

$$N_I \cdot K \quad (8d)$$

where ΔP_{net} is the net available pressure drop after substracting frictional losses, and v_{act} is the actual velocity in the flare stack.

Group II Equalities
(with losses accounted for)

$$N_{II} =$$

$$\frac{\dot{Q}_{act}}{PA_f\sqrt{(2gh)}} = \quad (9a)$$

$$\frac{C_p M}{R} \cdot \frac{(T' - 1)^{3/2}}{T'} \cdot \sqrt{K} = \quad (9b)$$

$$N_{II}^{\circ} \cdot \sqrt{K} \quad (9c)$$

where Q_{act} is the maximum heat release that can be supported by natural draft under actual conditions, accounting for losses.

Several methods are available for estimating K. The method chosen is to account for permanent pressure losses at each station (i.e., damper, friction, etc.) plus the pressure stored as specific kinetic energy using the loss estimations of fluid dynamics [4].

The permanent pressure loss can be summed over each station

$$\Sigma \Delta P_i = \frac{1}{2} \Sigma(\rho_i v_i^2 \cdot K_i) \quad (10)$$

where the subscript i denotes a particular station. Summing these losses over the entire natural draft incinerator gives the total permanent pressure loss. The permanent pressure loss substracted from the theoretical draft yields the net stack draft available to do useful work.

From a mechanical energy standpoint, friction in the stack (stack losses) can be modeled with the friction factor [5]:

$$\frac{v^2}{2} \cdot \frac{fh}{D} = \text{friction loss} \quad (11)$$

where D is the stack diameter, h is the stack height, and f is the friction factor defined by Equation (12). In Equation (11), friction loss is the specific-energy-rate loss due to stack friction (energy normalized by the mass flow rate, commonly known as head loss). The friction factor can be correlated by the Colebrook [6] equation below:

$$\frac{1}{\sqrt{f}} = -2 \cdot \log [\epsilon/3.7D + 2.51/N_{Re}\sqrt{f}] \quad (12)$$

where ϵ is the surface roughness measured in meters, D is the incinerator diameter, m; and N_{Re} is the Reynolds number.

Equation (12) taken with Equation (11) represents a reliable way to model stack loss, but the approach suffers from two major disadvantages. First, Equation (11) assumes that the velocity is already known (explicit in evaluating the Reynolds number), when in fact, the entire reason for evaluating the friction loss is to determine the velocity. The Reynolds number is defined by:

$$N_{Re} = \frac{D \cdot v \cdot \rho_f}{\mu}$$

where μ is the viscosity of the flue at the average operating temperature, Pa·s. Equation (11) can be used iteratively with Equation (5) as a first guess in computer routines. However, without a computer the tedium of the trial-and-error approach is burdensome. Second, Equation (12) is non-linear, requiring numerical methods to evaluate. In the overall derivation of the "loss factor" it will be shown that both these objections can be overcome.

With respect to damper losses, the sudden contraction and expansion can be modeled using the familiar K factors:

$$\frac{v_d^2}{2} \cdot (K_c + K_e) = \text{damper loss} \quad (13)$$

where v_d is the velocity through the damper, K_c is the loss factor for sudden contraction, and K_e is the loss factor for sudden expansion.

If Equations (11) and (13) are combined and v_d expressed in terms of the maximum stack velocity, and the sudden expansion of the flue gases through the stack accounted for, Equation (14) is obtained:

$$\frac{v^2}{2} \cdot \left[1 + \frac{fh}{D} + K_e + \frac{(A')^2}{(T')} \cdot (K_c + K_e)\right] \quad (14)$$

where A' is the dimensionless area (stack area/total damper area).

This dimensionless area may be modified to include a dimensionless burner area, if desired, using Equation (15) below:

$$A' = \sqrt{[(A_f/Ad)^2 + (A_f/A_b)^2 - 1]} \quad (15)$$

where A_b is the area of the flare stack unoccupied by the burner.

The loss term in Equation (14) is dimensionless and the basis for the loss factor, K:

$$K = 1/\left[1 + \frac{fh}{D} + K_e + \frac{(A')^2}{(T')} \cdot (K_c + K_e)\right] \quad (16)$$

The reciprocal is used so that Group I and II terms can be multiplied by a form of K. (Multiplying Group I by K gives an estimate of the actual stack velocity and draft, while Group II must be multiplied by $\sqrt{K}$ to correct the terms to estimated actual conditions. This is implicit in the derivation of K and Groups I and II. The reader should note the form $2gh$ takes in Group I versus Group II parameters.) Equation (16), though valuable, is cumbersome to use. The equation may be used in computer routines or iterative spreadsheets. However, the introduction of two simplifications yields K as a function of the dimensionless parameters A' and T', alone.

For common draft velocities on the order of 5 to 20 m/s (15 to 60 ft/s), $f \approx 0.023$ and is fairly constant over a wide range. Assuming an average h/D ratio of 3 introduces little error, as this is a common condition. Furthermore, fh/D is small compared with $1 + K_e$, and is relatively insignificant in the final form of the loss factor.

The majority of loss in a natural draft incinerator occurs due to air moving through the dampers. For a fluid undergoing a large contraction and expansion, K_c and K_e are generally taken to be 0.5 and 1.0, respectively [7]. Both the outside air reservoir and the internal incinerator di-

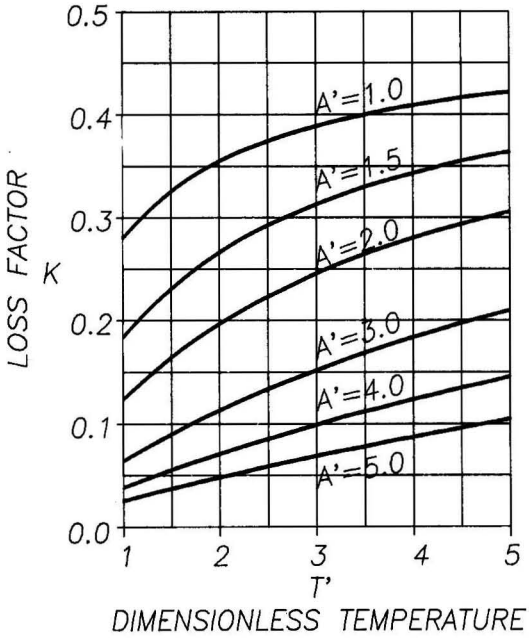

Figure 3. Correction factor for entropy losses.

mension are large when compared to the damper opening. The final effect of the simplifications is shown in Equation (17):

$$K = 1/\left[2.069 + 1.5 \cdot \frac{(A')^2}{(T')}\right] \qquad (17)$$

K is plotted against T' with A' as a parameter in Figure 3, based on Equation (17). For very slender stacks ($h/D >> 3$) the value 2.069 should be recalculated using Equations (16) and (12).

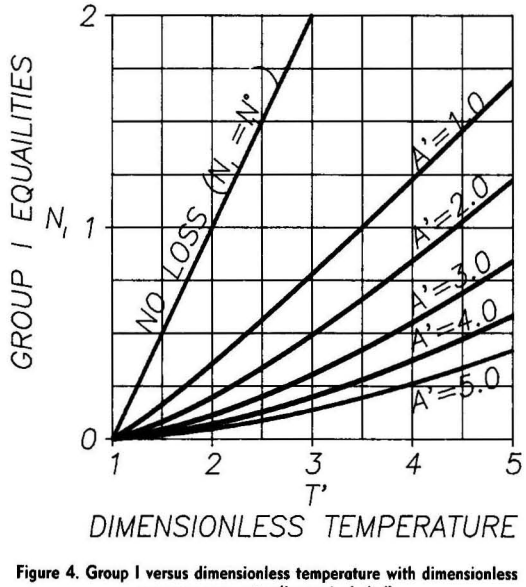

Figure 4. Group I versus dimensionless temperature with dimensionless area as a parameter (losses included).

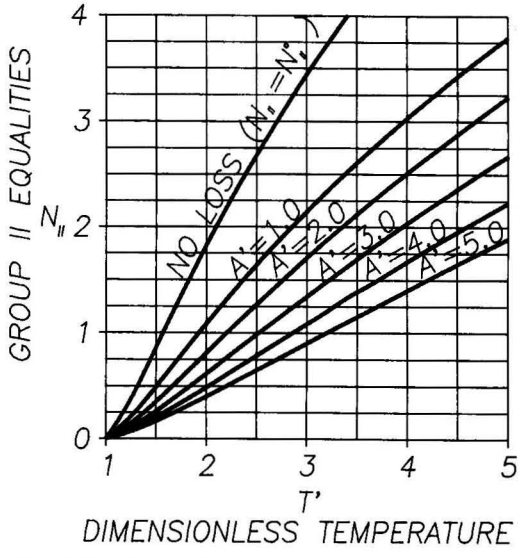

Figure 5. Group II versus dimensionless temperature with dimensionless area as a parameter (losses included).

If actual natural draft incinerators are currently in use, Equation (17) constants should be deduced as:

$$K = 1/\left[a + b \cdot \frac{A'^2}{T'}\right] \qquad [18]$$

using actual data. This will provide a reliable parameter for scale-up of similar designs. Group I parameters are multiplied by K to estimate actual values, while Group II parameters are multiplied by $\sqrt{K}$. These Groups, so modified, are presented graphically in Figures 4 and 5. In these figures the superscript ° has been removed to indicate that losses have been accounted for.

CONCLUSION

A consistent approach has been offered for the sizing and scale-up of natural draft incinerators. The equations presented reduce a large number of geometric and operating parameters to a small number of dimensionless groups that are functions of geometry and temperature alone. Design parameters have been deduced, however, in order to justify the actual constants in Equation (18), experimental work is required.

LITERATURE CITED

1. Perry, Robert H., and Cecil H. Chilton, Eds., *Chemical Engineering Handbook, 5th Edition*, 9–38, McGraw-Hill, New York (1973).
2. Welch, Harry J., Ed., *Transamerica Delaval Engineering Handbook, 4th Ed.*, 4–49, McGraw-Hill, New York (1970).
3. Welty, J. R., C. E. Wicks, and R. E. Wilson, *Fundamentals of Momentum, Heat, and Mass Transfer, 3rd Ed.*, 755, John Wiley and Sons, New York (1984).
4. Peters, M. S., and K. D. Timmerhaus, *Plant Design and Economics for Chemical Engineers, 3rd Ed.*, 514, McGraw-Hill, New York (1980).
5. McCabe, W. L., and J. C. Smith, *Unit Operations of Chemical Engineering, 3rd Ed.*, 86, McGraw-Hill, New York (1976).
6. Giles, R. V., *Fluid Mechanics and Hydraulics, 2nd Ed.*, Schaum's Outline Series, McGraw-Hill, New York (1962).
7. Perry, Robert H., and Cecil H. Chilton, Eds., *Chemical Engineering Handbook, 5th Edition*, 5–53, McGraw-Hill, New York (1973).

Fundamental Experiments on Thermal Desorption of Contaminants from Soils

JoAnn S. Lighty, Geoff D. Silcox, David W. Pershing
Department of Chemical Engineering, University of Utah, Salt Lake City, Utah 84112

Vic A. Cundy
Department of Mechanical Engineering, Louisiana State University, Baton Rouge, Louisiana 70803

and

David G. Linz
Environment and Safety Research, Gas Research Institute, Chicago, Illinois 60631

The goals of this research are to develop an understanding of the transport phenomena that occur during the desorption of contaminants from soil and to obtain rate information. This information can then be used to develop a model to predict the performance of full-scale thermal treatment systems for optimization and cost reduction.

INTRODUCTION

Hazardous-waste incineration is an effective technology for the remediation of contaminated solids and results in permanent destruction of most organic hazardous compounds. Due to wide commercial availability, future advances in this technology and other thermal-destruction technologies are expected [*1*]. Present research [*2, 3*] has focused on the chemical kinetics and decomposition of the hazardous off-gas in the secondary combustor or afterburner. However, to understand the primary-combustor process fundamentals, i.e., volatilization of contaminant, mass transfer, and heat transfer, it is necessary to model the transient behavior of the system. Knowledge of the transient primary-combustor processes will lead to optimum afterburner design and prediction of possible failure modes or "puffs" as studied by Linak, McSorley, and Wendt [*4*].

A three-fold fundamental, experimental program is underway at the University of Utah to understand the transport phenomena that occur during the desorption of contaminants from solids during thermal treatment. A Particle-Characterization Reactor (PCR) is used to evaluate the transport phenomena occurring on a particle basis, where the controlling resistances are largely intraparticle. Desorbent gas is passed through a thin bed of soil such that the surface-temperature and concentration of the particle are known and bulk gas-phase gradients are negligible.

The Bed-Characterization Reactor (BCR) represents a one-dimensional mass-transfer and heat-transfer experiment where resistances within a soil bed are considered.

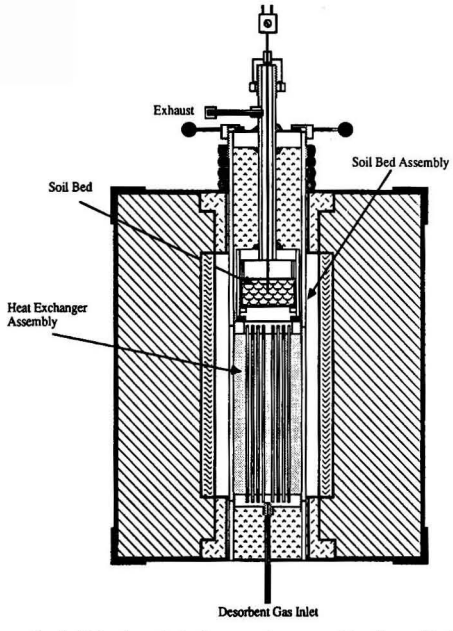

Figure 1. Particle-characterization reactor assembly. From *Nuclear Chemical Waste Management*, [5]. Reproduced by permission of Pergamon Press.

Desorbent gas is swept across the top of a bed of solid; heat is transferred to the bed and contaminant is evolved from the solid to the bulk stream. Gradients exist within the depth of the bed only.

PCR and BCR results are directly applicable to several industrial incineration processes, for example, a moving grate, a multiple hearth, or a fluidized bed. To evaluate the transport processes occurring in a full-scale rotary-kiln system, where the effects of solids mixing and heat-transfer (flame radiation, wall conduction) must be taken into account, a third facility, a rotary-kiln simulator, has been built.

EXPERIMENTAL EQUIPMENT

Particle-Characterization Reactor

The Particle-Characterization Reactor (PCR) has been designed to examine the transport phenomena occurring in a particle where the resistances are largely intraparticle. The reactor (Figure 1), designed to operate up to 1200°C, is constructed in two major pieces, a soil-bed assembly and heat-exchanger assembly, both of which are placed in a high-temperature furnace. The heat-exchanger assembly is constructed from a series of concentric tubes designed to preheat the desorbent gas prior to its passing up through the soil bed. The soil-bed assembly supports a thin bed of soil (1.3-cm thick) and rests on top of the heat-exchanger assembly. After the gas has been preheated, the gas passes up through the soil bed, exits out the top of the soil-bed assembly and is then pumped to a gas-chromatograph (GC) system equipped with a flame-ionization detector (FID). The data obtained from this reactor result in time-resolved contaminant evolution curves.

Bed-Characterization Reactor

The Bed-Characterization Reactor (BCR) is a one-dimensional equipment exploring heat-transfer- and mass-

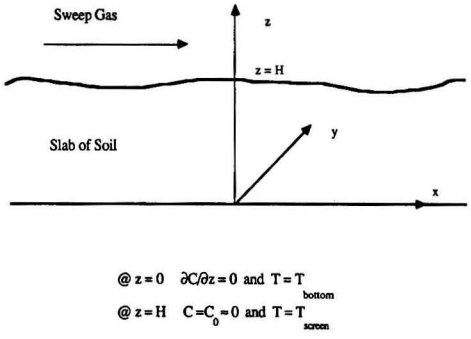

Figure 2. Bed-characterization reactor concept.

transfer resistances through a bed of soil. Temperature and concentration gradients exist within the depth of the soil only (see Figure 2); these gradients are used to obtain the effective thermal conductivity and diffusivity for the selected solid, contaminant, and temperature. As illustrated in Figure 3 two trays are placed in a high-tempera-

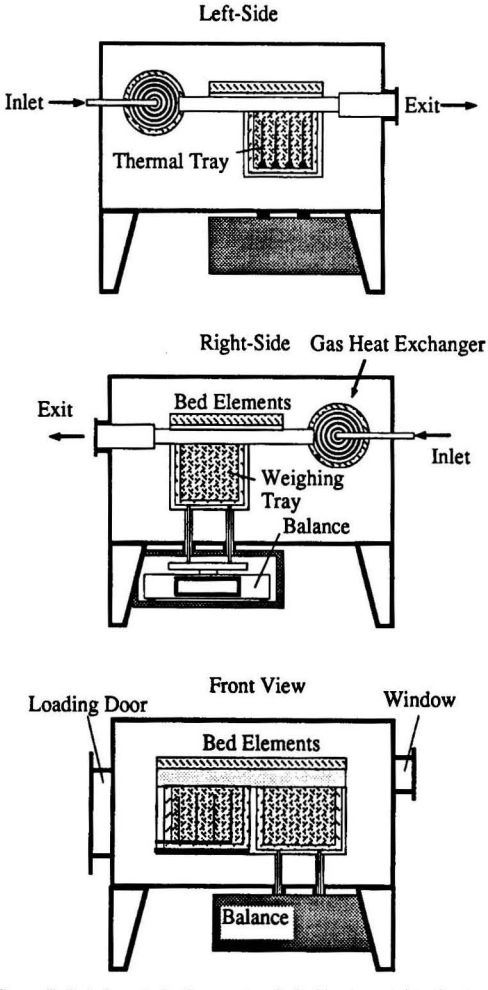

Figure 3. Bed-characterization reactor: Left-side view, right-side view, and front view.

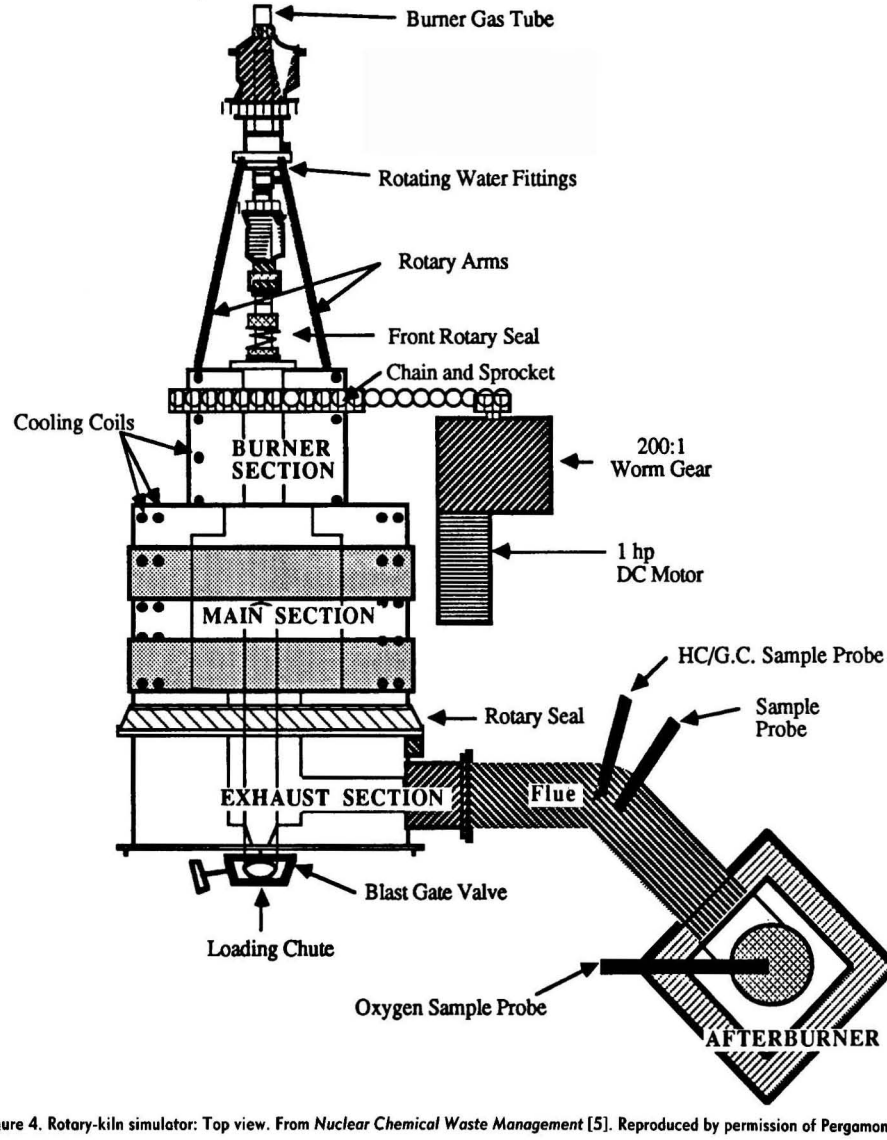

Figure 4. Rotary-kiln simulator: Top view. From *Nuclear Chemical Waste Management* [5]. Reproduced by permission of Pergamon Press.

ture furnace (1200°C) and desorbent gas passes over the top of the trays. The exhaust gas is analyzed using GC/FID and GC/MS (mass spectrometry) techniques. One tray is equipped with twelve Type-K thermocouples located at different depths and cross-sectional locations. The second tray is placed on a Mettler PM-4000 electronic balance (0-4000 g with 0.01 g sensitivity). This tray is used to measure the transient weight loss resulting from the evolution of residual moisture, soil organics, and contaminant. A radiant heater is located above both trays to maintain the temperature of the system. The bottom temperatures are known, defining the boundary conditions for temperature at this location; the solid bottom insures a zero concentration-gradient boundary condition.

Rotary-Kiln Simulator

The rotary-kiln simulator has been used to study the transient evolution of contaminants from solids in a realistic mixing and temperature environment. The 73 kW kiln is constructed in three major sections: a burner section, main section, and exhaust section. The burner section and main section rotate while the exhaust section is stationary and connected to an afterburner system. The gases from the kiln are continuously analyzed for CO, CO_2, and O_2, and semi-continuously for hydrocarbons using GC/FID and GC/MS. The simulator is a batch system, that is, a batch of contaminated solid is loaded into the main section of the kiln through a rear loading location (see Figure 4) and combusted for a determined residence time. This batch of solid represents a control volume of solid moving down the length of a continuous-feed, full-scale rotary kiln. The variable of distance in a full-scale system is replaced with time in the simulator so the measurement of transient hydrocarbon evolution from a control volume of solid is possible.

The afterburner system consists of two opposing burners, rated at 73 kW each, placed in a rectangular combustion chamber. Oxygen is measured at the exit of the afterburner.

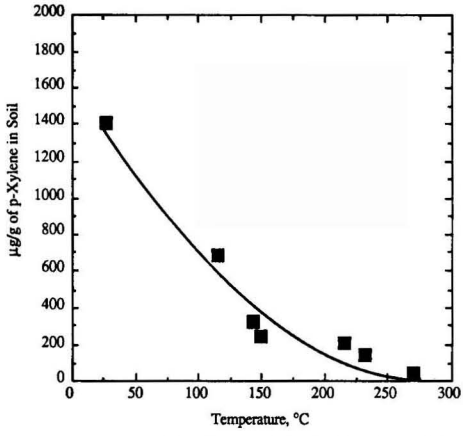

Figure 5. Concentration of p-xylene remaining in the clay soil after desorption for 1 hour in the PCR at several temperatures. Data obtained from Ref. [5].

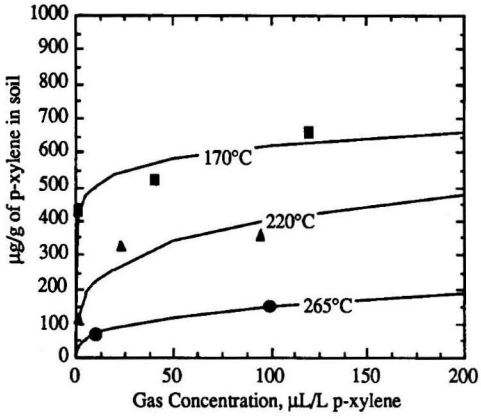

Figure 6. Adsorption data from the PCR for clay compared with Freundlich isotherm model.

DISCUSSION OF RESULTS

This paper reports on results from experiments in all three reactor systems — the PCR, BCR, and rotary-kiln simulator — using a clay soil contaminated with p-xylene. A series of BCR results, examining the effects of temperature and bed depth on the desorption of contaminants, are also presented and discussed.

Particle-Characterization Reactor Results

Experiments in the PCR have shown that several variables are important in the desorption of contaminant from the soil, including temperature and soil type. Higher temperatures result in faster desorption rates and a lower concentration of contaminant remaining in the soil, as shown in Figure 5 which is a graph of the concentration remaining in the soil as a function of temperature. Soil type affects the desorption rate and the amount of contaminant evolved. The adsorption characteristics, a function of temperature, appear to strongly influence the rate of desorption. Even at low gas-phase concentrations and at temperatures above the contaminant boiling point, contaminant can adsorb onto the soil, as illustrated in Figure 6 for clay contaminated with p-xylene. The adsorption data can be represented by the Freundlich-isotherm model. This isotherm assumes that the heat of adsorption increases logarithmically with decreasing surface coverage.

Bed-Characterization Reactor Results

Temperature was also found to be an important variable in the BCR experiments. The temperature of the sweep gas and radient heaters in the BCR experiment affected the rate of desorption and total evolution of contaminant, as illustrated in Figure 7 for a 7.6-cm bed of clay soil desorbed at gas temperatures of 175, 240, and 315°C. The data are shown as percent of p-xylene evolved versus time, where the initial p-xylene concentration in the soil was 0.5% by weight (a total of approximately 17.2 g of p-xylene). At 175°C, the p-xylene evolved slowly and by 7.5 h the concentration near the top of the bed was approximately 600 µg/g while the concentration on the bottom was 1450 µg/g. The rate of evolution increased at 240°C and the concentration was approximately 20 µg/g at the top and 400 µg/g at the bottom. For 315°C, the p-xylene evolved rapidly and was essentially completely driven from the bed after 6 h. The data show a period of constant evolution followed by a falling-off period. During the constant-rate region, contaminant evaporates from the soil and heat of desorption is simply the latent heat of vaporization. When the soil contaminant concentration reaches a critical concentration, the heat of desorption becomes a function of surface coverage (as discussed in the PCR results), and the rate of evolution decreases.

The effect of bed depth was also studied. Data for 5.1-cm and 7.6-cm beds are shown in Figure 8 as percent soil weight evolved as a function of time. The thermal resistances in the thinner bed were reduced; therefore, the contaminant evolved from the bed faster and more completely, as expected.

PCR, BCR, and Kiln-Simulator Results Comparison

As previously discussed, the BCR represents a system with large gradients within the bed of soil while the PCR has small gradients due to the gas flow through the bed. Figure 9 shows the fraction of p-xylene evolved versus time for a PCR experiment (280°C gas temperature), a BCR experiment (top of the bed calculated at 290°C), and a rotary-kiln simulator experiment (280°C gas tempera-

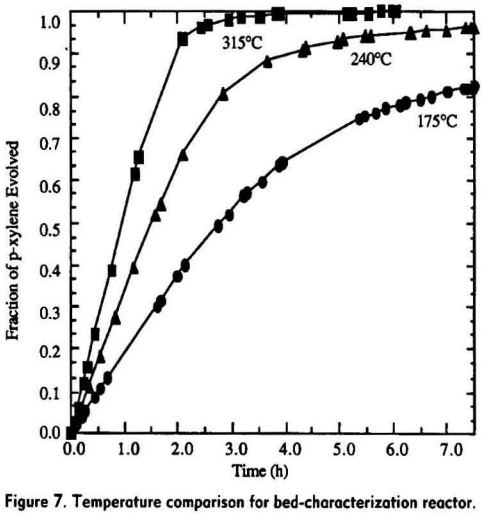

Figure 7. Temperature comparison for bed-characterization reactor.

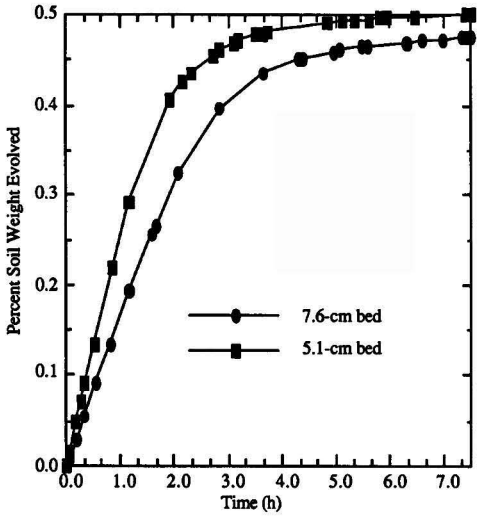

Figure 8. Illustration of bed depth effects in BCR.

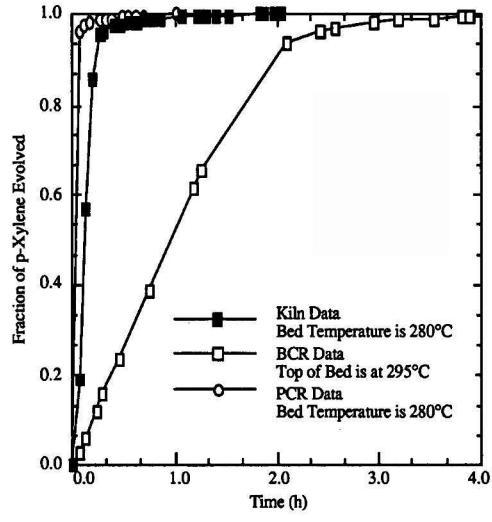

Figure 9. Comparison of results from the three reactors at a desorption temperature of ~280°C.

ture). The figure illustrates the importance of the degree of mixing and gas/solid contacting in the soil bed. In the PCR experiment, the contaminant evolved rapidly, within 0.4 h, while for the BCR run, at the end of 0.4 h, only 20% of the contaminant evolved (based on an average of the top and bottom concentrations in the bed). As expected, the kiln data are intermediate between the PCR and BCR data. The PCR evolution rate was the highest due to gas flow through the bed of particles, resulting in rapid heat-up of the bed and excellent gas/solid contacting. The soil in the PCR comes to 90% of the final operating temperature in approximately 0.2 h. Gradients of temperature are high in the BCR system, resulting in slower desorption of contaminant. Due to the mixing and wall conduction in the kiln, the kiln soil bed heats up rapidly (90% in 0.3 h), accounting for the similarity of the kiln experiment and the PCR experiment. Still, gas/solid contacting and heating rates in the kiln bed are intermediate between the PCR and BCR.

CONCLUSIONS

Thermal desorption data have been obtained for three reactors using a clay soil contaminated with p-xylene. The PCR data suggest that: Local temperature is a key parameter governing the rate of desorption of contaminant from soil.

The functional form of the adsorption isotherm influences the rate of desorption and causes the decreased desorption rate prior to complete removal. The adsorption characteristics are strongly dependent upon temperature, accounting for the strong temperature dependence of the desorption data. The adsorption data can be represented by the Freundlich isotherm, where the heat of adsorption varies logarithmically with surface coverage.

The BCR data have shown that higher temperatures yield faster desorption rates.

Thermal and mass-transfer resistances within the soil bed are important to the rate of evolution and the amount of contaminant evolved. This result was confirmed in experiments comparing two different bed depths and in a comparison of PCR and BCR data.

Desorption rates follow a constant-rate period followed by a falling-off regime. The falling-off region indicates that desorption of the final monolayer of contaminant is a function of the adsorption characteristics of the soil. Mathematical modeling of the BCR system indicates that the gas/solid equilibrium at the particle surface can be represented by the Freundlich isotherm which is in agreement with the PCR results. The results from the kiln experiment show the importance of bed mixing and bed heating rate. The evolution rate is faster in the kiln than in the BCR due to increased bed heat-up rates and gas/solid contacting.

ACKNOWLEDGMENTS

This work was funded by the Gas Research Institute, Dave Linz, Project Manager, the National Science Foundation-Presidential Young Investigator Program, and the Advanced Combustion Engineering Research Center (NSF/ACERC). Funds for the ACERC center are received from the National Science Foundation, the State of Utah, 22 industrial participants, and the U.S. Department of Energy. The assistance of Warren Owens, Department of Mechanical Engineering, University of Utah, and Chris Leger, Department of Mechanical Engineering, Louisiana State University, is also appreciated.

LITERATURE CITED

1. Oppelt, E. T., *J. Air Pollut. Control Assoc.*, 8, p. 558 (1987).
2. Dellinger, B., et al., "PIC Formation under Pyrolytic and Starved Air Conditions"; U.S. Environmental Protection Agency, EPA/600/S2-86/006 (1986).
3. Cundy, V. A., J. S. Morse, and D. W. Senser, *J. Air Pollut. Control Assoc.*, 36, p. 824 (1986).
4. Linak, W. P., J. A. McSorley and J. O. L. Wendt, *J. Air Pollut. Control Assoc.*, 37, p. 934 (1987).
5. Lighty, J. S., D. W. Pershing, and V. A. Cundy, *Nucl. Chem. Waste Manag.*, 8, 225 (1988).

Evaluation of Alternative Processes for Final Treatment of Hazardous Waste Effluents

John A. Meardon
Kirk-Mayer Inc., Livermore, CA

Sol Lyandres
John T. Rees
TENERA, LP, Berkeley, CA

and

Stuart Shealy
International Technology Corp., Knoxville, TN

Five process unit operations were evaluated for effectiveness in treating aqueous effluent from a hazardous waste treatment facility. The aqueous effluent contained residual amounts of various organics and heavy metals. The objective of the pilot test program was to produce an aqueous product which could meet requirements for discharge to a POTW, or directly to the environment, and a solid product which could be disposed of in a Class I landfill. Processes evaluated included one primary, evaporative crystallization, two secondary, activated sludge bio-treatment and reverse osmosis, and two tertiary, carbon adsorption and ultraviolet peroxidation. Test results from these process operations identified several processing configurations whereby the final treated product could meet discharge criteria. Performance results of each process unit operation are summarized and discussed.

INTRODUCTION

IT Corporation owns and operates a hazardous waste treatment, storage and disposal (TSD) facility in Contra Costa County, California. The TSD facility provides primary treatment for a variety of industrial wastes. The effluent from these predominantly batch treatments is held in surface impoundments for solar evaporation.

The California State Toxic Pits Cleanup Act of 1984 (TPCA) prohibits the storage or disposal of liquid hazardous wastes in some surface impoundments beyond specified dates and in other surface impoundments unless in accordance with specific statutory requirements. Compliance with TPCA legislation as well as a desire to modernize its existing TSD facility were the primary objectives in IT's pursuing a program to evaluate alternate treatment technologies on a pilot scale. The pilot demonstrations were focused on the processing of aqueous effluents resulting from the primary treatment of incoming hazardous wastes to the TSD facility.

In regard to compliance with the TPCA legislation the pilot unit operations were intended to demonstrate a treatment and processing scheme by which residual liquids in the impoundments could be rendered acceptable for discharge from the facility. In meeting this criteria it was also desired that any solid by-product would be acceptable for disposal in a Class I landfill. Pilot scale demonstration of an acceptable process scheme would provide viable information and data from which the units could be scaled. Pilot tests would also provide actual performance results for the permitting process which must precede installation and operation. In conjunction with IT's goals to modernize the existing TSD facility it was highly desirable that the selected processing scheme be directly adaptable, or easily modified, for use in that facility. Thus, a modernized TSD facility would use the same equipment as that needed for TPCA compliance, satisfy the processing needs and discharge requirements of the new facility and minimize additional capital investment.

The pilot program was initiated in November, 1986 by conducting a variety of laboratory tests on samples of impounded liquids. The impounded liquids consist primarily of concentrated salt brines contaminated with a variety of organics. The tests were conducted for "Proof of Principle" as well as for generating information from which a focused pilot demonstration could be planned. Laboratory testing centered around the processes of evaporation, stripping, carbon adsorption, and chemical oxidation. Results of the laboratory testing, along with a review of a

TABLE 1. FEEDSTOCK SUMMARY

	Modernized Plant Feedstock	TPCA Feedstock
DISSOLVED METALS, mg/l		
Antimony	ND	0.93
Arsenic	3.5	ND
Beryllium	TR<0.2	TR<0.005
Boron	200	460
Cadmium	ND	0.28
Chromium, (Total)	13	12
Copper	510	38
Lead	0.64	3.8
Mercury	0.004	0.011
Nickel	27	48
Selenium	0.017	ND
Silver	ND	0.06
Vanadium	1.4	10
Zinc	7:2	15
MISCELLANEOUS CHEMICALS, mg/l		
Ammonia	256	4960
Calcium	30	1060
Chloride	13000	58000
Cyanide	1.8	1.2
Fluoride	1500	520
Magnesium	43	93
Potassium	1160	1900
Sodium	30200	71800
Sulfate	17000	38000
Sulfide	53	109
MISCELLANEOUS PARAMETERS		
pH, units	8.9	8.9
Conductivity, μmhos/cm	48000	100000
Density, mg/l	1030	1116
Alkalinity, mg/l	6700	12200
BOD5, mg/l	670	146
COD, mg/l	7550	19700
TOC, mg/l	3900	13000
TKN, mg/l	380	5100
TDS, mg/l	53300	158000
TSS, mg/l	1320	80
SELECTED VOLATILE ORGANICS, μg/l		
Acetone	5300	970
Benzene	ND	TR<5
2-Butanone (MEK)	ND	74
N-Butanol	TR<240	ND
Chloroform	TR<75	TR<5
Ethylbenzene	TR<51	TR<5
1,1,1-Trichloroethane	ND	TR<5
Toluene	TR<83	12
Xylenes	320	22
SELECTED SEMI-VOLATILE ORGANICS & HERBICIDES, μg/l		
Naphthalene	TR<2000	ND
Bis(2-Ethylhexyl)phthalate	TR<2000	ND
Benzoic Acid	ND	80000
2-Methylnaphthalene	4800	ND
2,4,5-TP	16	150
SELECTED PHENOLS, μg/l		
2-Chlorophenol	4700	ND
2,4-Dichlorophenol	7300	ND
2-Nitrophenol	1500	ND
Phenol	57000	ND

NOTES:
ND = Not Detected
TR = Trace amount detected; Not quantified below indicated limit.

number of other alternate processing technologies, provided the basis for selecting specific process units to be piloted.

To replace and deinventory the existing solar evaporation impoundments three alternates were identified. These alternates were to discharge to: 1) a local POTW; 2) a local waterway or; 3) to the atmosphere via direct evaporation. Discharge to a POTW requires compliance with local sewer discharge criteria, whereas effluent discharges to the local waterways require California State Regional Water Quality Board acceptance and the issuance of an NPDES permit. Atmospheric emissions are governed by the local Bay Area Air Quality Management District via air permit. The preceding options are listed in

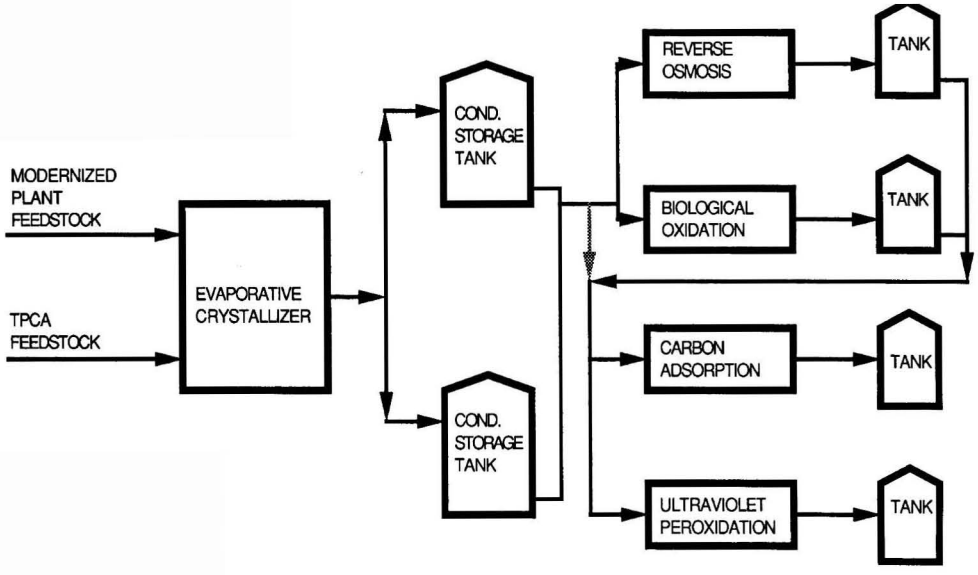

Figure 1. Pilot test program block flow diagram.

order of technical and economic preference and perceived order of decreasing political difficulty to implement.

FEEDSTOCK SOURCE AND DESCRIPTION

The objective of the pilot demonstration was twofold. First was the demonstration of a successful process configuration for the treatment and discharge of existing aqueous impoundments to comply with pending TPCA legislation deadlines. Second was a comparable demonstration for expected effluent from a modernized treatment plant.

The first feedstock was plentiful with more than 300 acre-feet of impounded liquids available at the time of pilot testing. The second feedstock could only be simulated since effluent from a yet to be constructed facility was not available. Although the new facility is to have modern and more efficient treatment technologies, a synthetic feedstock to represent the expected effluent is still only a "best guess" based on assumed incoming waste streams and process performance. Effluent derived from the existing treatment facility is considered to represent a "worst case" effluent for the modernized facility.

TPCA feedstock was an "aged" effluent from prior years treatment operations at the facility. This "aged" effluent was more concentrated in inorganic salts and had a different organic character than the modernized facility feedstock. The modernized facility feedstock was effluent which had been impounded for less than sixty days. Key analytical parameters of the two pilot demonstration feedstocks are summarized in Table 1. It is evident that the TPCA feedstock was more concentrated in inorganic salts (TDS) as well as residual organics (TOC) than the modernized plant feedstock. Organic analyses also indicated differences between the two feedstocks. These differences were attributed primarily to the aging of the material through solar evaporation and biological action which took place over prolonged impoundment.

PILOTED PROCESSES

Unit operations selected for pilot demonstration at the TSD facility consisted of a single primary treatment process, two secondary treatment processes and two tertiary treatment processes. The process selected as the primary treatment was forced circulation evaporative crystallization. No alternate to this process was contemplated due to very successful laboratory results. Secondary treatment processes chosen were biological oxidation via an activated sludge system, and membrane separation via reverse osmosis. The secondary processes were limited to processing the resultant aqueous condensate feedstock which was generated by the evaporative crystallizer. Tertiary processes consisted of liquid-phase carbon adsorption and an ultraviolet peroxidation process. Both tertiary processes were intended for any polishing of effluent from the secondary processes if needed to meet acceptable discharge levels. The unit operations included in the pilot testing program are shown in a simplified block flow diagram presented in Figure 1. A brief description of each unit operation follows.

Crystallization

To perform demonstration testing at IT's TSD facility a pilot scale forced circulation crystallization unit was leased from HPD, Incorporated of Naperville, Illinois. The unit was rated at two to four liters per minute of evaporative capacity and was constructed predominantly of Alloy 825. The crystallizer consisted of a vapor body, an external heater, recirculation pump, primary and vent condensers, and associated instrumentation and controls. As part of the crystallization unit a batch perforated bowl centrifuge was supplied to purge and dewater the crystallized salts from the system. The heater was supplied with an external source of steam but operated under conditions to simulate a vapor recompression unit. The crystallizer system is depicted in Figure 2.

Biological Oxidation

A small scale activated sludge system was constructed to perform testing at the treatment site. The biological oxidation system consisted of a feed and nutrient tank, a 750 liter bioreactor and clarifier and effluent receiver. The reactor contents were continually mixed and supplied with oxygen via compressed air fed through air diffusers mounted on the reactor base. Feed and recycle flows were controlled using metering pumps. The biological oxidation system is depicted in Figure 3.

Reverse Osmosis

A small reverse osmosis unit capable of processing 20 liters per minute of feed material at pressures of up to 6900 KPa was purchased for demonstration testing at the treatment facility. The unit consisted of a skid frame equipped with a feed supply reservoir, a high pressure positive displacement pump, piping and mounting structure for two membrane pressure vessels and associated instrumentation and controls. The unit was operated in a total recycle mode as well as a once through semi-continuous production mode for the generation of performance data and feedstock for tertiary treatment processes. The reverse osmosis system is depicted in Figure 4.

Granular Activated Carbon Adsorption

Two one-meter sections of 2.5-centimeter diameter glass column were assembled for use in the granular activated carbon adsorption demonstration testing. In addition to the column the system included a feed tank, feed pump, product receiver and manual instruments and controls. The unit was packed with Calgon Filtrasorb 300 activated carbon for all testing. The configuration of the activated carbon adsorption unit is shown in Figure 5.

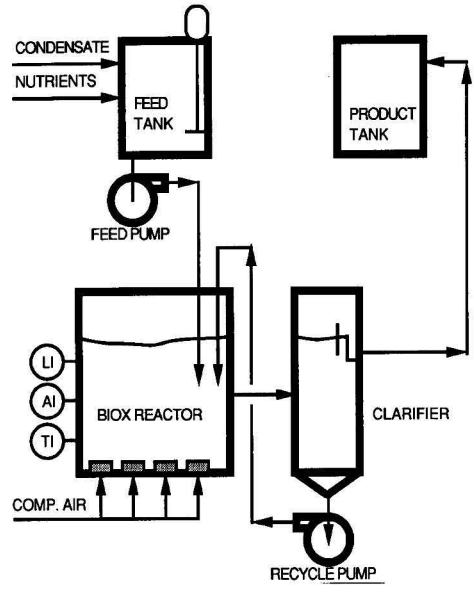

Figure 3. Biox test unit.

Ultraviolet Peroxidation

A 750 liter batch recirculating pilot unit was leased from Peroxidation Systems, Inc. Tucson, Arizona for demonstration testing at the treatment facility. The Peroxidation unit consisted of a feed-recirculation tank, recir-

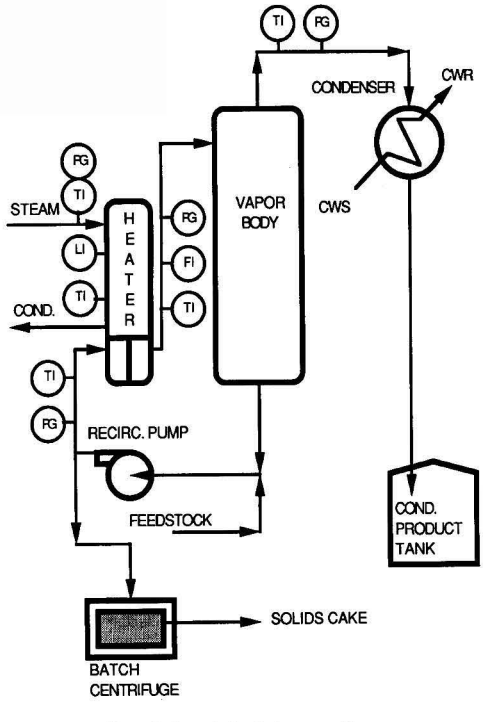

Figure 2. Forced circulation crystallizer.

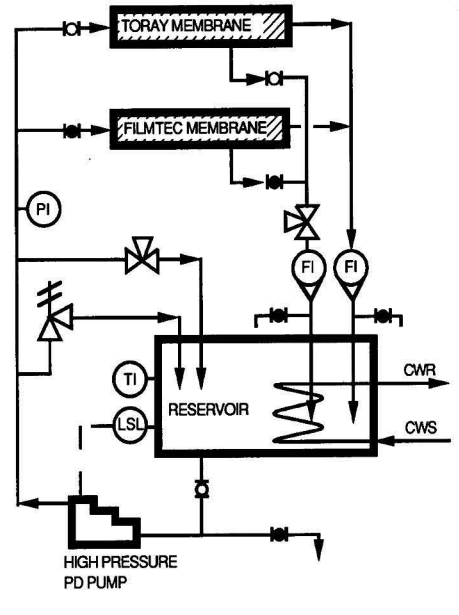

Figure 4. Reverse osmosis test unit.

culation pump, reaction chamber equipped with eight independent 5 Kw UV lamps, associated instrumentation and controls. The UV peroxidation system is depicted in Figure 6.

UNIT PERFORMANCE

General

The two primary feedstocks described previously (TPCA feedstock, and Modernized facility feedstock) were evaluated for the pilot test program. Both of these feedstocks were processed through the crystallizer unit for performance testing as well as subsequent secondary feedstock production. The condensate product from the crystallizer became in turn the feedstock for both secondary units. Treated product from each secondary treatment unit was collected to provide feedstock for evaluation in the tertiary treatment units. Each unit operation feedstock and product was sampled and analyzed to assess process performance. Selected treatment unit products were retained in sufficient volume for more detailed analytical evaluation.

Crystallizer

As the primary treatment process the forced circulation crystallizer was selected based on its ability to provide a gross separation of inorganic and organic contaminants from the aqueous feed. Operation of such units for decontamination is standard and has been practiced in a variety of industrial applications [*1*]. Details of the crystallizer performance for this pilot test program are reported elsewhere [2] and therefore will only be summarized here.

In both test runs the crystallizer performed as well as, or better than, originally anticipated. The condensate products exhibited total organic carbon (TOC) concentration an order of magnitude less than their respective feedstocks. The product condensates contained a variety of low to moderately volatile organics (50-200 °C Boiling Point). These organics consisted primarily of carboxylic acids, alcohols, ketones, and aromatic compounds.

Overall the crystallizer unit performed well. For both feedstocks tested there was no appreciable permanent fouling to the heat transfer surface. Fouling which did occur was readily removed through routine operating practices such as feed, hot water, or mild acid washing.

The resultant boiling point rise of the saturated mother liquor for both feedstocks tested was within an acceptable range (10-12 °C) for utilization of a mechanical vapor recompression evaporator.

The solid product from both feedstock evaluations was effectively dewatered to pass the paint filter test and thus was acceptable for disposal in a Class I landfill. The removal of inorganic salts through the crystallization process also provided an adequate purge for the residual heavy organics which were potential foulants to the system. These organics were removed through adsorption on or entrainment within the crystalline product.

A summary of key analytical parameters for each feedstock and its respective condensate and solid products is presented in Table 2.

Biological Oxidation

Use of biological oxidation treatment systems for the destruction of organic contaminants has been demonstrated successfully for contaminated ground water as well as for treatment of a variety of industrial waste waters [*3, 4, 5*]. The biological treatment unit was piloted as a secondary treatment process for the purpose of demonstrating the biodegradability of crystallizer condensates. Information obtained from the testing program would also be used to define the process equipment for IT's own installation if required and warranted. Acceptable biodegradation was obtained for both condensate feedstocks. The source of activated sludge for the bioreactor pilot unit was from a large petroleum refinery biotreatment system in the local area. Nutrients (nitrogen and

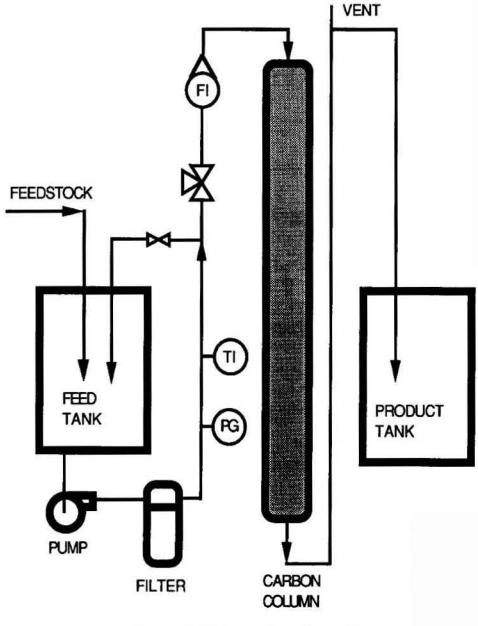

Figure 5. Carbon adsorption unit.

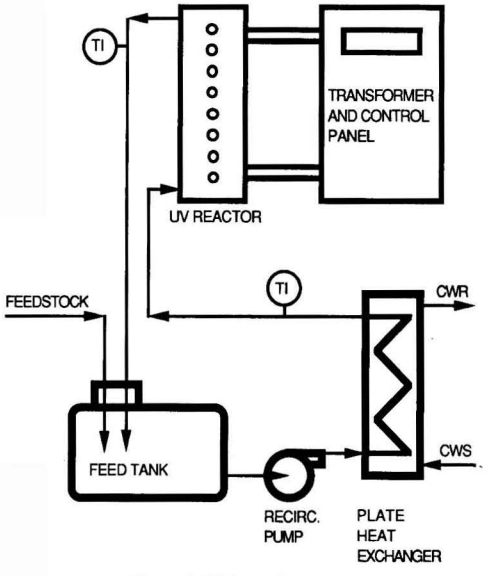

Figure 6. UV-Peroxidation unit.

TABLE 2. FORCED CIRCULATION CRYSTALLIZER PILOT TESTING SUMMARY

Run No.	Feedstock	Feed TOC Wt %	Feed TDS Wt %	Condensate TOC Wt %	Condensate TDS Wt %	Mother Liq. TOC Wt %	Mother Liq. TDS Wt %	Solids O&G Wt %	Solids Moist Wt %
1	TPCA	1.23	16.2	0.17	0.01	1.8	25.2	NA	NA
2	TPCA	2.27	17.5	0.16	0.03	3.7	38.1	NA	NA
3	TPCA	1.81	16.2	0.15	0.01	8.3	44.7	2.1	~5
4	Modern Plant	0.47	4.8	0.05	NA	3.1	28.2	NA	NA
5	Modern Plant	0.46	4.8	0.05	0.04	5.9	37.9	NA	NA
6	Modern Plant	0.46	4.8	0.05	0.02	3.3	38.1	2.1	~5

NA = Not Analyzed

phosphorous) necessary for proper microbial metabolism were added to the activated sludge system in the standard ratio of BOD5:N:P = 100:5:1. A pH buffer solution and a small amount of commercial fertilizer for micro-nutrients were also added to the system. Biodegradation of organics in both condensate feedstocks, as measured by TOC reduction, was usually in excess of 80 percent at hydraulic retention times (HRTs) in the order of 2 to 3 days. The food to micro-organism (F/M) ratios for the respective TPCA and modernized facility condensate feedstocks were demonstrated at levels of 0.30 and 0.45 for both condensate feeds. Mixed liquor volatile suspended solids (MLVSS) concentrations were maintained between 2200-2500 mg/l throughout all test runs. Table 3 summarizes key operating parameters for the biological tests conducted.

Reverse Osmosis

Reverse osmosis was selected as an alternate secondary treatment process based on reported performance of organic removal from a variety of aqueous streams [6, 7]. The condensates produced by the crystallizer are essentially free of scaling salts and suspended solids, therefore typical pretreatment requirements are not necessary for the operation of a reverse osmosis system. In essence, the feed stream is ideal with respect to unit operation. Both condensate products derived from the crystallizer operations were used in the tests conducted with the reverse osmosis unit. Test results for the reverse osmosis unit are reported in detail elsewhere [8] and will only be summarized here.

Two spiral wound thin-film composite membranes were tested under a variety of conditions. The two membranes tested were the Toray PEC-1000 and the Filmtec SW30-HR2540. Testing focused on two key parameters (1) effect of condensate feed pH on overall TOC rejection through the membrane, and (2) effect of TOC concentration in the feed on overall TOC rejection through the membrane. Results of the reverse osmosis test program demonstrated a slight effect of feedstock pH on the resultant permeate quality (TOC removal efficiency). A maximum permeate quality, and thus minimum permeate TOC concentration, was observed in the pH range of 3 to 8. Both membranes exhibited in excess of 98 percent rejection of TOC content for up to a tenfold increase in feedstock TOC concentration. This performance represented a system recovery of 90 percent. Analysis of the reverse osmosis concentrate indicated that this stream could be further concentrated and is acceptable for disposal via direct injection incineration. Typical performance characteristics for the reverse osmosis system are presented in Figures 7 and 8.

Carbon Adsorption

Removal of organic compounds from wastewaters by use of carbon adsorption is a widely used and accepted technology. Carbon adsorption is very effective in removing most hydrocarbons and chlorinated solvents and can be effective on many other complex and high molecular weight compounds. Carbon adsorption has not been found effective in removing organic compounds which exhibit significant water solubility [9, 10].

The carbon adsorption process was included in the pilot test program in order to evaluate its use as a tertiary treatment for secondary effluents derived through biological oxidation or reverse osmosis.

TABLE 3. BIOLOGICAL OXIDATION UNIT PILOT TESTING SUMMARY

Run No.	Feedstock	System HRT* Days	Feed Rate l/D	Feed TOC mg/l	Product TOC mg/l	Avg. TOC Reduction %
6	Modern Plant	2.2	290	600	160	73
7	Crystallizer	2.0	325	600	120	80
8	Condensate	1.8	370	600	120	80
1		15.5	32	1500	90	94
2		12.1	40	1500	88	94
3		7.5	65	1500	120	92
4	TPCA	5.5	90	1500	145	90
5	Crystallizer	4.1	120	1500	170	89
9	Condensate	4.5	145	1500	120	92
10		3.8	165	1500	120	92
11		3.3	195	1500	130	91
12		2.5	250	1500	150	90

*HRT = Hydraulic Retention Time

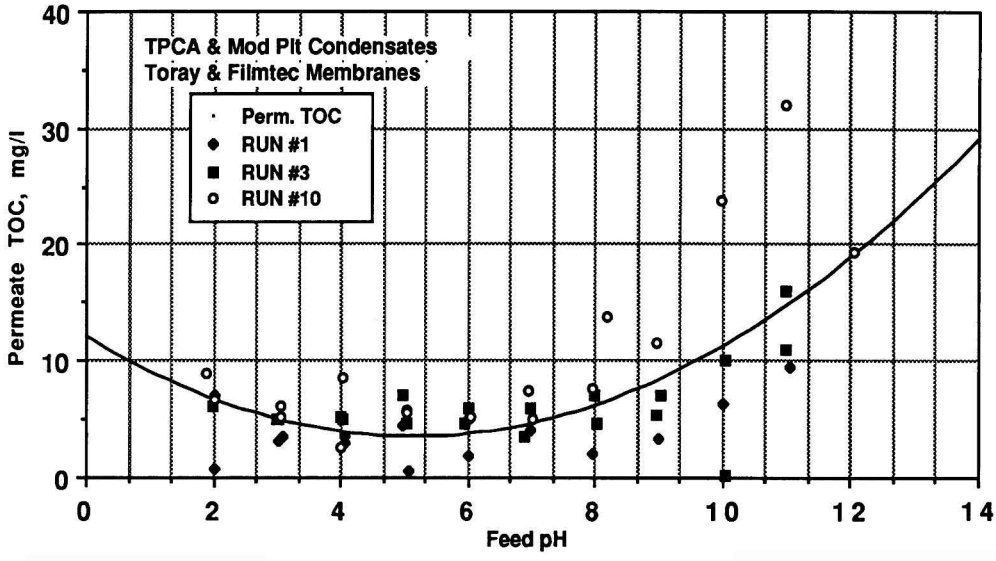

Figure 7. Effect of pH on permeate quality.

Carbon adsorption tests were conducted on three classes of feedstock: 1) Condensate from modernized facility feedstock; 2) Biological effluent from both condensate products and; 3) Reverse osmosis permeate from both condensate products. A summary of carbon adsorption performance is provided in Table 4. A typical isotherm generated for biological effluent derived from TPCA feedstock is presented in Figure 9.

As confirmed by the pilot test results the effectiveness of carbon adsorption on the condensate feedstock is marginal due to its high TOC content and the low organic loading of the carbon. Carbon adsorption of reverse osmosis permeates did reduce TOC levels by 30 to 50 percent. However, additional reduction of this already low TOC content stream is not considered warranted. Biological effluent is effectively treated by carbon adsorption to levels of less than 20 mg/l. For the biological effluents tested, removals of influent TOC content from 75 to 90 percent were demonstrated.

Better adsorption performance for the biological effluents is attributed to a different character of organic constituents remaining in the biological effluent than those remaining in the reverse osmosis permeate for the same condensate feed source. In the case of biological oxidation a chemical change occurs to the various molecules whereas reverse osmosis results in a purely physical separation based mostly on molecular size.

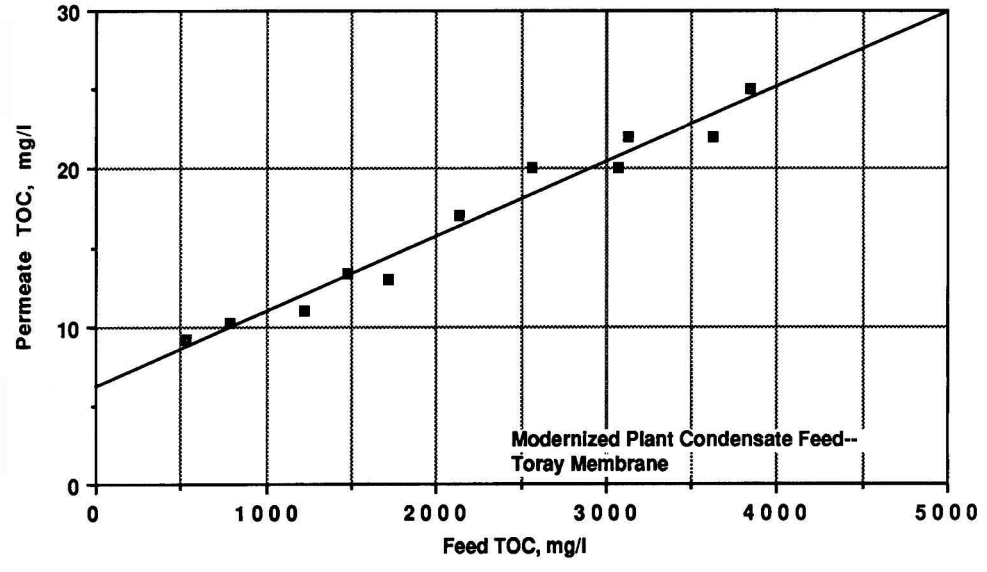

Figure 8. Permeate quality vs. feed TOC quality.

TABLE 4. CARBON ADSORPTION COLUMN PILOT TESTING SUMMARY

Run No.	Feedstock	Run Time Hr	Feed pH –	Feed TOC mg/l	Product TOC mg/l	Carbon Use** gm/l
	Modern Plant Crystallizer Condensate					
1	Undiluted	1.5	8.1	550	112	40.7
2	Undiluted	1.5	8.1	550	110	–
8	RO Permeate	24	8	15	10	2.7
10	Biological Effluent	23	7.5	132	28	2.9
11	Biological Effluent	23	3.6	132	28	2.9
	TPCA Crystallizer Condensate					
4	RO Permeate	7.5	8	38	21	8.5
7	RO Permeate	5	4	38	22	–
5	Biological Effluent	14	3.6	130	8	0.8*
6	Biological Effluent	11	6.8	130	8	0.8*

*Based on extrapolation of column run using Isotherm data.
**Grams of carbon required to treat one liter of feedstock in the continuous carbon column.

Carbon Column Conditions: Feed Rate @ 100ml/min
Empty Bed Volume @ 890 ml
Carbon Bed Weight @ 385 gms
Carbon: Calgon Filtrasorb 300

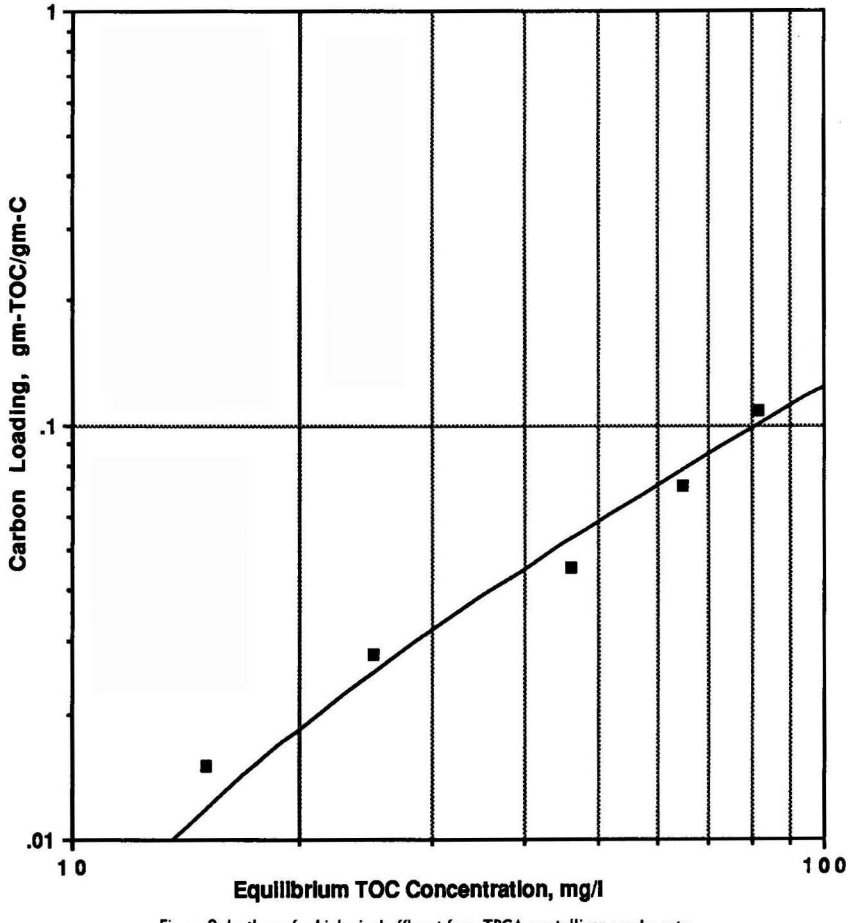

Figure 9. Isotherm for biological effluent from TPCA crystallizer condensate.

TABLE 5. ULTRAVIOLET PEROXIDATION PILOT TESTING SUMMARY

Run No.	Feedstock	Reaction			H_2O_2 Dose mg/l	TOC		
		Time min	Temp C	Power W/l		SOR* mg/l	EOR* mg/l	T-1/2 min
	Modern Plant Crystallizer Condensate							
1	Diluted 2:1	130	30-35	26	1720	141	102	146
2	Diluted 2:1	215	35-45	26	4230	141	12	60
3	Undiluted	196	40-50	58	3667	525	146	--
6	Undiluted	240	40-50	53	3500	525	50	55
11	Biological Effluent	60	30-43	41	1393	122	11	--
12	Biological Effluent	40	35-44	83	992	130	23	--
9	RO Permeate	60	35-48	33	1115	19	10	92
10	RO Permeate	45	40-54	66	796	15	5	27
	TPCA Crystallizer Condensate							
4	RO Permeate	30	33-49	74	1770	27	5	13
5	RO Permeate	90	35-48	33	1274	59	8	44
7	RO Permeate	90	34-52	33	2070	33	11	51

*SOR = Start of Run
EOR = End of Run

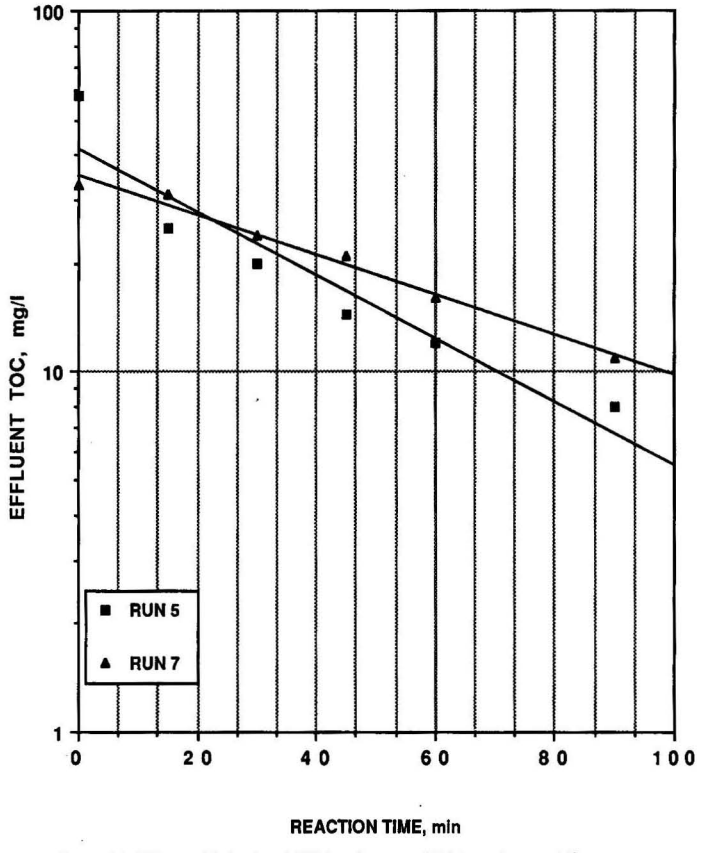

Figure 10. UV peroxidation batch RXN performance TPCA condensate-R/O permeate.

Ultraviolet Peroxidation

Destruction of residual TOC content using the process of ultraviolet peroxidation was evaluated as an alternate tertiary treatment to carbon adsorption. Ultraviolet peroxidation is, according to the literature [*11, 12*], most effective in the destruction of chlorinated, aromatic, and higher molecular weight organics and least effective on low molecular weight alcohols, amines and carboxylic acids.

Similar feeds were tested in the ultraviolet peroxidation unit as those tested for carbon adsorption. Tests were run at varying peroxide dose and UV light input. Results of these tests are summarized in Table 5. A typical TOC reduction profile for biological effluent from TPCA feedstock is presented in Figure 10.

The test results indicate successful reduction of the TOC content for all feedstocks given sufficient peroxide dose, UV-light power, and reaction time. When compared to carbon adsorption, the UV-peroxidation process is not an economically attractive option for tertiary treatment of biological effluents or reverse osmosis permeates derived from the condensate feedstocks. The relatively unattractive performance of the UV-peroxidation system is attributed to the high percentage of TOC content in the feedstocks tested being low molecular weight alcohols, ketones, and carboxylic acids.

CONCLUSION

The pilot test program successfully demonstrated that effluents and impounded liquids, comparable to those evaluated, can be treated to reduce organic, and inorganic contaminants to very low levels in the aqueous effluent. A solid waste with low moisture content is also produced.

The pilot test results confirm that a number of process configurations will provide aqueous effluents suitable for discharge to a POTW, a local waterway or to the atmosphere. Test results also indicate that the produced aqueous effluent is a good candidate for reuse within a treatment facility.

In relation to the proposed TPCA compliance and modernized plant goals, two process configurations provided highest quality aqueous effluents. Both configurations include evaporative crystallization as primary treatment followed by either biological plus carbon treatment or reverse osmosis plus carbon treatment. The reverse osmosis plus carbon treatment option is judged to be more advantageous from the standpoint of operability, minimizing air emissions, and overall economics. Due to resultant low TOC concentrations of the permeate product the reverse osmosis plus carbon treatment configuration has potential for eliminating carbon adsorption as a tertiary treatment and still meet discharge criteria. Selection of a treatment configuration is, however, ultimately dependent upon specifically imposed regulatory criteria coupled with economic considerations of the processes involved.

LITERATURE CITED

1. Gachot, D., and J. W. Walcott, "Waste Water Management Process Improvements," ASME Meeting, Paper No. 82-WA/HT-77, (1982).
2. Gorgol, R. G., and J. A. Meardon, "Cleanup of Contaminated Surface Impoundments Using Evaporation," AICHE Summer National Meeting, Denver, CO (August, 1988).
3. DeRenzo, D. J., Ed., *Biodegradation Techniques for Industrial Organic Wastes*, Noyes Data Corporation, Park Ridge, New Jersey (1980).
4. Blackburn, J. W., "Prediction of Organic Chemical Fates in Biological Treatment Systems," *Environmental Progress*, Vol. 6, No. 3, (August, 1987).
5. Chakrabarty, A. M., Ed., *Biodegradation and Detoxification of Environmental Pollutants*, CRC Press, Inc., Boca Raton, FL (1982).
6. Gooding, C. H., "Reverse Osmosis and Ultrafiltration Solve Separation Problems," *Chemical Engineering*, (January 7, 1985).
7. Cartwright, P. S., "New Advances in the Use of Membranes for Waste Water Treatment," Presented at the 1985 Third Annual Membrane Technology/Planning Conference, Cambridge, MA, (October, 1985).
8. Lyandres, S., J. A. Meardon, and J. Rees, "Evaluation of Membrane Processes for the Reduction of Trace Organic Contaminants," AICHE Summer National Meeting, Denver, CO (August, 1988).
9. Knox, R. C., L. W. Canter, D. F. Kincannon, E. L. Stover, and C. H. Ward, "Treatment of Groundwater-Carbon Adsorption," *Aquifer Restoration-State of the Art*, Noyes Publications, (1986).
10. Parmele, C. S., and R. D. Allan, "Steam-Regenerated Activated Carbon: An Emission-Free, Cost Effective Groundwater Treatment Process," *Environmental Progress*, Vol. 5, No. 2, (May, 1986).
11. Sukol, R. B., "Principles and Applications of Photodegradation for Treating Organic Pollutants," Report for the USEPA Office of Research and Development, Contract No. 68-03-3413-Perox (1987).
12. Hager, D. G., C. G. Loven, and C. L. Giggy, "Chemical Oxidation of Organic Contaminants in Ground Water," Presented at HMCRI National Conference and Exhibition, Washington, DC, (November, 1987).

Book Reviews

Analytical Groundwater Modeling Flow and Contaminant Migration, by William C. Walton. Lewis Publishers, Inc., Chelsea, MI 48118 (1989) 105 Pages + 2 Computer Diskettes, U.S. List Price: $68.00.

The quantitative prediction of groundwater flow and contaminant migration has blossomed into a full scientific discipline since its inception in the late 19th century. With today's easy access to large, fast computers, three-dimensional transient calculations are routinely performed for complex flow and geologic geometries. In many cases, the basic data and scale of decisions are insufficient to warrant a rigorous, costly numerical solution while analytical models may be more appropriate, efficient, and cost effective. The author of this book, William C. Walton, presents a compendium of elegant groundwater flow and solute transport analytical solutions. Four computer programs, tailored for the IBM PC and compatible microcomputers, are supplied with the text for performing easy simulation and graphing of uncomplicated, two-dimensional groundwater flow and contaminant migration.

Chapter 1 provides an introduction to the text and the four microcomputer programs written in BASIC: WELFUN (well functions), WELFLO (well and groundwater flow), CONMIG (contaminant migration), and GWGRAF (graphics). Chapters 2 and 3 discuss analytical solutions to the well function for such conditions as non-leaky and leaky artesians, water table with slow gravity yield, fractured rock, and partial penetration. The attributes of WELFLO, a groundwater flow simulator are discussed in Chapters 4 and 5. The following conditions are supported: leaky and nonleaky artesians, water table, and nonleaky artesian fractured rock. Partial penetration with or without well-bore storage and boundaries and discontinuities are also included. Analytical solutions for contaminant migration are discussed in Chapters 6 and 7. Graphical techniques are considered in Chapters 8 and 9. Eight appendices are provided in the text. These appendices discuss such topics as: source code, operating instructions, representative aquifer and contaminant data base values, and program verification and example input/output displays.

The text is well structured and easy to read. Emphasis is placed on practice rather than theory. Relevant expressions are presented without derivation. The microcomputer programs are simple to use and can be readily modified to fit specific needs. The book is highly recommended for practicing hydrologists, geologists, civil and chemical engineers, water well contractors, educators and students, and any other readers with a keen interest in quantitative hydrogeology.

David Tomasko
Energy & Environmental Systems Division
Argonne National Laboratory
9700 South Cass Avenue
Argonne, Illinois 60439

Improving Safety in the Chemical Laboratory: A Practical Guide by Jay A. Young, John Wiley & Sons, New York, NY, (1987) 350 pages, U.S. List Price $45.00

The authors are to be congratulated for preparing a timely and vitally needed book focusing on the paramount concern of safety in the chemical laboratory. There is a greater need for incorporation of a comprehensive safety program into the operation of governmental, industrial, research, and especially, academic laboratories. Although many chemical laboratories require certain minimum safety standards, several lack effective enforcement of these regulations, many lack personal protective equipment, proper chemical handling and storage, and general safety rules. It is time that the importance of safety be an integral part in the operation of all chemical laboratories.

The authors of *Improving Safety in the Chemical Laboratory*, present and discuss comprehensive and authoritative guidelines which should be studied and implemented by any person using, or having responsibility for the use, of chemicals.

Part I of this text discusses effective methods and procedures for identification and rectification of conditions which could contribute to the occurrence of accidents. This part also focuses on the role of management and its interaction with personnel in organizing a safe chemical laboratory. Part 2 takes a scientific approach to understanding the hazards and a comprehensive coverage of the laws and regulations pertaining to chemical safety. This book is highly recommended for managers, engineers, scientists, laboratory technicians, and especially faculty and students in engineering and science curricula.

Hamid R. Kavianian
Argonne National Laboratory
Argonne, IL 60439

When Your Health Is At Stake, You Look For A Board Certified Specialist...

a doctor with proven special expertise

Why Not Apply The Same Common Sense In Selecting Engineers?

Beginning with Opthalmologists in 1915, medical doctors have recognized that increasing complexity in the practice of medical specialties required self-regulation, a mechanism to protect the public. They have established a series of 23 specialty boards to examine and certify those doctors who have *proven* their special qualifications to master these complexities.

This mechanism, board certification, has achieved almost universal acceptance in the practice of medicine. Dermatologists don't perform brain surgery and vice versa. Equally important, people requiring brain surgery don't look to hire a dermatologist, although both have the same state professional license to practice medicine. Common sense? Yes! Effective? Yes!

Engineering today has more practicing engineers, 1.6 million, and more specialties than medicine. But, the proven effective methods for self-regulation of specialties in medicine, the methods that provide assurance and guidance so that the client/patient gets the right kind of doctors, largely have been overlooked in engineering. There is an exception.

The American Academy of Environmental Engineers has been certifying environmental engineering specialists since 1955. The Academy's peer-controlled certification process, modeled on the medical specialty boards, requires each person certified to have a college education, to be licensed to practice engineering, to have a minimum of 8 years environmental engineering expertise and to demonstrate (by written examination and oral interview) their special capabilities in air pollution control, hazardous waste management, industrial hygiene, radiation protection, solid waste management, public health, or water supply and wastewater treatment.

At the Academy, we are working to improve engineering quality, to reduce the cause for liability insurance problems and to protect the environment. We help those who hire environmental engineers get the right engineer.

If you would like to get the environmental engineer with the *proven* special capabilities you require, please write or call The American Academy of Environmental Engineers.

A copy of *Who's Who in Environmental Engineering* which lists ALL certified environmental engineers is available for $50.00 (US Funds) from the Academy. A *FREE* copy of the Academy's *Environmental Engineering Selection Guide* is provided to all purchasing *Who's Who in Environmental Engineering.*

AMERICAN ACADEMY OF ENVIRONMENTAL ENGINEERS

132 Holiday Court, Suite 206 • Annapolis, Maryland 21401 • 301-266-3311 • William C. Anderson, P.E., Executive Director

Quality in Engineering begins with PROVEN competence.

find information fast

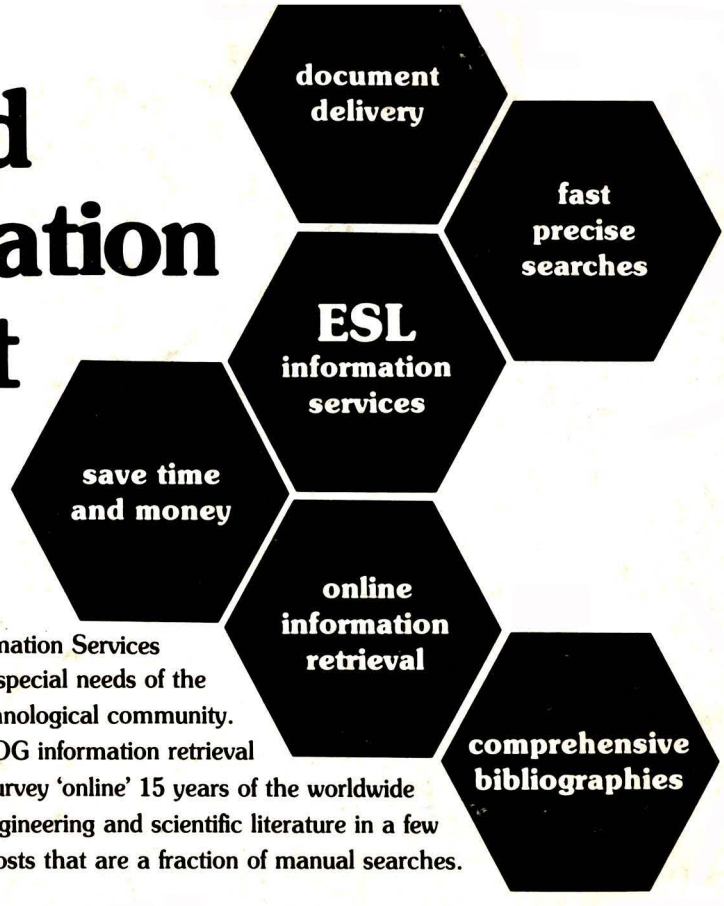

ESL Information Services addresses the special needs of the Engineering and Technological community. Through the DIALOG information retrieval system, we can survey 'online' 15 years of the worldwide engineering and scientific literature in a few minutes at costs that are a fraction of manual searches.

WHAT ESL INFORMATION SERVICES HAS TO OFFER YOU

- Fast precise searches of the Engineering Literature
- Immediate access to engineering journals, numerous conference proceedings, reports, and books
- Over 65 databases covering engineering, physics, computers, energy, materials, patents, and chemistry
- Flexible and extensive search terms - authors, title words, subject categories, chemical abstracts register numbers
- More for your money and time... save hours of library research over manual techniques
- Document delivery... tap the vast resources of the Engineering Societies Library's engineering and technological literature... over 5000 serials from some 50 countries in 25 languages

For more information on this indispensable research tool, please call or write:

ESL Information Services

Engineering Societies Library

345 East 47th Street New York, New York 10017 (212) 705-7610

(L20932